REMARKS

Claims 20, 49-51, 54-57, and 59 were pending in the subject application. Applicants have herein canceled claims 54 and 55, and amended claims 20, 49, 51, 56, 57, and 59. Applicants have added new claims 65-67. The amendments and new claims are fully supported in the specification as follows: Claim 20: page 3, lines 14-16; Claims 49, 56 and 57: page 7, line 28 to page 8, line 2; page 15, lines 1-9; Claim 51: page 14, lines 14-31; page 7, line 28 to page 8, line 2; page 15, lines 1-9; and Claim 59: page 15, lines 10-18. Specifically, applicants point out that language regarding injection of hMSCs and delivery of hMSC via catheter provide *de facto* support for the language "site-specific" in claims 49 and 57. Thus, applicants maintain that these amendments do not present new matter. Accordingly, applicants respectfully request that the Examiner enter this Amendment. Upon entry of this Amendment, claims 20, 49-51, 56, 57, 59 and 65-67 will be pending and under examination.

Rejection of claims 20, 49-51, 54-57 and 59 under 35 U.S.C. §112, First Paragraph (Written Description)

The Examiner rejected claims 20, 49-51, 54-57 and 59 under 35 U.S.C. §112, second paragraph, as allegedly failing to comply with the written description requirement because amendment of the claims to recite the term "effective" is considered new matter. The Examiner stated that the specification provides support for a sufficient amount but not for an effective amount, and since a minimal amount may be sufficient, it would be different in scope if changed to an effective amount to create an ion channel or induce a pacemaker current.

Applicants respectfully disagree. Applicants maintain that in the context of the instant claims the terms "effective" and "sufficient" are synonymous, since any amount which is sufficient to create an ion channel or induce a pacemaker current is effective to do the same. Nevertheless, to advance prosecution of the subject application, applicants have amended claims 20, 51, 57 and 59 to recite "sufficient" instead of "effective." As noted by the Examiner, the specification provides explicit support for the expression of HCN2 in an amount "sufficient" to

create an ion channel. Accordingly, the instant amendments render this ground of rejection moot, and applicants respectfully request that it be withdrawn.

Rejection of claims 20, 49-51, 54-57 and 59 under 35 U.S.C. §112, First Paragraph (Enablement)

The Examiner stated that to the extent the claimed compositions and/or methods are not described in the disclosure, claims 20, 49-51, 54-57 and 59 are also rejected as not enabled.

In response, applicants maintain that the amendment of claims 20, 51, 57 and 59 to recite "sufficient" instead of "effective" renders this rejection moot. Accordingly, applicants respectfully request that the Examiner withdraw this ground of rejection.

The Examiner also rejected claims 20, 49-51, 54-57 and 59 under 35 U.S.C. §112, first paragraph, as allegedly failing to comply with the enablement requirement on the basis that one of ordinary skill in the art would have had to perform undue experimentation to make and/or use the invention. The Examiner also referred to the factors for evaluating "undue experimentation" set forth in *In re Wands*, 858 F.2d at 737, 8 USPQ 1400, 2d at 1404, and in analyzing these factors, enumerated four main issues to support his contention that the specification does not provide specific guidance to practice the claimed invention in humans.

More specifically, regarding the enablement rejections, the Examiner first contended that the specification provides no guidance on how to obtain a purified, homogeneous population of hMSCs.

Applicants respectfully disagree with the Examiner's conclusions regarding the alleged difficulty cited by the Examiner in obtaining a homogeneous population of human MSCs. First, applicants note that the specification teaches a method for isolating human and canine MSCs from marrow aspirate. See page 29, lines 1-14. The specification also teaches that cell purity can be tested by flow cytometry and by the ability of hMSCs and cMSCs to differentiate into

osteogenic, chondrogenic, adipogenic and cardiogenic lineages. See page 29, line 22 to page 30, line 3, and page 30, line 26 to page 31, line 2. In addition, methods for isolating homogeneous (> 98% pure) hMSC populations were well known to those skilled in the art prior to the January 13, 2003 effective filing date of the subject application. See, for example, Haynesworth et al., Bone (1992), 13, 69-80 ("Haynesworth") and U.S. Patent No. 5,486,359 ("the '359 patent"), issued January 23, 1996, at col. 4, lines 35-38, and col. 16, line 7 to col. 17, line 24 (both of which are attached here to as **Exhibit 1**). Accordingly, applicants maintain that methods for preparing a homogeneous population of hMSCs, which are fully described in the specification and were known in the art prior to the effective filing date of the subject application, could be readily performed by a skilled artisan without undue experimentation.

The Examiner stated (citing Javazon et al. (2004) Exp Hematol 32: 414-425; Barry et al. (2004) Intl J Biochem Cell Biol 36: 568-584; Gepstein (2005) Expert Opin Biol Ther 5: 1531-1537; and Beyer Nardi et al. (2006) Handbook Exp Pharmacol 174: 249-282) that it has been difficult to predict the efficacy and outcome of a transplanted hMSC.

Applicants disagree with the Examiner's assessment and conclusions based on the above cited references. Applicants first note that Javazon summarizes the characterization of MSCs and merely speculates on potential issues surrounding the use of MSCs in tissue maintenance and repair. In contrast, the present application is directed to the use of MSCs to express HCN channels and to deliver pacemaker current at the site of delivery, and not to the use of MSCs in tissue maintenance and repair.

Regarding the Barry reference, applicants also note that it merely summarizes recent findings and speculates on issues to consider regarding host immune response, homing mechanisms and differentiation of implanted cells. Again, Barry does not address the present claimed invention relating to the use of engineered MSCs to express the HCN2 gene.

Regarding the Gepstein reference, in contrast to Javazon, it addresses the use of MSCs as biological pacemakers. However, Gepstein provides no data to support the speculation of

potential issues. Rather, Gepstein actually favorably reviews the applicants' work in the use of engineered MSCs to express the HCN2 gene, referencing their Potapova et al. paper (Cir. Res. (2004) 94:952-959) stating that:

> the result was the generation of an idioventricular rhythm localised at the site of cell transplantation. Subsequent histological examination revealed the presence of the grafted cells as well as the presence of gap junctions (positive connexin staining) between donor and host cells.

Gepstein at page 1534, first column. Gepstein further notes that "the approach above [referring to Potapova reference (inventor's own work)] may be attractive for a number of reasons." Accordingly, none of the cited references undermine enablement of the presently claimed invention.

Further, applicants respectfully point out that enablement does not require the resolution of all potential issues surrounding a particular claimed composition or methods, but only requires one of skill in the art to practice the claimed invention without undue experimentation. Applicants respectfully submit that clinical trials are undertaken to consider and resolve all efficacy and safety issues, and that results from clinical trials are not necessary for enablement and allowance of certain subject matter. See MPEP 2164:

> However, to comply with 35 U.S.C. 112, first paragraph, it is not necessary to 'enable one of ordinary skill in the art to make and use a perfected, commercially viable embodiment absent a claim limitation to that effect.' (citing *CFMT, Inc. v. Yieldup Int'l Corp.*, 349 F.3d 1333, 1338, 68 USPQ2d 1940, 1944 (Fed. Cir. 2003)).

In addition, there are several cases that clearly indicate that applicants do not have to demonstrate an invention is completely safe to be patentable under 35 U.S.C. 112, first paragraph. These cases focus on safety not undermining the utility of the invention, even when the rejection is based on lack of enablement under 112, first paragraph. For example, in *In re Brana*, 51 F.3d 1560 (Fed. Cir. 1995), the Examiner rejected claims to anti-tumor compounds under 112, first paragraph on the basis that the tests described "were not sufficient to establish a reasonable expectation that the claimed compounds had a practical utility (i.e. antitumor activity in humans)." See pp. 1563-1564. The Fed. Cir. Reversed, stating:

> The Commissioner counters that such *in vivo* tests in animals are only preclinical tests to determine whether a compound is suitable for processing in the second stage of testing, by which he apparently means *in vivo* testing in humans, and therefore are not reasonably predictive of the success of the claimed compounds for treating cancer in humans. The Commissioner, as did the Board, confuses the requirements under the law for obtaining a patent with the requirements for obtaining government approval to market a particular drug for human consumption. *See Scott v. Finney,* 34 F.3d 1058, 1063, 32 USPQ2d 1115, 1120 (Fed.Cir.1994) ("Testing for the full safety and effectiveness of a prosthetic device is more properly left to the Food and Drug Administration (FDA). Title 35 does not demand that such human testing occur within the confines of Patent and Trademark Office (PTO) proceedings.").

See *In re Brana*, 51 F.3d at 1567. The Federal Circuit also noted that FDA approval is not a prerequisite for finding a compound useful within the meaning of the patent laws, citing to *Scott,* 34 F.3d 1058, 1063. The Federal Circuit continued:

> Usefulness in patent law, and in particular in the context of pharmaceutical inventions, necessarily includes the expectation of further research and development. The stage at which an invention in this field becomes useful is well before it is ready to be administered to humans. Were we to require Phase II testing in order to prove utility, the associated costs would prevent many companies from obtaining patent protection on promising new inventions, thereby eliminating an incentive to pursue, through research and development, potential cures in many crucial areas such as the treatment of cancer. In view of all the foregoing, we conclude that applicants' disclosure complies with the requirements of 35 U.S.C. § 112 ¶ 1.

See *In re Brana*, 51 F.3d at 1568. As such, applicants respectfully assert that the Examiner's enablement rejections based on the recitation of references speculating on issues and potential safety concerns is misplaced.

In any event, applicants address herein below each of the safety concerns voiced by the Examiner. Regarding the potential for differentiation of transplanted stem cells, applicants have shown that no differentiation of hMSCs was observed over a 42-day period following injection of mHCN2-transfected hMSCs into left ventricular (LV) subepicardium of 6 non-immunosuppressed adult dogs (see Plotnikov et al. (2005) Circulation 112: II-126; submitted as Exhibit A in the March 7, 2006 Amendment). Thus, applicants maintain that uncertainties noted by the Examiner concerning mechanisms of engraftment and *in vivo* differentiation of

transplanted MSCs do not undermine enablement of the claimed invention. Importantly, the Examiner has not pointed to any reference documenting the actual occurrence of appreciable undesirable differentiation in any study relevant to the claimed invention. Accordingly, applicants maintain that the alleged theoretical risk of unwanted differentiation of transplanted hMSCs does not diminish the enablement of the present invention.

Regarding the question of host immune responses to implanted MSCs, applicants note that these cells are thought to be immunoprivileged. See Liechty et al. (2000) Nat Med 6: 1282-1286, attached hereto as **Exhibit 2** (see page 1283 noting that there was an apparent lack of immune response of hMSCs implanted into a sheep fetus). Indeed, the specification also notes that hMSCs transplanted into fetal sheep even after the expected development of immunologic competence engrafted and persisted in multiple tissues for as long as 13 months after transplantation, and suggests a possible reason may be because hMSCs express class I human leukocyte antigen but not class II, which may limit immune recognition. See page 29, line 26 to page 30, line 8; and Liechty et al. (2000; **Exhibit 2**) for more detail. More than not eliciting an immune response, there is evidence that MSCs may actually suppress such a response. See the Javazon reference cited by the Examiner at page 417, right col. In addition, consistent with the immunoprivileged status of hMSCs, applicants showed that there was no cellular or humoral rejection six weeks following injection of hMSCs into canine hearts. (Reported in Plotnikov et al., 2005; previously submitted as Exhibit A in the March 7, 2006 Amendment). Accordingly, applicants maintain that the question of host immune responses to transplanted hMSCs does not militate against the enablement of the claimed invention.

As to questions regarding the mechanism of homing of transplanted cells, applicants note that the claims, as amended herein, recite the site-specific introduction of HCN2-expressing hMSCs directly into the heart, thereby obviating any requirement for specific homing of systemically introduced hMSCs. The appropriate sites in the heart for introduction of hMSCs to treat different conditions would be well known to a person of ordinary skill in the art. Applicants note that in a study involving injection of HCN2-expressing hMSCs into canine heart and monitoring over 42 days, Plotnikov et al. (2005; submitted as Exhibit A in the March 7, 2006

Amendment) reported that nests of hMSCs were found adjacent to the injection site but not at a distance. Applicants submit, therefore, that the Examiner's comments concerning the mechanism of homing of transplanted cells are moot.

Applicants wish to emphasize that their citation herein of Plotnikov et al. (2005) and other post-filing date references is not meant to supplement the disclosures in the specification so as to render it enabling, or to show what was known at the time of filing. Rather, these publications are cited as evidence that the disclosures in the specification as filed are sufficient to enable a person skilled in the art to practice the invention being claimed without undue experimentation, i.e., to demonstrate that the disclosure was enabling as of the filing date. Several Federal Circuit decisions, for example *Gould v. Quigg* 3 U.S.P.Q.2d 1302 (Fed. Circ. 1987), confirm the utility of post-filing date references for this purpose:

> As to the technical article, it is true that a later dated publication cannot supplement an insufficient disclosure in a prior dated application to render it enabling. In this case, the later dated publication was not offered as evidence for this purpose. Rather, it was offered as evidence of the level of ordinary skill in the art at the time of the application and as evidence that the disclosed device would have been operative.... It was not legal error for the district court to accept the testimony of an expert who had considered a later publication in the formulation of his opinion as to whether the disclosure was enabling as of the time of the filing date of the '540 application. *Gould v. Quigg* 3 U.S.P.Q.2d 1302, 1305.

In this regard, applicants note the Examiner's assertion on page 16 of the Office Action that post-filing date art cannot be used for the enabling support of the instant claims as the cited art uses a method that is different from the instant disclosure and does not provide guidance to other issues raised in the office action.

Applicants respectfully disagree with the Examiner's failure to consider Potapova et al. (2004), submitted as Exhibit C in the March 7, 2006 Amendment in support of enablement. Applicants note that the specification discloses a method for injecting HCN2-transfected hMSCs into canine heart as a means for introducing HCN channels into the heart, and provides data indicating that implantation of these cells results in the generation of pacemaker current in the heart. See the specification at page 7, line 28 to page 8, line 18, and Fig. 10. The same

procedures are reported in Potapova et al. In contrast to Potapova et al.'s disclosure that hMSCs were obtained from a commercial source and that 10^6 transfected hMSCs were injected into the heart, the specification provides a method for preparing hMSCs and does not disclose the number of cells injected. Applicants maintain, however, that determining an appropriate number of hMSCs to be injected into the heart, in effect determining the dosage of cells to be administered, does not require undue experimentation by a skilled artisan. As to the source of the cells, applicants have noted hereinabove the isolation and purification of hMSCs was known in the art. Accordingly, applicants maintain that the post-filing date Potapova et al. (2004) reference can be properly used to show that the disclosures in the specification are enabling.

The Examiner also argued (citing Boheler(2004)) that the alleged presence of a mixed distribution of channels in hMSCs argues for a heterogeneous cell population. In response, applicants reiterate that methods for preparing homogeneous populations of hMSCs are disclosed in the specification and in the prior art. See the specification at page 29, lines 1-14, and the '359 patent at col. 4, lines 35-38, and col. 16, line 7 to col. 17, line 24. Applicants maintain that even if, *arguendo*, such cell populations contained small numbers of one or more cell subpopulations, such subpopulations do not interfere with the use of isolated hMSCs as a delivery platform for introducing HCN channels into the heart, as was demonstrated in experiments disclosed in the specification. See page 7, line 28 to page 8, line 18; see also Potapova et al. (2004), submitted as Exhibit C in the March 7, 2006 Amendment.

The Examiner also noted (citing Gepstein et al., 2005) that pacemaker function is the result of a combination of the activity of a number of ionic current, and thus, overexpression of the HCN current alone will not fully recapitulate all the properties of a SA node cell. Applicants agree with the Examiner that overexpression of a HCN current alone in a hMSC does not fully recapitulate all the properties of a SA node cell. However, applicants emphasize that an engineered hMSC overexpressing a HCN current is not intended to recapitulate the properties of a SA node cell. Instead, the rationale of using hMSCs as delivery platforms for biological pacemaking is that the hMSC expressing the HCN channel will pair with a cardiomyocyte via

gap junctions, whereby the paired cells will then operate together as a single functional unit that in conjunction with a tightly-coupled myocyte generates spontaneously initiated, or automatic action potentials that serve the same function as automatic action potentials initiated by the sinus node. This rationale is illustrated in the drawing attached hereto as **Exhibit 3**. The top panel shows that in a natural pacemaker cell, i.e., a SA node cell, action potentials (inset) are initiated via inward current flowing through transmembrane HCN channels. These channels open when the membrane repolarizes to its maximum diastolic potential and close when the membrane has depolarized during the action potential. Current flowing via gap junctions to adjacent myocytes results in their excitation and the propagation of impulses through the conducting system. The lower panel shows a hMSC genetically engineered to incorporate HCN channels in its membrane. These channels can only open, and current can only flow through them (inset) when the membrane is hyperpolarized; however, because the stem cell lacks the different ion channels required for hyperpolarization, such hyperpolarization can only be delivered if an adjacent myocyte is tightly coupled to the stem cell via gap junctions. In the presence of such coupling and the opening of the HCN channels to induce local current flow, the adjacent myocyte will be excited and initiate an action potential that then propagates through the conducting system. The depolarization of the action potential will result in the closing of the HCN channels until the next repolarization restores a high negative membrane potential. Thus, whereas wild-type and genetically engineered pacemaker cells incorporate in each cell all the machinery needed to initiate and propagate action potentials, an engineered hMSC lacks this machinery and depends on gap junction-mediated pairing with a myocyte to form a functional unit that operates similarly to a SA node cell or other automatic cardiac cell. As discussed in detail in their March 7, 2006 Amendment, applicants note that the specification provides evidence of robust gap junction-mediated coupling between hMSCs and cardiomyocytes.

The Examiner further noted (citing Boheler, 2004) a number of questions in the art concerning the best way (local or systemic) to introduce cells for therapeutics, and the survival and homing capacity of the cells in host tissues following transplantation. The Examiner stated that applicants' post-filing art (not identified) indicates that catheterization is not usable for hMSC transplantation due to problems associated with

cell size and potential of injury to the cell.[1]

Applicants remind the Examiner that "[a]s long as the specification discloses at least one method for making and using the claimed invention that bears a reasonable correlation to the entire scope of the claim, then the enablement requirement of 35 U.S.C. §112 is satisfied." See M.P.E.P §2164.01(b). The claims, as amended herein, specify that the HCN2-expressing hMSCs are site-specifically introduced into the heart. Notably, the specification discloses the result of an experiment whereby the site-specific introduction of HCN2-transfected hMSCs into the LV wall of a canine heart by injection (i.e., site-specific introduction) resulted in the induction of pacemaker activity in the ventricle. See page 7, line 30 to page 8, line 2. The specification also teaches that hMSCs may be introduced into the heart by a variety of site-specific methods, including injection, topical application to the cells of the heart, microinjection and catheterization. See page 15, lines 1-9. Accordingly, applicants maintain that this disclosure relating to the site-specific introduction of HCN2-expressing hMSCs into canine heart enables the now pending claims.

Applicants disagree with the Examiner's assessment regarding catheterization. Applicants provide herein several references indicating that delivery of hMSCs by catheterization is viable and was enabled by the present application in view of the knowledge of one skilled in the art. For instance, others had successfully delivered viable cells to a heart via catheterization by the filing date of the present application. In 2000, an abstract of Weinstein, et al. was presented in Sweden showing that myoblasts were successfully delivered to a heart via catheterization: "[c]atheter advance into the left ventricle through the aorta was guided with fluoroscopy followed by endocardial mapping with the electromagnetic NOGA system. . . . Vital dye staining of the myoblasts before versus after the procedure showed no significant difference in cell viability. Furthermore, cell passage through the injection catheter showed less than 5% cell death." (Abstract

1 In seeking clarification from the Examiner regarding his comments that inventors' own work indicates that catheterization would not work, the Examiner indicated in a telephone conversation with applicants' representative that the argument in the Office Action was actually the Examiner's "interpretation of the references of record" and that he was not referencing a specific journal article or paper by the inventors.

attached hereto as **Exhibit 4**). Thus, this reference shows that those skilled in the art at the time the present application was filed could successfully deliver cells to the heart and also knew how to test for cell viability to be able to optimize the procedure. Applicants respectfully submit that one skilled in the art could use the teachings of Weinstein regarding delivery of myoblasts to the heart via catheterization to successfully deliver MSCs to the heart via catheterization without undue experimentation.

Further, others have continued in using/studying the delivery of cells to the heart through catheterization:

Exhibit 5: Texas Heart Institute Stem Cell Center – "Ongoing studies at the Stem Cell Center inject the stem cells directly into the muscle of the heart from inside the heart chamber. This is performed with a catheter that is inserted into the groin. The exact area of disease is located through a sophisticated mapping system know as the NOGA® Cardiac Navigation system and the cells are injected using a Myostar® Injection Catheter."

Exhibit 6: Kornowski, et al., Catheter Cardiovasc Interv. 2001 Mar;52(3):400-6 - "The NOGA system maps regional myocardial function and delivers local catheter-based therapeutics. . . . In conclusion, catheter tip trajectories at any location are highly stable throughout the cardiac cycle."

Exhibit 7: Sherman et al., Nature Clinical Practice Cardiovascular Medicine, March 2006, Vol. 3, supplement 1, S57-S64 – "The catheters described in this article have been shown in both animal and clinical studies to be effective in cell delivery and to be safe." "Two catheter-based methods have been used in clinical trials to deliver cells to the heart. . . ."

Exhibit 8: Perin et al., "Methods of Stem Cell Delivery in Cardiac Diseases," Nature Clinical Practice Cardiovascular Medicine, March 2006, Vol. 3, supplement 1, S110-S113 – "Two catheter systems are currently available for transendocardial cell delivery: the Stilleto™ . . . and the Myostar™." "The Myostar catheter allows assessment of myocardial viability at each specific injection site." (emphasis added).

Exhibit 9: Smits, et al., Journal of the American College of Cardiology, Vol. 42, No. 12 2003, pp.2063-2069 – " . . . we believe that catheter-based cell transplantation in HF patients is feasible and that the transendocardial catheter-based cell delivery technique is safe from a procedural point of view."

Thus, notwithstanding that the delivery of hMSCs via catheterization may continue to be improved and optimized through ongoing clinical trials, the delivery of hMSCs via catheterization was clearly enabled in the present application.

The Examiner also stated (citing Mocini et al. (2005) Ital Heart J 6: 267-271, and Zhang (2002) Circulation 106: 1294-9) that the unpredictability related to undesired cell lineage differentiation and unordered activation and contraction could potentially induce cardiac arrhythmia as discussed in the previous Office Action dated December 7, 2005.

Regarding the potential for inducing cardiac arrhythmias by introducing hMSCs expressing HCN channels into the heart, applicants previously explained in their March 7, 2006 response to the December 7, 2005 Office Action that Zhang (2002) does not apply to the claimed invention. Briefly, Zhang relates to pluripotent embryonic stem cells that have innate pacemaking function whereas the hMSCs of the subject invention are multipotent, have no innate pacemaking function, and exhibited no evidence of differentiation or generating arrhythmias even after six weeks of monitoring (see Plotnikov et al. (2005), submitted as Exhibit A in the March 7, 20076 Amendment). Thus, the arrhythmias generated by the embryonic stem cells in Zhang's study are not predictive of arrhythmias generated in the claimed invention. Mocini et al. (2005) also raises the possibility of arrhythmias after stem cell transplantation, but notes that such complications have been shown only in the case of skeletal myoblast transplantation. Again, applicants note that skeletal myoblasts are different from the undifferentiated hMSCs used in the claimed invention. Moreover, because the pacemaker current, I_f, flows only at diastolic potentials, inducing I_f in the heart should not affect action-potential duration and is therefore not expected to generate arrhythmias. In this regard, applicants note that the Examiner has not pointed to any reference indicating that transplantation

of undifferentiated hMSCs expressing HCN channels into the heart causes arrhythmias. Applicants maintain, therefore, that the theoretical risk of arrhythmias is not a proper basis for asserting nonenablement of the claimed invention. Moreover, as mentioned above, the inventors' own work study reported in Plotnikov et al. (2005) shows that no arrhythmias were seen in a 42-day study.

Applicants respectfully submit, as previously noted in their March 7, 2006 response to the December 7, 2005 Office Action, that several of the Examiner's grounds of rejection appear to be predicated on the absence of optimized protocols for inducing biological pacemaker activity using the claimed methods. For example, rejections based on uncertainties concerning the homogeneity of the hMSC preparation used, the degree of coupling between cell types, the optimal way of delivering the cells into the heart, and the potential for unwanted differentiation of transplanted hMSCs and for generating arrhythmias, fit into this category. Applicants maintain, however, that optimization of the claimed methods requires only routine experimentation by a skilled practitioner, and the lack of optimized protocols does not mean the method is not enabled. Applicants emphasize that the specification discloses the experimental demonstration of certain aspects of the claimed invention that the Examiner contends are not enabled. Thus, a composition comprising a hMSC expressing a HCN2 ion channel (claim 20) was experimentally made (see the specification at page 7, lines 11-14 and 28-30); a method of expressing a functional ion channel in a syncytial structure such as a mammalian heart comprising preparing the above composition site-specifically introducing it into the a canine heart (claims 49 and 50) has been experimentally performed (see page 7, line 28 to page 8, line 18); and a method of inducing a pacemaker current in a mammal's heart comprising site-specifically introducing the above composition into the heart (claim 57) has been experimentally performed (see page 7, line 28 to page 8, line 18). Applicants are therefore perplexed by the Examiner's arguments that these methods and composition, among others, are not enabled by the disclosures in the specification.

Based on the foregoing remarks, applicants maintain that the specification as filed enables one skilled in the art to make and use the invention recited in the presently amended claims

employing only routine experimentation. Accordingly, applicants respectfully request withdrawal of this ground of rejection.

Regarding claim 20, the Examiner noted that although claim 20 is drawn to a composition, the Examiner has "analyzed [claim 20] for its intended use in the treatment of heart failure and other cardiac disorders." Applicants agree that while the composition is useful in methods of treating a cardiac rhythm disorder, the composition is also useful for inducing a pacemaker current in a mammal's heart and in a cell. Further, the specification notes that the compositions are useful for causing a contraction of a cell, for shortening the time required to activate a cell and changing the membrane potential of a cell. See paragraphs [016-018] of the published application. As such, the compositions are also useful for research purposes. For example, the specification notes that the transfected stem cells are useful in studying membrane properties of adult heart cells. See paragraph [0125] of the published application. Accordingly, applicants submit that it is improper for the Examiner analyze enablement of the composition claim based on only one intended use. See MPEP 2164.01(c):

> In contrast, when a compound or composition claim is not limited by a recited use, any enabled use that would reasonably correlate with the entire scope of that claim is sufficient to preclude a rejection for nonenablement based on how to use. If multiple uses for claimed compounds or compositions are disclosed in the application, then an enablement rejection must include an explanation, sufficiently supported by the evidence, why the specification fails to enable each disclosed use. In other words, if any use is enabled when multiple uses are disclosed, the application is enabling for the claimed invention. (emphasis added).

Accordingly, applicants respectfully submit that the Examiner's enablement analysis of claim 20 based solely on one intended use is in error.

Double Patenting Rejections

The Examiner provisionally rejected claims 20, 49-51, 54-57 and 59 under the judicially created doctrine of obviousness-type double patenting as allegedly unpatentable over claims 20-59 of co-pending Application No. 10/342,506 ("the '506 application) which corresponds to U.S. Publication No. 20040137621.

In response, applicants note that this is a "provisional" rejection over the '506 application which is not an allowed application. Accordingly, if the claims of the subject application are otherwise allowable, the "provisional" double patenting rejection should be withdrawn and the claims in the subject application should be allowed and issued, whereby the claims of the '506 application would become subject to an obviousness-type double patenting rejection.

Rejection of claim 20 under 35 U.S.C. §103(a) (Obviousness)

The Examiner rejected claim 20 under 35 U.S.C. 103(a) as allegedly unpatentable over Marban et al. (U.S. Patent Application Publication No. US2004/0254134, published February 16, 2004; effective filing date February 29, 2002; henceforth "Marban"), Heubach et al. (2002) Circulation 106 Suppl. p. II-68; henceforth "Heubach"), and Jansen et al. (U.S. Patent No. 6,979,532, issued December 27, 2005, effective filing date February 12, 2000; henceforth "Jansen").[2]

The Examiner stated that Heubach teaches that novel therapeutic strategies for heart failure include the injection of autologous mesenchymal stem cell into the heart but does not teach MSCs comprising HCN2. The Examiner also stated that Marban discloses that a composition of modified cells could be implanted in cardiac tissue to induce or modulate pacemaker activity and that genes encoding HCN channels could be used to affect cardiac firing rate. The Examiner conceded, however, that Marban does not teach the use of a composition of MSCs comprising HCN2. The Examiner additionally stated that Jansen teaches a process comprising determining the membrane potential of mammalian cells that express HCN2 but does not explicitly teach a composition of MSCs comprising HCN2.

The Examiner asserted that it would have been obvious for one of ordinary skill in the art

[2] Applicants note that in the previous Office Action, the Examiner cited U.S. Patent No.6,849,611 in a 103(a) rejection. Applicants had argued that the reference was not by "another." Upon closer review of the '611 patent, applicants note that the '611 patent and the present invention are owned by the same entity and as such are not available at under 102(e)(f) and (g). However, since the '611 patent and the present invention list different inventors, the '611 patent may still be applicable under 103(a). Nevertheless, applicants maintain that since the '611 patent does not teach or suggest the use of MSCs incorporated with a nucleic acid which encodes an HCN channel in an amount sufficient to create an ion channel in the cell, it does not anticipate nor render the claimed invention obvious. Further, as discussed above in the present response, because of Heubach's shortcomings, Heubach does not

at the time of invention to modify the cells taught by Heubach by expressing a nucleic acid encoding HCN isoforms taught by Marban, for expressing ion channel genes in a stem cell at sufficient level for pacemaker activity. The Examiner further contended that one of ordinary skill in art would have been motivated to combine the teachings of Heubach, Marban and Jansen and would have reasonable expectation of successfully producing a composition comprising mesenchymal stem cell incorporated with HCN2. The Examiner therefore concluded that the claimed invention would have been *prima facie* obvious to one of ordinary skill in the art at the time of the invention.

Applicants respectfully disagree. Applicants maintain that the Examiner has failed to establish a *prima facie* case of obviousness of claim 20 for the following reasons. First, although Heubach reports that MSCs contain "significant mRNA levels for the HCN2 channel" Heubach most importantly writes that they do not express endogenous "macroscopic pacemaker currents such as the hyperpolarization-activated current I_f . . . ." (emphasis added). The preliminary results disclosed in Heubach are presented in more detail in Heubach et al. (2004) J Physiol 554.3: 659-672, a copy of which is attached hereto as **Exhibit 10**. Heubach et al. (2004) also teaches that "[t]here was strong expression of mRNA for the hyperpolarization-activated and cyclic nucleotide-gated ion channel isoform 2 (HCN2) in all samples of hMSC, but the respective current I_f was not observed." (emphasis added). See page 668, left col; see also page 667, right col., Fig. 9, and the abstract. Heubach et al. (2004) further teaches at page 669, right col. that:

> Ion channel mRNA, though expressed at high levels, is not necessarily translated into functionally active channel molecules. The discrepancy between the presence of mRNA but lack of the respective current is most striking for [Kv4.2 and Kv4.3 channel subunits], but also for the hyperpolarization-activated and cyclic nucleotide-gated channel isoform 2 (HCN2), responsible for the I_f inward current. The reason for the lack of functional channel molecules remains unclear.

(emphasis added). Applicants assert that, based on the teachings of Heubach (cited by the Examiner, and elaborated upon by Heubach et al. (2004)), one skilled in the art would have clearly understood that hMSCs do not synthesize functional endogenous HCN2 channels even

---

provide the motivation or suggestion to combine the '611 patent with Heubach to arrive at the present invention.

when "high levels" of HCN2 mRNA were expressed in such cells. Applicants therefore submit that Heubach teaches that hMSCs are not appropriate host cells to transfect with an HCN2 gene for the purpose of delivering functional HCN2 channels into a heart, and thus teaches away from the composition recited in claim 20. Accordingly, a person of ordinary skill in the art would not be motivated to combine Heubach with Marban and Jansen.

Second, applicants maintain that contrary to the Examiner's contention, a skilled artisan would not have had a reasonable expectation of success that modifying the cells taught by Heubach by expressing a nucleic acid encoding HCN isoforms taught by Marban would result in the functional expression of HCN2 ion channels at a level sufficient for pacemaker activity. This is evident from Heubach's teaching that although MSCs contain "significant mRNA levels for the HCN2 channel," they do not express "macroscopic pacemaker currents such as the hyperpolarization-activated current I_f . . . ." One would not be motivated to express HCN2 channels in hMSCs since hMSCs already express HCN mRNA but nevertheless do not have functional endogenous HCN channels (as taught by Heubach). Applicants maintain that one would not be motivated to express HCN2 in hMSCs since Heubach showed that even with expression of HCN channel mRNA, the hMSCs did not have functional HCN channels. Heubach even noted, "[t]he reason for the lack of functional channel molecules remains unclear."

Third, none of the references cited by the Examiner envisages the use of engineered MSCs to express functional HCN2 channels or induce pacemaker current in a cell, as is claimed in the subject invention. Marban discloses the use of myocardial cells (see page 4, para. 46-48) and embryonic stem cell-derived cardiomyocytes (page 10, para. 121), whereas Jansen teaches the use of differentiated mammalian cells such as CHO or HEK293 cells (see col. 6, lines 5-7). As noted by the Examiner, Heubach does teach the injection of autologous mesenchymal stem cell into the heart as a novel therapeutic strategy for heart failure. However, the objective of Heubach's study is clearly to measure the electrophysiological properties of hMSCs as a means of evaluating the potential of these cells for acquiring the characteristics of excitable cells and differentiating into cardiomyocytes. The contemplated differentiation of implanted MSCs is explicitly stated in Heubach et al. (2004; **Exhibit 10**) at page 669, first para: "In the context of *in*

vivo and *in vitro* differentiation of human mesenchymal stem cells (hMSC) into excitable cells we describe the electrophysiological properties of undifferentiated hMSC." Further, Heubach et al. (2004) states at page 70, para. spanning left and right cols.: "Preliminary clinical studies have shown that the injection of undifferentiated bone marrow stem cells into the infarcted heart can improve cardiac function. The fate of the implanted cells, whether they differentiate into cardiomyocytes, contribute to neoangiogenesis, or just perish, remains unclear" (emphasis added). Thus, Heubach clearly did not envisage the implantation of MSCs to induce pacemaker current in the heart.

Applicants maintain that claim 20 is not obvious over the cited prior art because (1) Heubach teaches away from combining the cited references in the way suggested by the Examiner; and in any event, (2) a combination of the cited references does not result in the claimed invention. Applicants therefore respectfully request that the Examiner reconsider and withdraw this ground of rejection.

Conclusion

In view of the remarks made hereinabove, applicants respectfully request that the Examiner reconsider and withdraw the rejections set forth in the May 24, 2006 Final Office Action. Applicants respectfully submit that the now pending claims are in condition for allowance and earnestly solicit allowance of these claims.

If a telephone interview would be of assistance in advancing prosecution of the subject application, applicants' undersigned attorney invites the Examiner to telephone her at the number provided below. Authorization is hereby given to charge Deposit Account No. 11-0600 for any fees deemed necessary in connection with the filing of this Amendment, including the fee for a one month extension of time.

Respectfully submitted,
KENYON & KENYON LLP

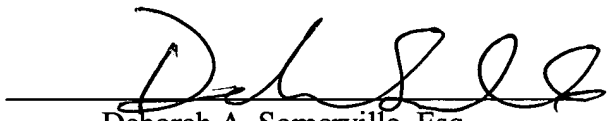

September 25, 2006
Date

Deborah A. Somerville, Esq.
Registration No. 31,995

Kenyon & Kenyon LLP
One Broadway
New York, New York 10004
(212) 425-7200 (telephone)
(212) 425-5288 (facsimile)
CUSTOMER No. 26646

ISSN 8756-3282 (677)

Bone

Volume 13, Number 1, 1992

AN INTERNATIONAL MULTIDISCIPLINARY JOURNAL OF
BONE CELL BIOLOGY, PHYSIOLOGY, AND PATHOLOGY

INDEXED IN Current Contents, CABS, BIOSIS Database, Index Medicus, MEDLINE, Excerpta Medica, PASCAL-CNRS Database

Published by
PERGAMON PRESS New York / Oxford / Seoul / Tokyo

Bone

Manuscript Submissions: Manuscripts should be addressed to any of the Editors or Associate Editors (see addresses listed above).

Publishing, Subscription, and Advertising Offices: Pergamon Press, Inc., 395 Saw Mill River Road, Elmsford, NY 10523, USA, INTERNET "PPI@PERGAMON.COM," or Pergamon Press plc, Headington Hill Hall, Oxford OX3 0BW, England.

Published Bimonthly. Annual institutional subscription rate (1992): £335.00 (US$535.00). Two-year institutional rate (1992/3): £636.50 (US$1016.50) Personal subscription rate for those whose library subscribes at the regular rate (1992): £157.00 (US$251). Sterling prices are definitive. US dollar prices are quoted for convenience only, and are subject to exchange rate fluctuation. Prices include postage and insurance and are subject to change without notice. Back issues of all previously published volumes, both hard cover and microform, are available direct from Pergamon Press. Subscription rates for Japan are available on request.

The Item-Fee Code for the publication is: 8756-3282/92 $5.00 + .00.

Bone, 13, 69–80, (1992)
Printed in the USA.

8756-3282/92 $5.00 + .00

Cell Surface Antigens on Human Marrow-Derived Mesenchymal Cells Are Detected by Monoclonal Antibodies

S. E. HAYNESWORTH, M. A. BABER and A. I. CAPLAN

Skeletal Research Center, Department of Biology, Case Western Reserve University, 2080 Adelbert Road, Cleveland, OH 44106, USA

Address for correspondence and reprints: Arnold I. Caplan, Skeletal Research Center, Department of Biology, 2080 Adelbert Road, Case Western Reserve University, Cleveland, OH 44106, USA.

Abstract

Human bone marrow has been shown to contain mesenchymal cells, which fabricate the connective tissue network of the marrow called the stroma. A subset of these marrow-derived mesenchymal cells can be isolated, expanded in culture, and then induced to differentiate into bone-producing osteoblasts and ultimately osteocytes when placed in the proper environment. At present, there are no methods for definitively identifying these cells in human marrow tissue or following their differentiation into osteogenic phenotypes. Therefore, we culture-expanded, marrow-derived mesenchymal cells from human donors and used these cells to immunize mice whose spleens were used to generate hybridoma cell lines, which secrete antibodies to antigens on the cell surface of these culture-expanded mesenchymal cells. Hybridoma culture supernatants were successively screened against highly enriched samples of culture-expanded, marrow-derived mesenchymal cells in cryosections and live cell cultures to identify unique cell surface antigens. Positive clones were then screened against cell suspensions of whole and fractionated marrow to identify hybridomas whose supernatants were nonreactive with marrow hemopoietic cells. Three hybridoma cell lines, SH2, SH3, and SH4, were identified; these hybridomas secrete antibodies that recognize antigens on the cell surface of marrow-derived mesenchymal cells, but fail to react with marrow-derived hemopoietic cells. Additional tissue screening reveals unique tissue distributions for each of the recognized antigens, which suggests different antigen recognition for each antibody. However, all three antibodies fail to react with the cell surface of osteoblasts or osteocytes, suggesting that the antigens recognized by these antibodies are developmentally regulated and specific for primitive or early-stage cells of the osteogenic lineage.

Key Words: Monoclonal antibodies—Human bone marrow—Mesenchymal cells—Cell surface antigens.

Introduction

Several studies with a variety of animals have shown that bone marrow contains mesenchymal cells, which can differentiate into cartilage and bone (Petrakova et al. 1963; Ashton et al. 1980, 1984, 1988; Bab et al. 1984a, 1984b, 1986; Oghushi et al. 1989a, 1989b; Beresford 1989, for review). Similar results have recently been reported with fresh cell suspensions derived from human marrow (Bab et al. 1988). Marrow-derived mesenchymal cells are also thought to differentiate into a connective tissue network within the marrow called the stroma (Zipori 1985); the cells of the stroma interact directly with hemopoietic stem cells and influence their differentiation (Dexter & Shadduck 1980; Lanoette et al. 1982; Sachs 1987).

Although mesenchymal cells are present at very low frequency in whole marrow (Bab et al. 1986), they can be grown in culture and their numbers expanded many fold (Ashton et al. 1984). We have recently developed methods to culture-expand mesenchymal cells from human marrow (Haynesworth et al. 1992). In culture these cells exhibit a uniform fibroblastic morphology. No adipocytic, round, cuboidal, or multinucleated cells are observed. Therefore, the culture conditions used in our previous study select for a small, highly enriched subset of mesenchymal cells from the very heterogeneous stromal cell population. After expansion and passage of the mesenchymal cells, their osteogenic potential was tested by loading them into porous calcium phosphate ceramic cubes and implanting the composite grafts into subcutaneous sites in athymic mice. Bone formed in the pores of ceramic cubes loaded with culture-expanded mesenchymal cells, but not in empty ceramic cubes. Furthermore, a monoclonal antibody specific for human tissue clearly identifies the bone-forming cells and osteocytes embedded in new bone in the pores of the ceramic cubes as being derived from the human cells and not from the athymic rodent host (Haynesworth et al. 1992).

Although these mesenchymal cells uniformly take on a fibroblastic morphology in culture (Ashton et al. 1984; Haynesworth et al. 1992), no characteristic markers, such as unique cell surface antigens, enzymatic activity, extracellular matrix molecules, or cellular structures, have been reported for these cells thus far. Markers for mesenchymal cell identification would be helpful to understand better the role that these cells play as components of marrow tissue. For example, specific cell surface markers would allow mapping of the position of mesenchymal cells in different regions of bone marrow and in marrow from different anatomical sites for better understanding of the potential stromal-hemopoietic cell interaction.

Markers for identifying mesenchymal cells would also be valuable in deciphering the role these cells play in osteogenesis. Recent data indicate that osteogenic cells pass through distinct lineage steps on the way to becoming osteoblasts and ultimately osteocytes (Pechak et al. 1986a; Caplan & Pechak 1987; Bruder & Caplan 1989a, 1989b, 1990a, 1990b, 1990c). Of particular

importance, Bruder and Caplan (1989b, 1990a, 1990b, 1990c) have identified developmentally regulated, stage-specific, cell surface antigens on several isoform variants of osteoblasts and osteocytes during chick tibia development. However, no stage-specific cell surface antigens on osteoprogenitor cells were identified or reported in the studies by Bruder and Caplan, nor have they been reported to our knowledge in any other study.

In this study, we report the presence of three developmentally regulated antigens on the surface of human marrow-derived mesenchymal cells. Given that we have previously shown that these cells are capable of forming bone (Haynesworth et al. 1992), we investigated the presence of these antigens in mesenchymal and nonmesenchymal tissues. Our results support the future use of these markers for studying not only the structural and functional roles of mesenchymal cells in marrow tissue, but the developmental position and control of these cells within the osteogenic lineage.

Materials and Methods

Source and preparation of human marrow mesenchymal cell cultures

Marrow from femoral head cancellous bone was obtained from patients with degenerative joint disease during total hip transplantation and from iliac crest by aspiration of normal donors or oncology patients having marrow harvested for future bone marrow transplantation, as described previously (Haynesworth et al. 1991). Preparation of marrow samples for isolation and culture-expansion of mesenchymal cells was essentially the same as detailed previously (Haynesworth et al. 1992). Briefly, plugs of femoral head cancellous bone marrow (0.5–5 ml) were transferred to sterile tubes to which were added 25 ml of BGJ_b medium (GIBCO, Grand Island, NY) with 10% fetal bovine serum from selected lots (complete medium). The tubes were vortexed to disperse the marrow and then centrifuged at 1000 × rpm for 5 min to pellet cells and bone pieces. The supernatant and overlying fat layer were removed, and the marrow and bone were reconstituted in 5 ml of complete medium and vortexed to suspend the marrow cells. Suspended cells were collected and separated into a single cell suspension by sequentially passing cells through syringes fitted with 18 and 20 gauge needles. Cells were then counted with a hemocytometer, red blood cells having been lysed with 4% acetic acid prior to counting, and plated into 100-mm dishes at 5–10 × 10^7 nucleated cells per dish.

Marrow aspirates (5–10 ml) were transferred to sterile tubes to which 20 ml of complete medium were added. The tubes were centrifuged at 100 × g for 5 min to pellet the cells, the supernatant and fat layer were removed, and the cell pellets (2.5–5.0 ml) were resuspended and fractionated on gradients of 70% Percoll (Sigma, St. Louis, MO). After these gradients were centrifuged at 460 × g for 15 min, the top 25% of the gradient (low density cells), pooled density = 1.03 g/ml, was collected, rinsed with three volumes of complete medium, and plated in 100-mm culture dishes at 5–10 × 10^7 nucleated cells per dish.

Culture and passage of marrow-derived mesenchymal cells

Marrow-derived mesenchymal cells from femoral head cancellous bone or iliac aspirate were cultured in complete medium at 37° C in a humidified atmosphere containing 95% air and 5% CO_2, with medium changes every 3–4 days. When culture dishes became near confluent, the cells were detached with 0.25% trypsin containing 1 mM EDTA (GIBCO) for 5 min at 37° C. The action of trypsin was stopped by adding ½ volume of fetal bovine serum. The cells were counted, split 1:3, and replated in 7 ml of complete medium. Aliquots of cells were cryopreserved in 90% fetal bovine serum with 10% dimethyl sulfoxide (freezing medium).

Harvest and preparation of culture-expanded cells for immunization

When passaged cells reached confluence, the culture medium was discarded from the plates and the plates were rinsed twice with Moscona's balanced salt solution (GIBCO) and incubated for 1 h at 37° C in 5 ml of 0.5 mM EGTA in Moscona's. This method of detaching the cells from the plates was chosen to minimize cleavage of cell surface proteins, which may occur when cells are treated with proteases like trypsin. Plates were swirled gently to detach cells that had rounded up and were lightly adherent to the plastic. Cells were collected with a pipet and centrifuged at 1000 rpm for 5 min. Cells were rinsed twice with 5 ml of Tyrodes balanced salt solution (GIBCO), suspended at 1–2 × 10^6 cells in 1 ml of Tyrodes, and taken up in 3-ml syringes fitted with 20-gauge needles.

A 14-week-old female CB6F/J mouse was immunized with cultured human marrow-derived mesenchymal cells by peritoneal injection. The initial injection was followed by four booster injections spaced one week apart. Each injection consisted of culture-expanded mesenchymal cells from a *different* donor to enhance the immune response to antigens common to each donor, relative to the immune response to donor-specific antigens.

On day 0, the initial injection consisted of cells derived from a femoral head marrow plug from donor H-20 (born 4-09-37). Cells from primary cultures were grown to confluence and replated 1:3. These first-passaged cells were also grown to confluence prior to harvest for immunization. Approximately 2 × 10^6 cells were used. On day 7, the first booster injection consisted of mesenchymal cells derived from femoral head plugs of marrow from donor H-21 (born 1-01-38) and H-23 (born 2-23-09), and collected at subconfluence of primary cultures. Approximately equal numbers from each donor were used with the total cell count equaling 1.5 × 10^6. On day 15, the second booster injection consisted of mesenchymal cells derived from a femoral head plug from donor H-27 (born 12-12-25). The cells were harvested at confluence of primary culture, with the total cell count equaling 1 × 10^6. On day 22, the third booster injection consisted of cells derived from a femoral head plug from donor H-31 (born 1929). Cells were harvested at confluence after the first passage, with the total cell count equaling 1 × 10^6. On day 29, the fourth booster injection consisted of cells derived from a femoral head plug from donor H-31. These cells had been harvested at confluence after the first passage and cryopreserved in freezing medium in liquid nitrogen. Immediately prior to injection, cells were thawed, rinsed with Tyrodes, and injected with the total cell count equaling 2 × 10^6. At day 25, blood was drawn from the tail vein of the mouse and serum was prepared, serially diluted, and then incubated on cryosections of pelleted culture-expanded mesenchymal cells to assay for immunoreactivity by indirect immunofluorescence as described below. Immunoreactivity to the sectioned cells was observed with serum that was serially diluted to 1:10,000, indicating that the immunization regimen had been successful in generating an immune response in the mouse to the cultured cells. Non-immune serum showed no immunoreactivity when incubated with similar cells and assayed by indirect immunofluorescence.

Fusion and hybridoma selection

The cell fusion, hybridoma selection, and cloning procedure were similar to those described by Bruder and Caplan (1989b). A

fusion was performed with 3.0×10^7 splenocytes and 1.0×10^7 SP 2/O-Ag-14 nonsecretor myeloma cells in the presence of 50% polyethylene glycol 1500 (Boehringer Mannheim Biochemicals, Indianapolis, IN). The fused cells were transferred into 96-well plates, which had been seeded with a feeder layer of 1×10^4 peritoneal macrophages per well and maintained in Dulbecco's modified Eagle's medium (GIBCO) containing 20% fetal bovine serum, 10% NCTC-109 (M.A. Bioproducts, Walkersville, MD), 1% Gentamicin sulfate (M.A. Bioproducts), and 1% L-glutamine. Cells were grown and selected in HAT medium at 37° C in 95% air, 5% CO_2, for two weeks with medium changes every third day. Hybridoma supernatants were first screened (see below) for the presence of mouse immunoglobulin, and then positive clones were tested for reactivity to the surface of culture-expanded, human marrow-derived, mesenchymal cells. Those hybridomas that tested positive in both screens were transferred to medium lacking aminopterin, cloned several times by limiting dilution, grown to substantial numbers, and then frozen in freezing medium in liquid nitrogen.

Initial hybridoma screening

Microtiter wells containing hybridoma colonies were screened for the presence of mouse immunoglobulin on ELISA plates coated with goat-antimouse IgG (Organon Teknika, Malvern, PA). Hybridoma culture supernatants were tested by adding 50 µl aliquots to wells on the ELISA plates and allowing the supernatants to incubate in a humidified chamber for 1 h at room temperature. Plates were rinsed four times with Tris-buffered saline containing 0.1% BSA (0.1% BSA-TBS). Alkaline phosphatase-conjugated goat antibody with specificity for mouse IgG, IgM, and IgA (Organon Teknika) was diluted 1:100–1:250 in 0.1% BSA-TBS, and 50 µl were added to each well and allowed to incubate for 1 h at room temperature in a humidified chamber. Plates were rinsed four times with BSA-TBS, and 50 µl of 0.09% p-nitrophenol phosphate substrate (Sigma) in 50 mM glycine, 1 mM $MgCl_2$, pH 10.5 were added to each well and allowed to incubate at 37° C for 1 h. A yellow color in the wells was interpreted as positive antibody reactivity. Positive and negative controls consisted of identical analysis of immunized mouse serum and culture medium, respectively.

Immunocytochemistry of tissue sections of culture-expanded human marrow-derived mesenchymal cells

Confluent human marrow-derived mesenchymal cells in 100-mm dishes were detached with trypsin-EDTA essentially as described above. The cells were pelleted by centrifugation at 1000 rpm, and the supernatants were discarded. The pelleted cells were rinsed two times with phosphate-buffered saline (PBS). After the second rinse the supernatant was removed and the unfixed cell pellet was dispersed into a small cup containing OCT Tissue Tek Compound (Miles Inc., Elkhart, IN), and frozen in liquid nitrogen.

The blocks of tissue were sectioned at 6 µm and placed on gelatin-coated slides. The cell sections were covered with 50–100 µl of hybridoma culture supernatant and incubated at room temperature for 1 h in a humidified chamber. The slides were rinsed four times with 0.1% BSA-PBS. The sections were then covered with 50 µl of fluorescein isothiocyanate (FITC)-conjugated goat-antimouse IgG (Organon Teknika), which had been diluted 1:100 in 0.1% BSA-PBS, and were incubated for 1 h at room temperature in a humidified chamber. The slides were rinsed four times with 0.1% BSA-PBS and coverslipped with a drop of PPD immunofluorescence mounting medium (Johnson et al. 1982) (Eastman Kodak, Rochester, NY), and observed on an Olympus BH-2 epi-fluorescence microscope. Negative control slides consisted of identical analysis of cells with culture medium that did not contain antibody. Separate controls were performed with the monoclonal antibody SB-1 as primary antibody. This antibody is a mouse-derived IgG antibody with specificity for chicken alkaline phosphatase, which does not cross-react with human tissue (Bruder & Caplan 1990). Isotyping of selected antibodies was performed with a mouse monoclonal antibody isotyping kit (Amersham International plc, Amersham UK).

Immunocytochemistry to culture-expanded cells in micromass

Cells from confluent marrow-derived mesenchymal cell cultures were released with trypsin-EDTA as described above. After stopping the activity of the trypsin with calf serum, the cells were pelleted by centrifugation and the supernatant was removed. Cells were rinsed once with 5–10 ml complete medium and then were suspended in complete medium at a concentration of 5×10^5 cells per ml. One 50-µl aliquot of cell suspension was transferred to the center of each 35-mm culture dish to produce a confluent cell density "spot" or "micromass" culture (Solursh et al. 1978). The micromass cultures were incubated overnight at 37° C and then rinsed three times with PBS. To each culture, 100-µl aliquots of hybridoma culture supernatant were added, and the cultures were incubated for 1 h at room temperature in a humidified chamber. Dishes were rinsed with 0.1% BSA-PBS, and then incubated for 1 h with FITC-conjugated goat antibody specific for mouse IgG. Dishes were rinsed with 0.1% BSA-PBS, and coverslipped after applying a drop of PPD immunofluorescence mounting medium. Immunofluorescent staining was observed on an Olympus BH-2 epi-fluorescence microscope.

Immunocytochemistry to cell suspensions of whole marrow and Percoll-fractionated marrow

Samples of whole marrow cell suspensions and Percoll-fractionated marrow cell suspensions were prepared as described above for cell culturing. Cell suspensions of whole marrow and the mesenchymal cell-rich fraction from Percoll-fractionated marrow were incubated with hybridoma culture supernatant for 1 h at 4° C. Cells were rinsed with PBS, pelleted by centrifugation at 1000 rpm, reconstituted with FITC-conjugated goat anti-mouse IgG, and incubated for 1 h at 4° C. Cells were again rinsed with PBS, pelleted by centrifugation, and then reconstituted in 50–100 µl of PPD immunofluorescence mounting medium and transferred to microscope slides. Immunofluorescent staining was observed on an Olympus BH-2 epi-fluorescence microscope.

Immunohistochemistry to human and non-human mesenchymal and non-mesenchymal tissues

The following tissues were obtained as surgical or autopsy specimens from human patients: breast skin, foreskin, small intestine, heart, skeletal muscle, lung, liver, brain, tendon, ligament, gall bladder, articular cartilage, femur, rib cartilage, and rib periosteum. Mesenchymal cells from human rib periosteum were culture-expanded as described by Nakahara et al. (1991). The following animal tissues were also obtained for screening: chicken bone and marrow, rabbit bone and marrow, rat bone, and dog iliac bone and marrow. Mesenchymal cells from dog cancellous bone and marrow were harvested and culture-expanded by the identical methods described above for human

cancellous bone and marrow. Bone samples were demineralized in RDO Rapid Bone Decalcifier (Dupage Kinetics Laboratories Inc. Plainfield, IL). The unfixed tissues were each embedded in OCT-Tissue Tek Freezing Medium, sectioned at 6 μm, and placed on gelatin-coated slides. Tissue sections were screened against hybridoma culture supernatants from cloned hybridomas by the same procedure described above for screening culture-expanded, human marrow-derived, mesenchymal cells in frozen sections. Some cryosections of demineralized bone, a whole marrow cell suspension, and a low-density Percoll gradient cell suspension were further treated with collagenase, trypsin, testicular hyaluronidase, chloroform-methanol, or sodium periodate in an attempt to expose masked epitopes. These agents did not uncover any additional antigenic sites.

Flow cytometric analyses

Culture-expanded cells were released from culture dishes with trypsin and incubated with the monoclonal antibodies SH2, SH3, and SH4, or control antibody (SB-1) for 1 h at 4° C. Cells were rinsed with Tyrodes and then incubated for 1 h at 4° C with goat anti-mouse IgG conjugated to FITC. After rinsing away unbound antibodies, the cells were adjusted to a concentration of 1×10^6 cells per ml, and the number of fluorescently labeled cells was quantified with a Flow Fluoragraph IIS (Becton Dickinson, MA).

Results

Hybridoma clone analysis

After splenocytes were fused with mouse myeloma cells, the resulting hybridoma cells were plated into ten 96-well plates and incubated until cell colonies were visible by macroscopic observation (2–3 weeks). Of the 960 wells plated with cells, 764 wells showed growth of at least one hybridoma colony. Screening of the supernatants from the 764 wells by ELISA to identify immunoglobulin revealed that 245 wells contained immunoglobulin. These were further screened with a two-step indirect immunofluorescence assay with culture-expanded, human marrow-derived, mesenchymal cells. First, supernatants were screened against cryosections of pelleted culture-expanded cells; 171 of the 245 supernatants showed positive reactivity to the cells in this assay. The patterns of reactivity varied, with some supernatants producing reactivity only to cell surface epitopes, others reacting to cell surface and intracellular epitopes, and still others reacting only to intracellular epitopes. It is important to note that staining patterns consisting of a substantial number of stained and unstained cells were not observed with any of the hybridoma culture supernatants. To confirm the identity of supernatants reacting to cell surface epitopes, the 171 supernatants were tested against living, culture-expanded cells in confluent micromass cultures. Since the cells in this assay are living, positive reactivity indicates monoclonal antibody binding to cell surface epitopes and not to intracellular epitopes, which are exposed in the cryosections discussed above. Supernatants from 15 of the 171 wells immunostained the cell surface of the living cells. Before further characterization, the hybridoma cells from the 15 positive wells were collected from their original wells and cloned by limiting dilution.

The monoclonal antibodies from the 15 cloned hybridoma cell lines were then screened against cell suspensions of whole marrow and low-density Percoll gradient fractions of marrow (mesenchymal stem cell-rich fraction) to identify those that selectively bind to cell surface epitopes on marrow-derived mesenchymal cells and not to marrow-derived hemopoietic cells. Of the 15 hybridoma cell lines, three showed essentially no reactivity to cell surface epitopes on the marrow-derived hemopoietic cells in the cell suspension assay. These three cell lines were named SH2, SH3, and SH4. Isotype analyses showed antibodies SH2 and SH4 to be of the IgG-1 isotype and antibody SH3 of the IgG-2b isotype. The reactivity of each of the three monoclonal antibodies in the screening assays described above is illustrated in **Figs. 1–3.** Figure 1 illustrates the immunoreactivity of the three antibodies to cryosections of culture-expanded mesenchymal cells. In each case the antibodies react with the outer rim or cell surface of most cells, although intracellular fluorescent staining is present in some cells with each of the antibodies. The intensity of fluorescence varies among the three antibodies, with SH4 yielding the highest fluorescent staining, followed by SH3 and finally SH2. These differences may indicate differences in the number of binding antigens for each antibody. Alternatively, the differences in intensity could arise from varying levels of antigen accessibility due to blocking of the cell surface antigens from binding to the antibodies by other molecules. Likewise, the intensity of fluorescence is different for each antibody in indirect immunofluorescent analysis of the culture-expanded cells in living micromass cultures (Fig. 2). Reactivity to the cell surface is clearly evident for each antibody; again, the staining intensity is greatest for SH4, then SH3, and least for SH2. With all three antibodies the culture-expanded cells in cryosections and micromass are not uniformly stained. Instead, some cells appear to be stained more than others. Although the reasons for this are not clear at present, the observations are interesting and may be important. Also, with all three antibodies, no staining is observed outside of the cell surface, which might suggest that the surface reactivity may be due to extracellular matrix components in close contact with the cell.

In contrast to the positive staining of the three antibodies to the cell surface of the culture-expanded mesenchymals cells, practically no cells are reactive when the antibodies are assayed against cell suspensions derived from whole marrow (Figs. 3A and B) or the low-density fraction of marrow cells generated by Percoll gradient fractionation (Figs. 3C and D). In both of these preparations the vast majority of cells are of the hemopoietic lineage and do not react with the antibodies. Positively stained cells are observed at very low frequency in both samples, and may indicate the presence of a few mesenchymal cells; however, the exact identity of the positively staining cells has not been definitely shown, since similar positively stained cells are infrequently seen in samples incubated with FITC-labeled second antibody in the absence of primary antibody.

In order to determine the percentage of culture-expanded, mesenchymal cells that express antigens recognized by the SH2, SH3, and SH4 monoclonal antibodies, the number of immunoreactive cells was quantified by flow cytometry. All three antibodies generated increased fluorescence on 95–98% of the culture-expanded cells relative to the level of fluorescence on cells after incubation with control antibody.

Reactivity of SH2, SH3, and SH4 to mesenchymal cells in intact marrow tissue

The three monoclonal antibodies were tested on cryosections of marrow tissue harvested from femoral head cancellous bone. With each antibody, immunofluorescent staining is observed on some fibroblastic cells within the connective tissue matrix of the marrow stroma (**Fig. 4**). For cells in the plane of focus, staining

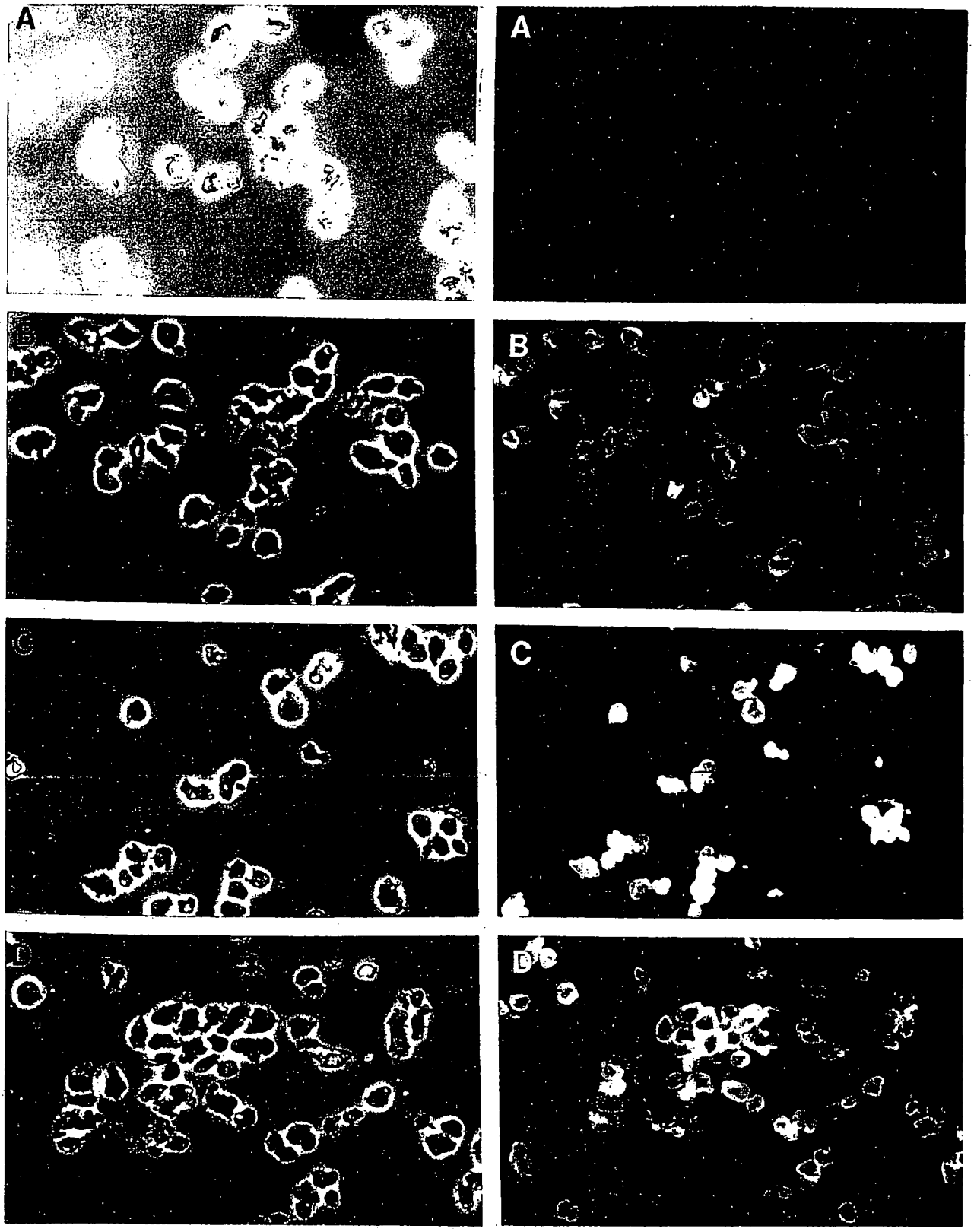

Fig. 1. Cryosections of culture-expanded, human marrow-derived mesenchymal cells after trypsin-mediated release from culture plates. Sections were incubated with negative control antibody (A) or with antibodies SH2 (B), SH3 (C), or SH4 (D), then FITC-goat antimouse immunoglobulin. The sections were then viewed with phase contrast (left) or immunofluorescent (right) optics. Note that each of the monoclonal antibodies stains the periphery of the sectioned cells, which indicates predominantly cell surface reactivity (×320).

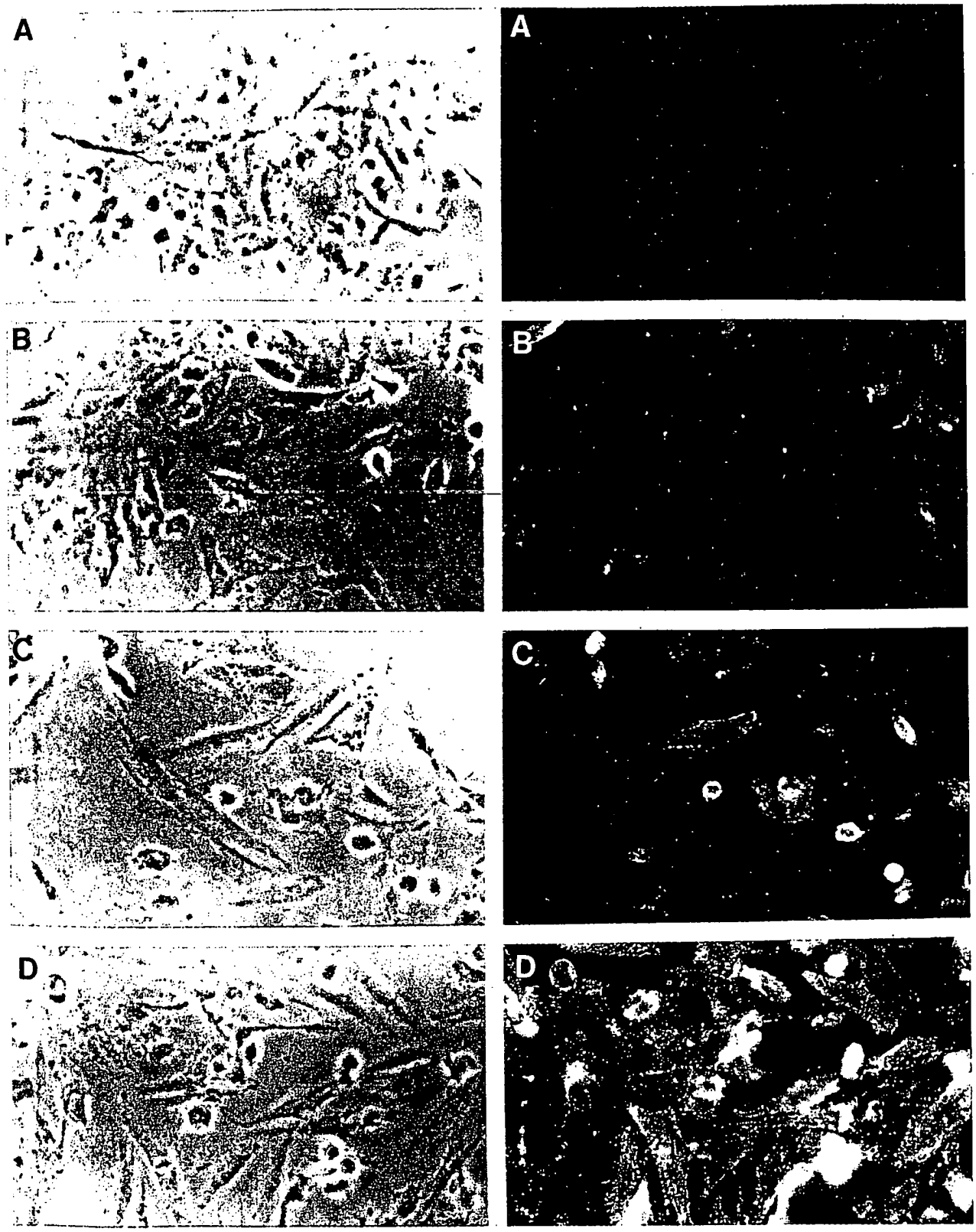

Fig. 2. Expressions of SH2, SH3, and SH4 antigens on live culture-expanded, human marrow-derived, mesenchymal cells. Micromass cultures of human marrow-derived mesenchymal cells were incubated with negative control antibody (A) or antibodies SH2 (B), SH3 (C), or SH4 (D), followed by FITC-goat antimouse immunoglobulin, and then viewed with phase contrast (left) or immunofluorescent (right) optics. Note that the live culture-expanded, human marrow-derived, mesenchymal cells express antigens on their surface recognized by each of these monoclonal antibodies (×184).

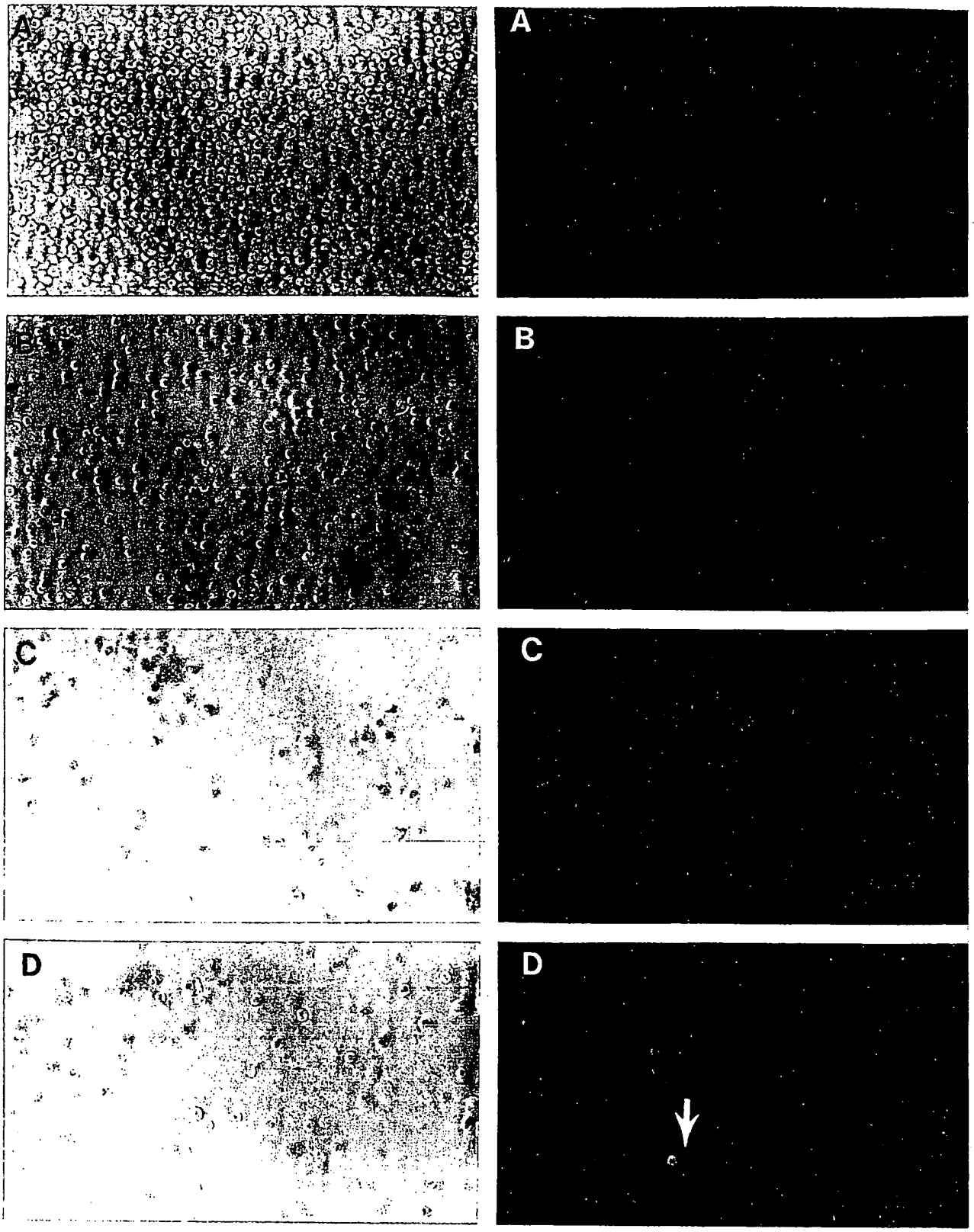

Fig. 3. Cell suspensions of whole marrow were incubated with control antibody (A) or monoclonal antibody SH4 (B), followed by FITC-goat antimouse immunoglobulin, and then viewed under phase (left) or immunofluorescent (right) optics. Almost all the cells are unreactive to the control and SH4 antibodies. A very small percentage of the cells show reactivity to both antibodies, although the frequency of positive reactivity is identical and likely indicates nonspecific binding. Similar binding is observed when whole marrow is treated with monoclonal antibodies SH2 or SH3. Cell suspensions of Percoll-fractionated marrow likewise were incubated with control antibody (C) or SH4 (D), followed by FITC-goat antimouse immunoglobulin, and then viewed under phase (left) or immunofluorescent (right) optics. Almost all the cells are unreactive in the sample treated with control antibody, as well as in the SH4-treated sample. A low percentage of reactive cells (white arrow) above that observed in the control sample are observed in the SH4-treated sample. Binding levels similar to that observed for SH4 are observed when monoclonal antibodies SH2 and SH3 are used (×299).

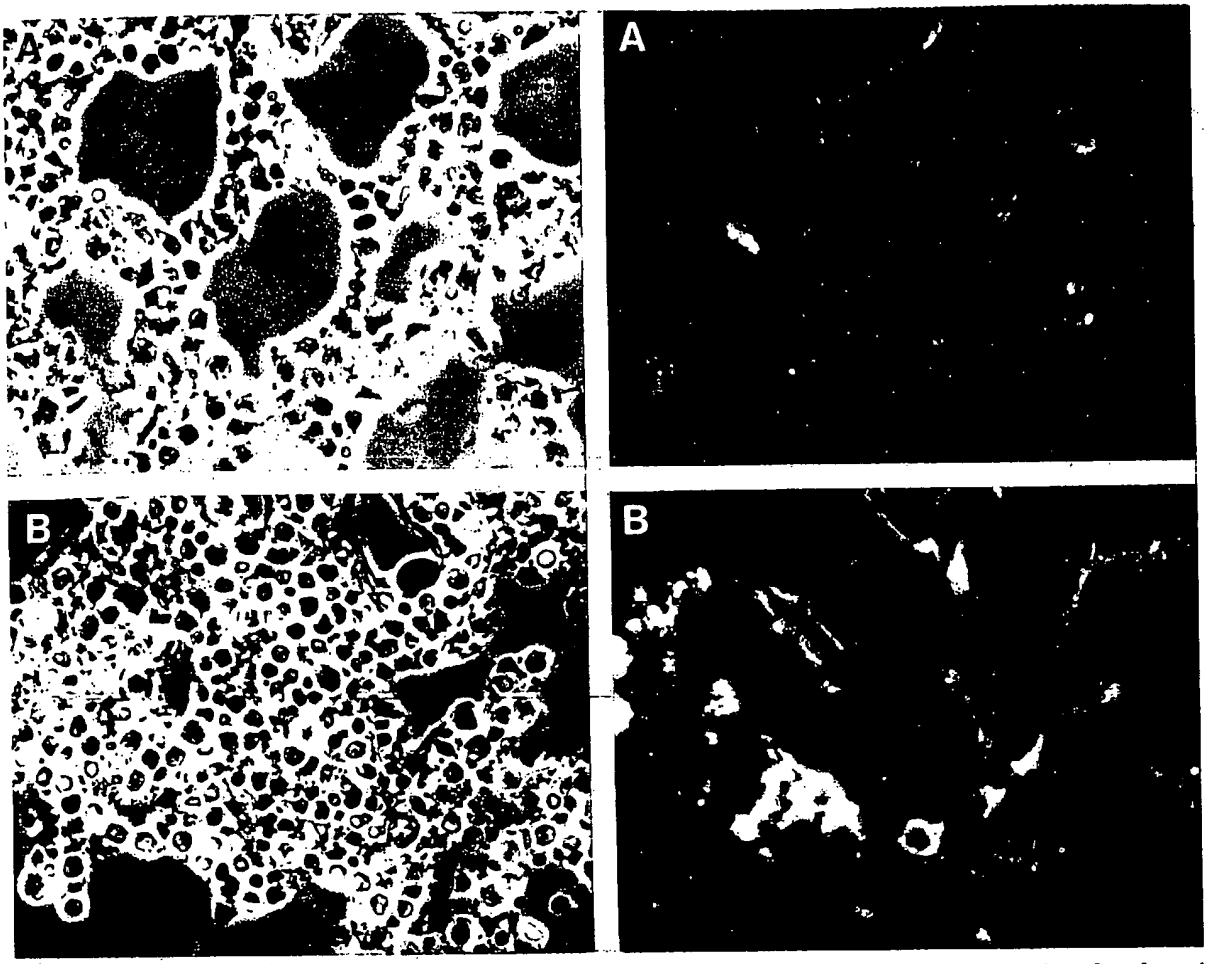

Fig. 4. Expression of the SH2 antigen on mesenchymal cells in intact human marrow tissue. Cryosections of human marrow tissue from femoral head cancellous bone were incubated with negative control antibody (A) or the SH2 antibody (B), followed by FITC-goat antimouse immunoglobulin, and then viewed with phase contrast (left) or immunofluorescent (right) optics. Note that the round clustered hemopoietic cells are not stained by the SH2 antibody, whereas some cells within the connective tissue stroma are stained. Some nonimmunoreactive autofluorescence of the tissue is observed in the negative control. The difference between the autofluorescence and specific immunostaining is clearly apparent during actual observations, but is difficult to capture on black and white film. SH3 and SH4 generated staining patterns similar to SH2 on cryosections of marrow tissue; however, it was not determined if the staining patterns were identical because of the technical difficulties of generating consecutive cryosections of the intact marrow tissue (×187).

is seen outlining the surface. For cells outside the plane of focus, the cell surface staining is not as easily observed in the photomicrographs, but is apparent under direct observations by manipulating the focus. For each antibody, only a subset of the stromal connective tissue cells are stained, indicating that the antibodies do not recognize all marrow stromal cell types. Staining is not observed on the round clustered hemopoietic cells.

Tissue specificity of SH2, SH3, and SH4 among mesenchymally-derived tissues

The three antibodies were tested on unfixed cryosections of a variety of mesenchymal tissues to characterize their selectivity for cell surface epitopes on marrow-derived mesenchymal cells in relation to other mesenchymal-derived tissues (**Table I**). All three antibodies fail to stain skeletal muscle cells, osteoblasts, osteocytes, and the extracellular matrix of femoral and rib bone. SH2 also does not react with chondrocytes from articular cartilage and rib cartilage, whereas SH3 and SH4 stain the cell sur-

Table I. Mesenchymal tissue distribution of antigens

	Monoclonal antibodies		
C. Mesenchymal-derived tissues	SH2	SH3	SH4
1. Femoral head (bone) (HCl)	−	−	−
2. Rib bone and marrow (RDO)	±	−	−
3. Rib cartilage	−	+	+
4. Skeletal muscle	−	−	−
5. Rib periosteum	+	+	+
6. Cultured periosteal cells (micromass)	−	+	+
7. Ligament	M	M	−
8. Tendon	−	−	M
9. Articular cartilage	−	+	+
10. Femoral shaft (RDO, HCL)	−	−	−
11. Skin (dermis)	±	±	±

+ = positive reactivity to the surface of the majority of the cells of the tissue. ± = positive reactivity to a small subset of cells in the tissue. M = reactivity to extracellular matrix components.

face of chondrocytes in both articular and rib cartilage (Fig. 5). All three antibodies stain the cell surface of a select group of cells in rib periosteal tissue. Stained cells are most frequent along the innermost layer of periosteum directly adjacent to the bone (Fig. 6.) The frequency of stained cells diminishes with increasing distance from the inner surface. SH3 and SH4, but not SH2, also stain culture-expanded cells derived from rib periosteum. In addition, all three monoclonal antibodies stain fibroblastic cells scattered throughout dermis, although the intensity and the amount of binding vary with each antibody.

Cross-reactivity with non-mesenchymal tissues

SH2, SH3, and SH4 were screened by indirect immunofluorescence on frozen sections of the following non-mesenchymal tissues: small intestine, heart, lung, liver, brain, gall bladder, and epidermis (**Table II**). All three monoclonal antibodies are nonreactive with brain and epidermis. SH2 is also negative with gall bladder, but reacts with extracellular matrix components of intestine, heart, lung, and liver. SH3 is negative with all the tissues except liver, where some extracellular matrix reactivity is observed. SH4 is nonreactive with all of the tissues except gall bladder, which shows positive reactivity in the tissue matrix.

Cross-reactivity with other species

SH2, SH3, and SH4 were tested for reactivity on unfixed cryosections of a variety of tissues and cells from rat, rabbit, dog, and chicken to determine the level of species cross-reactivity. SH2 and SH3 are nonreactive with frozen sections of culture-expanded dog marrow mesenchymal cells, day 7 chick hatchling tibia, day 12 chick embryonic heart, day 12 chick embryonic tibia, rabbit skin, rabbit femur, and rat femur. SH4 reacts with the cell surfaces of a subset of culture-expanded, dog marrow-derived, mesenchymal cells, but is not reactive with the other animal tissues listed above.

Discussion

Human marrow contains mesenchymal cells with the potential to differentiate into bone. These cells are present in marrow in very

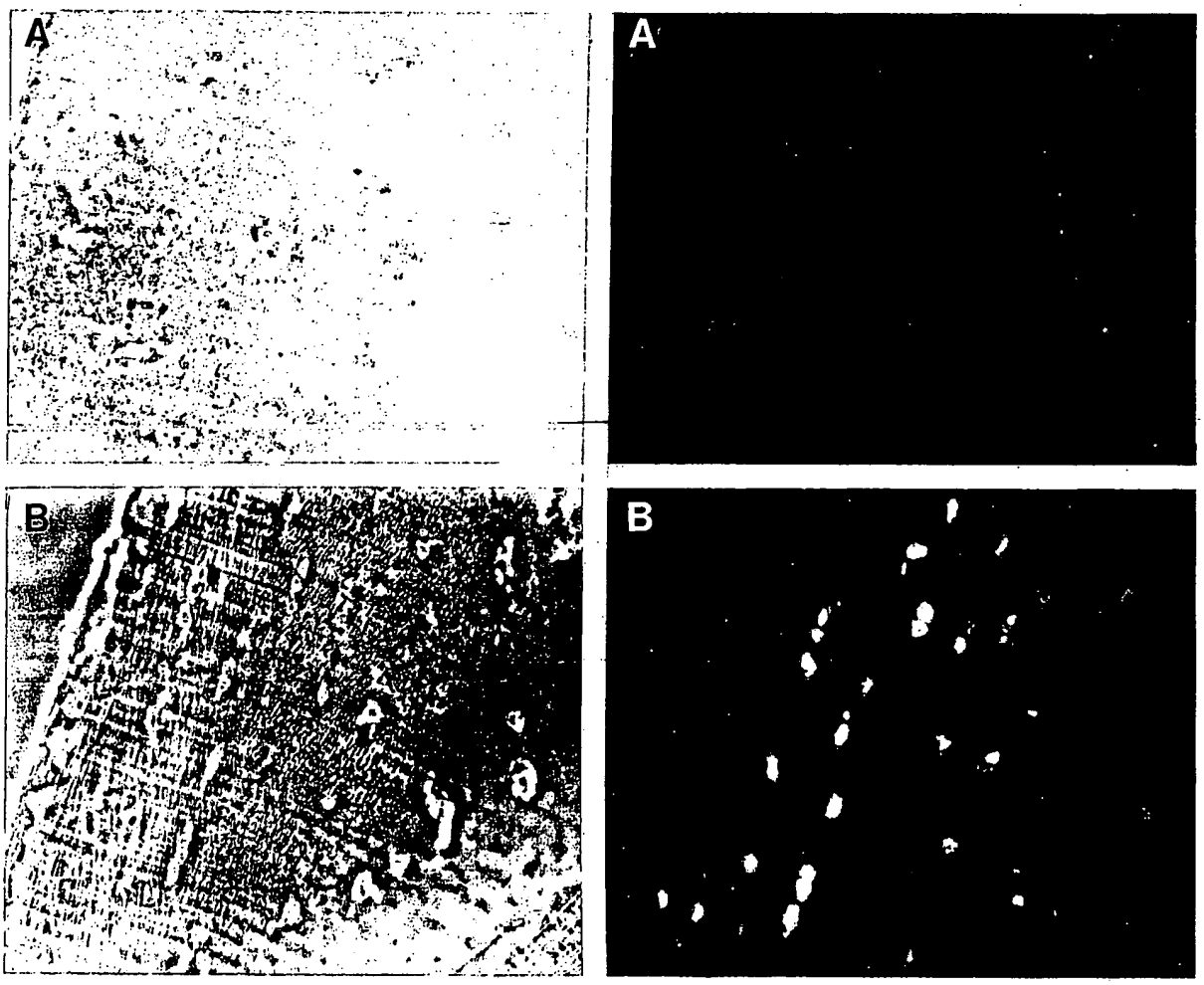

Fig. 5. Expression of the SH3 but not the SH2 antigen on chondrocytes in human articular cartilage. Cryosections of human articular cartilage were incubated with SH2 (A) or SH3 (B), followed by FITC-goat antimouse immunoglobulin, and then viewed with phase contrast (left) or immunofluorescence (right) optics. Note that the SH2 antibody fails to stain either the chondrocytes or the extracellular matrix in which they are embedded. In contrast, SH3 stains the cell surface of the chondrocytes and is nonreactive to the tissue matrix (×179). The SH4 antibody generates a staining profile very similar to the SH3 antibody.

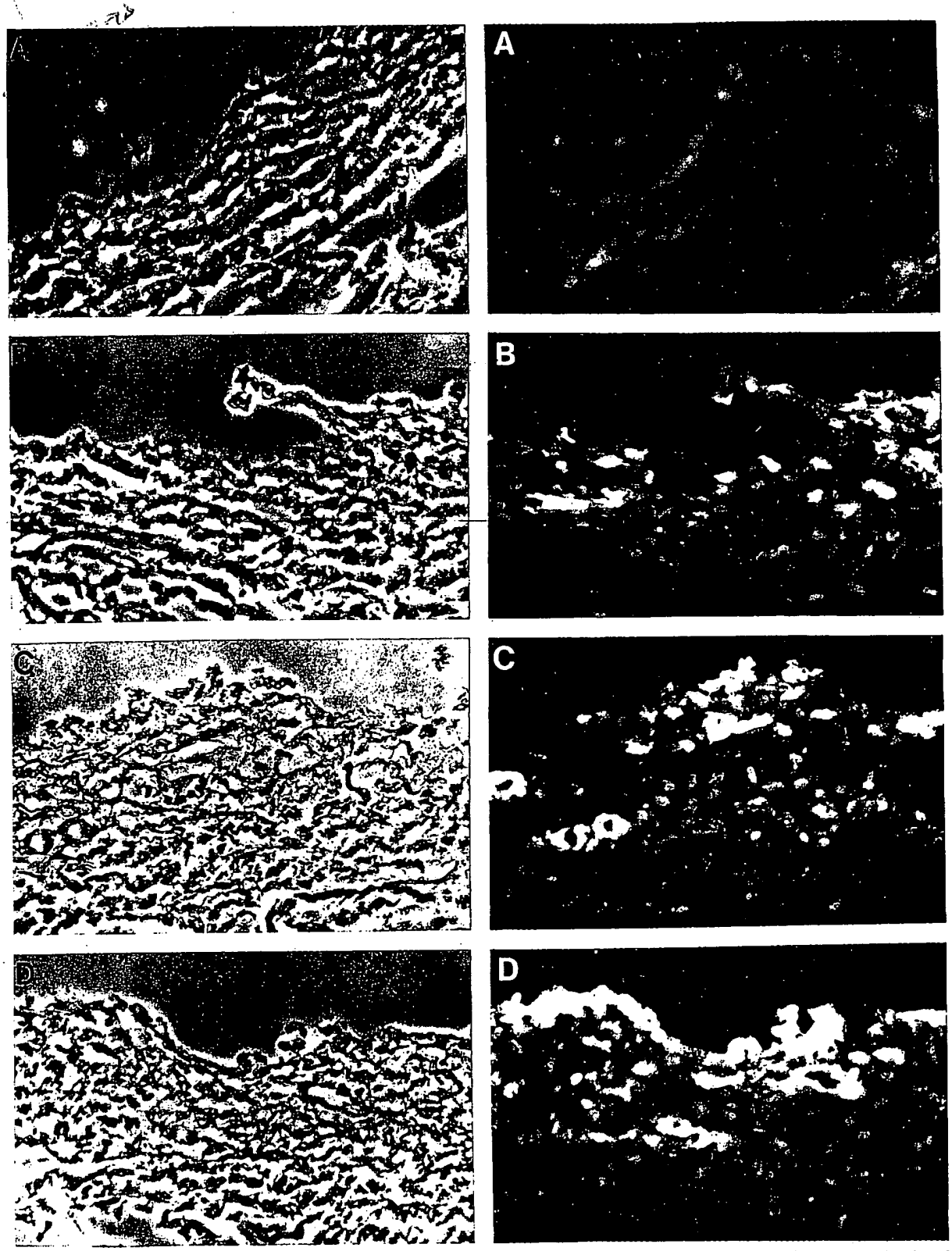

Fig. 6. Expression of SH2, SH3, and SH4 antigens in human periosteal tissue. Cryosections of human periosteum from rib bone were incubated with negative control antibody (A) or antibodies SH2 (B), SH3 (C), or SH4 (D), followed by FITC-goat antimouse immunoglobulin, and then viewed with phase contrast (left) or immunofluorescent (right) optics. The inner surface of periosteum, or side adjacent to the bone, is at the top. Note that each antibody stains a thin layer of cells along the inner surface of the periosteal tissue (×237).

Table II. Non-mesenchymal tissue distribution of antigens

D. Nonmesenchymal-derived tissues	Monoclonal antibodies		
	SH2	SH3	SH4
1. Intestine	M	–	–
2. Heart	M	–	–
3. Lung	M	–	–
4. Liver	M	M	–
5. Brain	–	–	–
6. Gall bladder	–	–	±
7. Breast skin (epidermis)	–	–	–

+ = positive reactivity to the surface of the majority of the cells of the tissue. ± = positive reactivity to a small subset of cells in the tissue. M = reactivity to extracellular matrix components.

low numbers; however, we have previously shown that they can be enriched and expanded in culture without the loss of their osteogenic capacity (Haynesworth et al. 1992). In this study, epitopes on the surface of these cells were detected by monoclonal antibodies. Immunostaining of intact marrow tissue confirms that these mesenchymal cells represent a small subset of the heterogeneous marrow stromal cell population. After culture-expanding this subset of mesenchymal cells from femoral head and iliac crest bone marrow, virtually all of the culture-expanded cells are stained by each of the monoclonal antibodies as measured by flow cytometry, suggesting that the culture system is selective for these mesenchymal cells with similar cell surface characteristics, in comparison to other stromal phenotypes and hemopoietic cells. These epitopes are, therefore, useful markers for distinguishing marrow mesenchymal cells from marrow hemopoietic cells, and for developing protocols that use the epitopes-specific monoclonal antibodies to quantify and purify marrow-derived mesenchymal cells from samples of whole marrow.

The three monoclonal antibodies likely react with different molecules, since they produce three distinct patterns of cross-reactivity with mesenchymal and non-mesenchymal tissues (Tables I and II). This cross-reactivity could arise from the presence of the same molecules on different cell types, different isoforms of the same molecules, or similar epitopes on different molecules. These considerations will be clarified as more information is gained through the identification and characterization of the cell surface antigens. However, it should be noted that identification and characterization of the cell surface antigens is not necessary in order to use these monoclonal antibodies as specific probes for mesenchymal cells in assays of marrow tissue and in studying the osteogenic lineage.

Some similarities in tissue specificity are observed among the three monoclonal antibodies. Of considerable interest is the cell surface cross-reactivity of antibodies SH2, SH3, and SH4 to human periosteal cells in intact tissue, and SH3 and SH4 to culture-expanded cells. These cells have been shown to have the capacity to differentiate into both cartilage and bone (Koshihara et al. 1989; Nakahara et al. 1990, 1991). The presence of these developmentally regulated antigens on periosteally-derived and marrow-derived mesenchymal cells suggests that the two groups of progenitor cells may possess similar structural characteristics, in addition to well documented similarities in developmental and lineage potentials. The antibody SH2, however, does not react with culture-expanded periosteal cells, which indicates that marrow-derived and periosteally-derived mesenchymal cells are likely similar but not identical. Also of interest is the cross-reactivity of all three monoclonal antibodies to a subset of human dermal fibroblast cells. The significance of this cross-reactivity cannot be determined by the data presented in this study, although the possibility exists that since marrow and dermal mesenchymal cells share common cell surface antigens, they may also share other structural properties and have similar developmental potentials.

All three monoclonal antibodies are nonreactive to osteoblasts and osteocytes from human bone. Since these cultured mesenchymal cells have clearly been shown to have the potential to differentiate into osteoblasts, these observations suggest that the antigens recognized by the monoclonal antibodies are lost as the marrow-derived mesenchymal cells differentiate and pass through the osteogenic lineage pathway. Because the antigens appear to be lost during osteogenesis, it may be possible to use them as markers for the very early stage progenitor cell (or stem cell), which matures by progressing through a series of transition steps on the way to developing into a secretory osteoblast and finally an osteocyte. Several of the transitional stages of osteoblast development have been identified by Bruder and Caplan (1989a, 1989b, 1990a, 1990b), who used monoclonal antibodies to study chick tibia development. A nonsecretory pre-osteoblast identified by the monoclonal antibody SB-1 (which is specific for alkaline phosphatase) differentiates into a transitory osteoblast and then a secretory osteoblast, which contains cell surface antigens recognized by monoclonal antibodies SB-1, SB-2, and SB-3. This cell can continue to develop into what is described as an osteocytic osteoblast, which has lost the SB-1 and SB-3 antigens, while acquiring a new antigen labeled by SB-5. Finally, an osteocyte with only SB-5 antigen is formed. However, no cell surface markers were identified for the primitive stem cells or progenitor cells that give rise to osteoblasts and osteocytes; moreover, no reports of specific cell surface markers for osteoprogenitor cells have ever been reported. Therefore, the monoclonal antibodies generated in this study may provide useful reagents for understanding the sequence of events in the early stages of osteogenic cell development.

With the availability of monoclonal antibodies to these antigens, assays can now be developed to quantify the number of mesenchymal cells in marrow and determine the variation in mesenchymal stem cell content in marrow from different sources of bone, and how the number of mesenchymal cells is affected by age. These data will help elucidate the relationship between mesenchymal cell number and the decreased level of bone formation that occurs with advanced age, often leading to osteoporosis. The monoclonal antibodies will also allow monitoring of the process of cell differentiation under various culture conditions and correlation of the abatement of antibody staining with the appearance of osteoblast-specific markers, such as alkaline phosphatase and osteocalcin. The information gained through the future use of these monoclonal antibodies will likely add to the understanding of osteogenic cell differentiation and osteogenic tissue homeostasis.

Acknowledgments: The authors wish to thank Dr. Scott P. Bruder for his valuable instructions and advice regarding hybridoma production, and for kindly supplying the monoclonal antibody SB-1, which was used in control experiments. We also thank Dr. Bruder and Dr. David A. Carrino for their constructive comments in reviewing drafts of the manuscript. We thank Dr. Victor M. Goldberg and Dr. Harry Figgie III (Department of Orthopaedics, University Hospital, Cleveland, Ohio) for samples of marrow plugs and Dr. Hillard Lazarus and Bob Fox (Department of Medicine, University Hospital, Cleveland, Ohio) for samples of aspirated marrow. We thank Dr. Thomas Pretlow and Dr. Rubin Ortiz (Department of Pathology, University Hospital, Cleveland, Ohio) for samples of a variety of human tissues. We also thank Dr. Haruhiko Nakahara for preparations of cultured human periosteum cells, and Dr. James

Fleming for technical assistance in the immunohistochemistry of periosteal tissue. We also thank Kerri Schimenti for expert technical operation of the flow cytometer. This research was supported in part by grant P30CA43703 from NIH, NCI, and USPHS, other grants from NIH, and grants from The Edison Biotechnology Program.

References

Ashton, B.; Allen, T.; Howlett, C.; Eaglesom, C.; Hattori, A.; Owen, M. Formation of bone and cartilage by marrow stromal cells in diffusion chambers *in vivo*. *Clin. Orthop.* **151**:294–307; 1980.

Ashton, B.; Eaglesom, C.; Bab, I.; Owen, M. Distribution of fibroblastic colony-forming cells in rabbit bone marrow and assay of their osteogenic potential by an *in vivo* diffusion chamber method. *Calcif. Tissue Int.* **36**:83–86; 1984.

Ashton, B.; Cave, F.; Williamson, M.; Sykes, B.; Couch, M.; Poser, J. Characterization of cells with high alkaline phosphatase activity derived from human bone and marrow: preliminary assessment of their osteogenicity. *Bone* **6**:313–319; 1985.

Ashurst, D.; Ashton, B.; Owen, M. Bone marrow stromal cells raised in diffusion chambers produce typical bone and cartilage matrices. *Calcif. Tiss. Int.* **42** [Suppl.]: 2; 1988.

Bab, I.; Ashton, B.; Syftestad, G.; Owen, M. Assessment of an *in vivo* diffusion chamber method as a quantitative assay for osteogenesis. *Calcif. Tissue Int.* **36**:77–82; 1984a.

Bab, I.; Howlett, C.; Ashton, B.; Owen, M. Ultrastructure of bone and cartilage formed *in vivo* in diffusion chambers. *Clin. Orthop.* **187**:243–254; 1984b.

Bab, I.; Ashton, B.; Gazit, D.; Marx, G.; Williamson, M.; Owen, M. Kinetics and differentiation of marrow stromal cells in diffusion chambers *in vivo*. *J. Cell Sci.* **84**:139–151; 1986.

Bab, I.; Passi-Even, L.; Gazit, D.; Sekeles, E.; Ashton, B.; Peylan-Ramu, N.; Ziv, I.; Ulmansky, M. Osteogenesis in *in vivo* diffusion chamber cultures of human marrow cells. *Bone and Mineral* **4**:373–386; 1988.

Beresford, J. Osteogenic stem cells and the stromal system of bone and marrow. *Clin. Orthop.* **240**:270–280; 1989.

Bruder, S.; Caplan, A. Discrete stages within the osteogenic lineage are revealed by alterations in the cell surface architecture of embryonic bone cells. Glimcher, M. J.; Lian, J. B., eds. *Third International Conference on the Chemistry and Biology of Mineralized Tissue*. New York: Gordon and Breach; 1989a: 65–71.

Bruder, S.; Caplan, A. First bone formation and the dissection of the osteogenic lineage in the embryonic chick tibia is revealed by monoclonal antibodies against osteoblasts. *Bone* **11**:359–375; 1989b.

Bruder, S.; Caplan, A. Terminal differentiation of osteogenic cells in the embryonic chick tibia is revealed by a monoclonal antibody against osteocytes. *Bone* **11**:189–198; 1990a.

Bruder, S.; Caplan, A. Osteogenic cell lineage analysis is facilatated by organ cultures of embryonic chick periosteum. *Develop. Biol.* **141**:319–329; 1990b.

Bruder, S.; Caplan, A. A monoclonal antibody against the surface of osteoblasts recognizes alkaline phoshatase in bone, liver, kidney, and intestine. *Bone* **11**:133–139; 1990c.

Caplan, A.; Pechak, D. The cellular and molecular embryology of bone formation. Peck, W. A., ed. *Bone and mineral research*. New York: Elsevier; 1987: Vol. 5, pp. 117–183.

Dexter, T.; Shadduck, R. The regulation of haemopoiesis in long-term bone marrow cultures: Role of L-cell CSF. *J. Cell. Phys.* **102**:279–286; 1980.

Haynesworth, S.; Goshima, J.; Goldberg, V.; Caplan, A. I. Characterization of cells with osteogenic potential from human marrow. *Bone* **12**:00–00; 1992.

Johnson, G.; Davidson, R.; McNamee, K.; Russell, G.; Goodwin, D.; Halborrow, E. Fading of immunofluorescence during microscopy: A study of the phenomenon and its remedy. *J. Immunol. Methods* **55**:231–242; 1982.

Koshihara, Y.; Kawamura, M.; Endo, S.; Tsutsumi, C.; Kodama, H.; Oda, H.; Higaki, S. Establishment of human osteoblastic cells derived from the periosteum in culture. *In vitro Cell. Devel. Biol.* **25**:37–43; 1989.

Lanoette, M.; Metcalf, D.; Dexter, T. Production of monocyte/macrophage colony-stimulating factor by preadipocyte cell lines derived from murine marrow stroma. *J. Cell. Phys.* **112**:123–127; 1982.

Nakahara, H.; Goldberg, V.; Caplan, A. Culture-expanded human periosteal-derived cells exhibit osteo-chondral potential *in vivo*. *J. Orthop. Res.* **9**:465–476; 1991.

Nakahara, H.; Bruder, S.; Haynesworth, S.; Holecek, J.; Baber, M.; Goldberg, V.; Caplan, A. Bone and cartilage formation in diffusion chambers by subcultured cells derived from the periosteum. *Bone* **11**:181–188; 1990.

Ohgushi, H.; Goldberg, V.; Caplan, A. Heterotopic osteogenesis in porous ceramics induced by marrow cells. *J. Orthop. Res.* **7**:568–578, 1989a.

Ohgushi, H.; Goldberg, V.; Caplan, A. Repair of bone defect with marrow cells and porous ceramic. *Acta Orthop. Scand.* **60**(3):334–339; 1989b.

Pechak, D.; Kujawa, M.; Caplan, A. Morphological and histochemical events during first bone formation in embryonic chick limbs. *Bone* **7**:441–458; 1986a.

Pechak, D.; Kujawa, M.; Caplan, A. Morphology of bone development and bone remodeling in embryonic chick limbs. *Bone* **7**:459–472; 1986b.

Petrakova, K.; Tolmacheva, A.; Friedenstein, A. Bone formation occurring in bone marrow transplantation in diffusion chambers. *Bull. Exp. Biol. Med.* (Russian) **56**(12):87–91; 1963.

Sachs, L. The molecular control of blood cell development. *Science* **238**:1374–1379; 1987.

Solursh, M.; Ahrens, P.; Reiter, R. A tissue culture analysis of the steps in limb chondrogenesis. *In Vitro* **14**:51–61; 1978.

Zipori, D. Stromal cell lines from the mouse bone marrow: a model system for the study of the hemopoietic microenvironment. Baum, S. J.; Pluznik, D. H.; Rozenzajn, L. A., eds. *Selected Papers from the 14th Annual Meeting of the International Society for Experimental Hematology*. New York: Springer-Verlag; 1985:55–63.

Date Received: September 13, 1990
Date Revised: September 3, 1991
Date Accepted: September 9, 1991

Human mesenchymal stem cells engraft and demonstrate site-specific differentiation after *in utero* transplantation in sheep

KENNETH W. LIECHTY[1], TIPPI C. MACKENZIE[1], AIMEN F. SHAABAN[1], ANTONETA RADU[1], ANNEMARIE B. MOSELEY[2], ROBERT DEANS[2], DANIEL R. MARSHAK[2] & ALAN W. FLAKE[1]

[1]*The Children's Institute for Surgical Science, The Children's Hospital of Philadelphia, 34th and Civic Center Boulevard, Philadelphia, Pennsylvania 19104-4399, USA*
[2]*Osiris Therapeutics, 2001 Allicianna Street, Baltimore, Maryland 21231-3043, USA*
K.L. & T.M. contributed equally to this work.
Correspondence should be addressed to A.F.; email: flake@email.chop.edu

Mesenchymal stem cells are multipotent cells that can be isolated from adult bone marrow and can be induced *in vitro* and *in vivo* to differentiate into a variety of mesenchymal tissues, including bone, cartilage, tendon, fat, bone marrow stroma, and muscle[1,2]. Despite their potential clinical utility for cellular and gene therapy, the fate of mesenchymal stem cells after systemic administration is mostly unknown. To address this, we transplanted a well-characterized human mesenchymal stem cell population[3] into fetal sheep early in gestation, before and after the expected development of immunologic competence. In this xenogeneic system, human mesenchymal stem cells engrafted and persisted in multiple tissues for as long as 13 months after transplantation. Transplanted human cells underwent site-specific differentiation into chondrocytes, adipocytes, myocytes and cardiomyocytes, bone marrow stromal cells and thymic stroma. Unexpectedly, there was long-term engraftment even when cells were transplanted after the expected development of immunocompetence. Thus, mesenchymal stem cells maintain their multipotential capacity after transplantation, and seem to have unique immunologic characteristics that allow persistence in a xenogeneic environment. Our data support the possibility of the transplantability of mesenchymal stem cells and their potential utility in tissue engineering, and cellular and gene therapy applications.

Although a heterogeneous population, the human mesenchymal stem cells (MSCs) used here[3] have been well characterized in their ability to proliferate in culture with homogeneous morphology, the uniform presence of a consistent set of surface marker proteins and their differentiation into multiple mesenchymal lineages in controlled *in vitro* conditions. Analysis of colonies derived from individual cells from cultured MSCs has confirmed the presence of a subpopulation of cells with at least tri-potential differentiative capacity (bone, cartilage and adipose tissue)[3]. Assessment of the engraftment, survival and long-term fate of human MSCs after transplantation would require a surrogate animal model in which transplanted cells could be easily detected and would not be rejected. We used the fetal lamb model because it has been used as an assay system for human hematopoiesis[4]. The fetal lamb is immunologically tolerant of allogeneic skin grafts[5] or of allogeneic[6] or xenogeneic[4] hematopoietic cells before 75 days of gestation, which allows avoidance of the immunologic barriers present in post-natal models. In this model, long-term, multilineage, human hematopoietic chimerism has been established by the pre-immune transplantation of human hematopoietic stem cells. Because human and sheep DNA and proteins are widely disparate with respect to sequence homology, human-specific markers can be used for the unequivocal detection and characterization of human cells by a variety of methodologies.

To assess the influence of stage of hematopoietic development and immune response on MSC engraftment, we transplanted equivalent doses per kilogram ($1\text{-}2 \times 10^6$ MSCs/kg fetal weight, or $5\text{-}20 \times 10^6$ cells/fetus) of MSCs by intraperitoneal injection at either 65 days or 85 days of gestational age (term is 145 days). We chose these times because they represent different developmental stages in the sheep for hematopoiesis and immune response. Hematopoiesis mainly occurs in the fetal liver at 65 days of gestation, with only minimal bone marrow formation, whereas active hematopoiesis is present in the bone marrow by 85 days of gestation[7]. In addition, fetal lambs develop the capacity to reject allogeneic skin grafts[5] and demonstrate allogeneic or xenogeneic hematopoietic engraftment failure[8] after 75 days of gestation.

We assessed the early and late tissue distribution of human cells after *In utero* transplantation using PCR for human-specific β-2 microglobulin DNA sequences on DNA isolated from multiple tissues (Fig. 1). Tissues were collected at 2 weeks, 2 months, 5 months or 13 months after transplantation. We determined the tissue distribution at the time of collection of human cells transplanted at 65 and 85 days of gestation (Fig. 1*c*). All sheep transplanted at 65 days of gestation ($n = 12$) and 16 of 17 transplanted at 85 days of gestation had demonstrable human cell engraftment at the time of tissue collection. Although the pattern of human cell distribution in individual sheep differed, human-specific sequences were detectable in 28 of 29 sheep (Fig. 1*b*).

These results show that despite their large size and fibroblastic morphology, MSCs can be transplanted and are capable of engraftment in multiple tissues, even when transplanted into the fetal peritoneal cavity. This requires migration across endothelial barriers, integration into host tissue microenvironments, and survival with available growth and regulatory signals. Our finding of a variable pattern of long-term human cell engraftment after detection of human cells at 2 weeks in nearly all tissues studied supports a model of nonselective hematogenous distribution, with subsequent selective long-term survival in specific tissues. This may be a function of the ability of specific microenvironments to support the engraft-

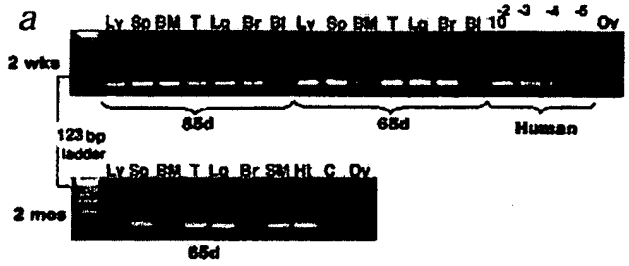

b

	65 d	85d
2 wks	2/2	5/6
2 mos	7/7	6/6
5 mos	3/3	3/3
13 mos		2/2
	12/12	16/17

c

	2 weeks		2 months		5 months		13 months
	65 d	85 d	65 d	85 d	65 d	85 d	85 d
Lv - Liver	1/2	4/6	3/7	1/6	0/4	0/3	1/2
Sp - Spleen	1/2	5/6	1/7	2/6	1/4	0/3	0/2
BM - Bone Marrow	2/2	4/6	2/7	1/6	1/4	0/3	1/2
T - Thymus	1/2	0/6	3/7	3/6	1/4	0/3	0/2
Lg - Lung	1/2	5/6	3/7	0/6	1/4	0/3	0/2
Br - Brain	1/2	4/6	0/7	0/6	0/4	1/3	0/2
Sk - Muscle	0/1	0/1	0/7	0/6	0/4	1/3	0/2
Ht - Heart	0/1	0/1	2/7	1/6	0/4	1/3	1/2
C - Cartilage	-	-	2/7	-	1/4	0/1	1/2
Bl - Blood	1/2	4/6	3/7	0/6	1/4	2/3	1/2

Fig. 1 Screening of sheep tissues (n = 29) after transplantation, by DNA PCR using probes specific for human β-2 microglobulin sequences. *a*, Gels represent samples from two sheep transplanted at 65 d and 85 d of gestation, followed by tissue collection 2 weeks (wks) after transplantation (top), or transplanted at 65 d of gestation, followed by tissue collection 2 months (mos) after transplantation (bottom). Left lane, molecular size markers (123-base-pair ladder). Human lanes represent samples of human cells diluted in sheep cells as indicated. Tissue abbreviations as listed in panel c; Ov, ovine control DNA. *b*, Frequency of human cell engraftment (in at least one tissue) at the time sheep were killed, assessed by PCR screening. wks, weeks; mos, months. *c*, Distribution of human-sequence-positive tissues at the times of tissue collection for sheep in the early and late transplantation groups. –, not analyzed.

ment and differentiation of MSCs or, alternatively, the loss of engraftment from some tissues may be due to heterogeneity of the transplanted population with respect to differentiation potential or replicative capacity and longevity. A third possibility is that the xenogeneic microenvironment can support the viability and differentiation of human MSCs, but not their self-replication. We have not quantitatively assessed expansion of the cells transplanted in this experiment. As the signals that stimulate MSC proliferation and differentiation are unknown, minimal expansion of donor cells in this xenogeneic, competitive model would not be unexpected. However, the apparent low frequency of donor cells indicated by immunohistochemistry here may be misleading. In the sheep model, exponential growth of the sheep occurred after transplantation. Experiments in the sheep model of human hematopoiesis in which human cells have been quantitatively assessed in chimeric bone marrow[9,10] have shown that even when low frequencies of donor cells can be detected, there is tremendous interval expansion in the total number of donor cells since transplantation.

The apparent lack of immune response indicated by the persistence of human cells transplanted at 85 days of gestation in the sheep fetus is interesting. Potential mechanisms for tolerance include failure of immune recognition, local immune suppression or thymic clonal deletion. Human MSCs express class I human leukocyte antigen but do not express class II, which may limit immune recognition[3]. *In vitro*, MSCs added to mixed lymphocyte cultures nonspecifically ablate alloreactivity by an as-yet-unknown mechanism (K. McIntosh, personal communication). As the involvement of thymic deletional mechanisms of tolerance when foreign antigen is presented after the development of a mature T-lymphocyte repertoire is unlikely, the persistence of human cells in this model may result from a combination of minimal immunogenicity and local immune suppression.

We confirmed the presence of human cells in PCR-positive tissues by immunohistochemistry using an antibody specific for human β-2 microglobulin, a component of the class I antigen complex (Fig. 2). Negative controls, consisting of tissues from transplanted sheep that were negative by PCR and age-matched tissues from normal sheep, were uniformly negative and confirmed the human specificity of the staining (data not shown). Many human MSCs were present in pre-natal (2 months) and post-natal (5 months and 13 months) hematopoietic and lymphopoietic tissues, including the fetal liver, bone marrow, spleen and thymus (Fig. 2*a–d*). We also identified human cells by β-2 microglobulin staining in non-lymphohematopoietic sites, including adipose tissue, lung (Fig. 2*e* and *f*), articular cartilage (Fig. 3*a* and *b*), perivascular areas of the central nervous system (Fig. 3*f*), and cardiac and skeletal muscle (Fig. 4*a* and *i–k*).

We assessed differentiation of human cells in various tissues using one of four techniques: characteristic morphology by staining with antibody against human β-2 microglobulin; immunohistochemical double staining for antibody against human β-2 microglobulin and a second non-human-specific differentiation marker; a combination of *in situ* hybridization for human sequences cleaved by *Arthrobacter luteus* (*Alu*) 1 restriction endonuclease combined with non-human-specific markers of muscle differentiation; or, where available, posi-

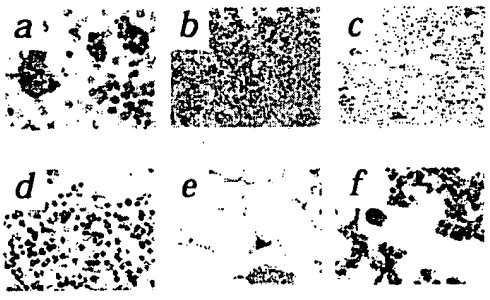

Fig. 2 Immunohistochemistry with human-specific antibody against β-2 microglobulin. *a*, Fetal liver at 2 months after transplantation (transplanted at 65 d of gestation), showing large human cells in clusters of hematopoiesis. *b*, Bone marrow 5 months after transplantation, showing many human cells per field. Original magnification, ×20. *c*, Frozen section of fetal spleen 2 weeks after transplant, showing large human cells with distinct nuclei. Original magnification, ×40. *d*, Thymus at 5 months after transplantation, showing a large human cell. *e*, Human adipocyte at 13 months after transplantation. *f*, Large human cell in alveolar space of fetal lung at 2 months after transplantation. Original magnification (*a* and *d–f*), ×100.

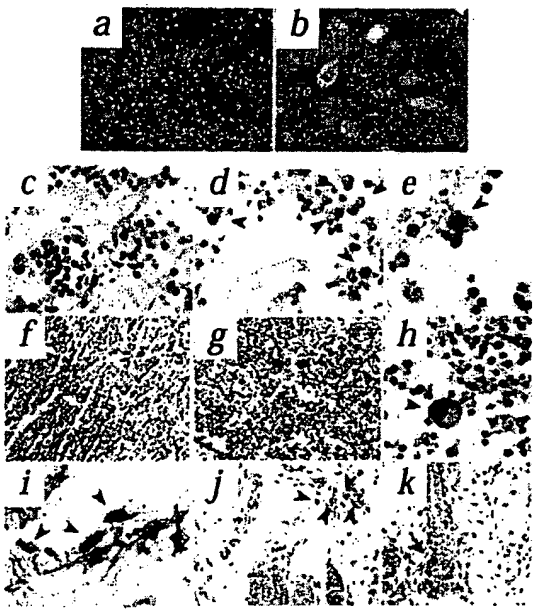

Fig. 3 Evidence for human cell differentiation. *a* and *b*, Low- and high-power magnification of staining of PCR-positive articular cartilage with human-specific antibody against β-2 microglobulin. *a*, Human cells in three separate lacunae of the cartilage (arrowheads). *b*, Higher-power magnification of human lacunar cell (arrowhead). *c–e*, Staining of bone marrow 5 months after transplantation with human-specific CD23. *c*, Negative control marrow from age-matched normal sheep. *d*, CD23 staining of PCR positive bone marrow, showing many large human cells. *e*, High-power magnification of CD23-positive bone marrow cells (arrowhead). *f–h*, Staining of thymus 5 months after transplantation with human-specific CD74. *f*, Negative control thymus from age matched normal sheep. *g*, Low-power magnification of CD74-positive cell (arrowhead). *h*, High-power magnification of a human thymic stromal cell (arrowhead). Original magnification, 200×. *i*, Double staining of PCR-positive brain tissue with anti β-2 microglobulin (dark brown granules, arrowheads) and anti glial fibrillary acid protein (GFAP-purple). *j*, Staining with antibody against β-2 microglobulin at 2 months after tail wounding. Multiple human cells are seen at the wound in the dermis (arrowheads) and in dermil appendages, *k*.

tive staining with human-specific differentiation markers proven not to cross-react with sheep cells. We confirmed site-specific differentiation for many cell types. We identified chondrocyte differentiation by finding human β-2 microglobulin-positive cells in the lacunae of articular cartilage (Fig. 3*a* and *b*). The immunohistochemical identification of human cells within the lacunae of cartilage specimens that were PCR-positive for human β-2 microglobulin sequences represented definite evidence of human chondrocyte differentiation. We identified human adipocytes in PCR-positive specimens by staining with antibody against human β-2 microglobulin and characteristic morphology (Fig. 2*e*). We assessed differentiation of human MSCs in bone marrow by immunohistochemistry using a human-specific antibody against CD23. CD23 is the low-affinity immunoglobulin E receptor and is expressed on a variety of cell types, including B-cell progenitors and bone marrow stromal cells[11]. At 2, 5 and 13 months after *in utero* transplantation, many human cells were present in the marrow and expressed CD23 (Fig. 3*d* and *e*). These human CD23-positive cells seemed to be large cells clustered in areas with ovine hematopoietic elements, consistent with bone marrow stroma. Staining of CD23-positive bone marrow with antibody against human CD45 was consistently negative, confirming that the human cells in the bone marrow were non-hematopoietic. We assessed differentiation of human MSCs in the thymus using immunohistochemistry with a human-specific antibody against CD74. At 2 and 5 months after *in utero* transplantation, multiple human cells detected in the thymus strongly expressed CD74 (Fig. 3*g* and *h*), a major-histocompatibility-complex-associated invariant chain expressed on thymic stromal cells[12]. These cells were large and were similar in morphologic appearance to epithelial cells, supporting our interpretation of the cells as thymic epithelial cells. The precursor of thymic dendritic cells is thought to be the hematopoietic stem cell, whereas the origin of the thymic epithelial cell is controversial. Our data supports but does not prove a mesenchymal origin for the thymic epithelial cell as a stromal-supporting cell in the thymus. Although human cells in the central nervous system were identified by PCR, these cells were located in the perivascular spaces in the gyral sulci rather than in the brain parenchyma and, on double staining, did not co-localize with cells expressing glial fibrillary acid protein, a marker for glial cell differentiation (Fig. 3*i*). Finally, we documented cardiomyocyte and skeletal myocyte differentiation by a combination of approaches. In cardiac muscle, β-2 microglobulin staining (Fig. 4*a*) or *in situ* hybridization

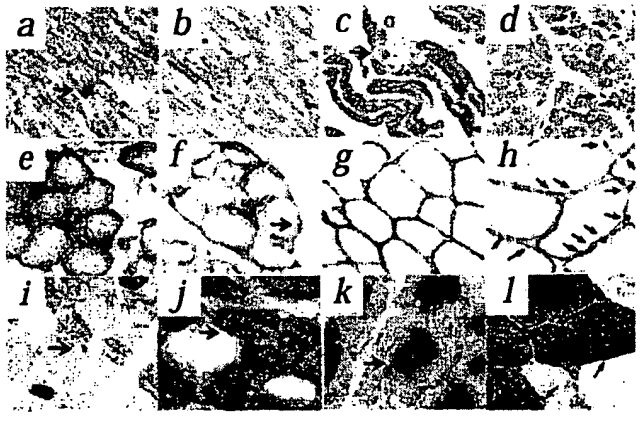

Fig. 4 Evidence for cardiac and skeletal myocyte differentiation. *a–d*, Cardiac muscle assessed at 5 months. *a*, Human cell (arrow) in the heart identified using antibody against β-2 microglobulin (dark brown) and counterstaining (pink) with antibody against SERCA-2. Original magnification, ×100. *b*, Age-matched sheep heart; negative control for staining with antibody against β-2 microglobulin and counterstaining with SERCA-2. *c* and *d*, *In situ* hybridization for human *ALU* sequences and counterstaining with SERCA-2. *c*, Human nucleus (arrow) within sheep cardiomyocyte. *d*, Human heart (positive control). *e–h*, Skeletal muscle analyzed by *In situ* hybridization for human ALU sequences and counterstained with dystrophin. *e* and *f*, Sheep skeletal muscle in cross-section with human nuclei (arrows) on the periphery of the cell. *g*, Age-matched sheep muscle (negative control). *h*, Human skeletal muscle (positive control). The arrows show human nuclei identified by *in situ* hybridization for human *ALU* sequences. *i–l*, Skeletal muscle stained with human-specific antibody against β-2 microglobulin and various counterstains. *i*, Counterstaining with SERCA-2, showing a human nucleus (arrow) on the periphery of a myocyte. *j*, Counterstaining with antibody against slow myosin, showing a human nucleus (arrow) on the periphery of a myocyte. *k*, Counterstaining with antibody against fast myosin, showing a human nucleus (arrow) on the periphery of a myocyte. *l*, Human skeletal muscle (positive control), counterstained with SERCA-2.

for human *ALU* sequences (Fig. 4*c*) were combined with double staining with antibody against smooth endoplasmic reticulum ATPase-2 (SERCA-2), a cytoplasmic protein specific for smooth or skeletal muscle[13]. We confirmed skeletal muscle differentiation by staining with antibody against dystrophin[14] combined with *in situ* hybridization for human ALU sequences (Fig. 4*e* and *f*), or by double staining for β-2 microglobulin and SERCA-2 (Fig. 4*i*), fast myosin (Fig. 4*j*) or slow myosin (Fig. 4*k*).

We also localized human cells at the site of wounds (tail clipping) inflicted at the time of MSC transplantation. These cells were in the dermis and dermal appendages and had fibroblastic features, indicating possible participation in wound healing (Fig. 3*j* and *k*).

Many reports have documented donor-derived stromal elements after bone marrow transplantation[15,16], indirectly supporting the possibility of the presence of a 'non-hematopoietic' stem cell in whole bone marrow that gives rise to stromal supporting elements. Similarly, a report documenting donor derived skeletal muscle in a muscle injury model after bone marrow transplantation[17] supports the possibility of a bone-marrow-resident stem cell with mesenchymal differentiative capacity. Evidence supporting the presence of osteoprogenitors in bone marrow has been reported in clinical[18] and experimental[19] studies. All of these studies used whole bone marrow as a donor source rather than more-defined 'stem cell' populations. Muscle reconstitution has been shown in irradiated mice with X-linked muscular dystrophy (*mdx*) after transplantation of highly enriched hematopoietic stem cells[20]. Those findings[20] indicate that the MSC may be an intermediate population and that the hematopoietic stem cell is more pluripotent than previously realized. More relevant here are studies that monitored the fate of MSCs or MSC-like populations after intravenous or intraperitoneal transplantation. In two studies in mice, cultured mouse adherent cell populations systemically transplanted persisted after transplantation[21,22]. Donor cells were detected in bone marrow, spleen, bone, cartilage and lung up to 5 months later by PCR or fluorescence *in situ* hybridization assays for the Y chromosome. Although these studies support the possibility of the presence of a bone-marrow-resident MSC, our study has directly documented multipotential differentiation of a relatively well-characterized MSC population *in vivo* after transplantation. Our finding of long-term persistence of MSCs with multipotential, site-specific differentiation supports the potential of these cells in transplantation, gene therapy and tissue engineering applications. However, clinical use will require the delivery of adequate numbers of MSCs to specific sites for therapeutic effect. This will require further insight into normal and disease-induced regulation of MSC proliferation and differentiation, a better understanding of the transplant immunology of MSCs and the development of strategies for diffuse or site-specific delivery for therapeutic applications.

Methods

Mesenchymal stem cell isolation and preparation. Fresh bone marrow was obtained by iliac crest aspiration from normal human donors after informed consent was given. MSCs were isolated as described[3]. Bone marrow aspirate (10 ml) was added to control medium (20 ml Dulbecco's modified essential media; Life Technologies) containing 10% FBS (Hyclone, Logan, Utah) from selected lots, and was centrifuged to pellet the cells and remove the fat. The cell pellet was resuspended in control medium and fractionated on a density gradient generated by centrifugation of a 70% percoll solution (Sigma) at 13,000*g* for 20 min. The MSC-enriched, low-density fraction was collected, rinsed with control medium and plated at a density of 1×10^7 nucleated cells per 60-mm² dish. The MSCs were cultured in control medium at 37°C in a humidified atmosphere containing 5% CO_2. Upon reaching near confluence, the cells were detached for 5 minutes at 37 °C with 0.25% trypsin containing 1 mM EDTA (Life Technologies). The cells were washed with control medium and were resuspended at a density of 5×10^6 MSCs/ml in control medium containing 5% DMSO (Sigma). The cells were then stored in liquid nitrogen.

Animals and transplant procedure. Pregnant Western Cross sheep (Thomas Morris, Reisterstown, Maryland) carrying twin pregnancies of confirmed gestational age were housed in the large animal facility at the Children's Hospital of Philadelphia, approved by the Assocoation for Assessment and Accreditation of Laboratory Animal Care (ALAAC). After induction of anesthesia and exposure of the fetus by maternal laparotomy and hysterotomy, MSCs were injected (1×10^6–2×10^6 human MSCs/kg estimated fetal weigh), with direct visualization, into the fetal peritoneal cavity.

Tissue processing. Fetal sheep were killed at 2 weeks or 2, 5 or 13 months after injection, and liver, spleen, lung, bone marrow, thymus, brain, heart, skeletal muscle, cartilage and blood were collected and analyzed for the presence of human cells by DNA isolation and immunohistochemistry. Tissues positive by PCR were analyzed by immunohistochemistry. Tissues negative by PCR and tissues from normal age-matched sheep were used as negative controls. In a subset of 65-day gestation recipients, the fetal tails were cut off at the time of MSC injection, and the tail wounds were obtained at 1 week or 2 months after wounding. Fetal tissues were fixed overnight at 4 °C in 10% neutral buffered formalin (Fisher Scientific). Bone marrow samples were then decalcified in Cal-EX (Fisher) for 12 h to 2 weeks (depending on size), followed by a 30-minute wash in 3% H_2O_2, and a 1-hour wash with distilled water. Samples were then embedded in paraffin as described[23]. In addition, samples from each tissue were 'snap-frozen' in liquid nitrogen and stored at –80 °C for subsequent total cellular DNA extraction. Skeletal muscles were frozen in isopentane-chilled in liquid nitrogen for subsequent frozen section analysis.

DNA isolation. Total cellular DNA was isolated using DNAzol (Molecular Resource Center, Cincinnati, Ohio). Approximately 100 mg tissue was homogenized in 1 ml DNAzol. The DNA was precipitated with 0.5 ml 100% ethanol. The DNA precipitate was pelleted by centrifugation and then washed twice with 95% ethanol. The DNA pellet was then dissolved in sterile water at a concentration of 15 µg/ml.

PCR analysis. Total cellular DNA was analyzed by PCR for human-specific β-2 microglobulin using a modification of published methods[24]. Specific primers for human β-2 microglobulin were selected based on the published human sequence (upstream primer, 5′-GTGTCTGGGTTTCATCAATC-3′; downstream primer, 5′-GGCAGGCATACTCATCTTTT-3′) and were shown to specifically amplify human, not ovine, DNA. Amplification conditions were: 95 °C for 9 min, followed by 45 cycles of 95 °C for 30 s, 55 °C for 30 s and 72 °C for 15 s, followed by an extension at 72 °C for 5 min. All samples were also amplified to detect the β-actin gene (upstream primer, 5′-CGGGACCTGACTGACTAC-3′; downstream primer, 5′-GAAGGAAGGCTGGAAGAG-3′) as a control for the presence of amplifiable DNA. For these controls, the reaction conditions were the same except 35 cycles of amplification were used. The sensitivity of the assay was assessed by human/sheep cell dilution studies with a sensitivity of detection of 1 human cell in 10,000 cells.

Immunohistochemistry. Immunohistochemical staining was also done for human CD74, human CD23, SERCA-2, dystrophin, myosin heavy chain (fast and slow) and glial fibrillary acid protein. For all tissues except skeletal muscle, paraffin sections 4–5 µm in thickness were collected on Superfrost Plus slides (Fisher) from each of the

paraffin-embedded tissues. Slides were incubated for 16 h at 55 °C and then deparaffinated by immersion in xylene followed by rehydration over 10 min through a graded alcohol series to deionized water. To enhance antigen retrieval, the slides were immersed in 1% Antigen Unmasking Solution (Vector Laboratories, Burlingame, California) and microwaved for 3 min. Samples were blocked for 30 min at room temperature with non-immune serum from the species in which the primary antibody was raised (1:10 dilution), followed by a 16-hour incubation with the specific primary antibody. The primary antibodies and dilutions used were: human β-2 microglobulin, 1:50–1:400 (PharMingen, San Diego, California); human CD74, 1:20 (Novocastra Laboratories, Newcastle upon Tyne, UK); and human CD23, 1:20 (Vector Laboratories). The slides were then washed with PBS followed by a second blocking step of 30 min at room temperature in methanol containing 0.6% hydrogen peroxide. Slides were then rinsed with deionized water and then PBS, followed by incubation for 30 min at room temperature with biotinylated secondary antibody (1:200 dilution; Vectastain ABC kit AK-5002; Vector Laboratories). The slides were washed with PBS, and avidin–biotin complex was added for 30 min at room temperature. The slides were then rinsed well in PBS and developed with chromagen 3,3′-diaminobenzidine. For sections stained for human β-2 microglobulin, CD74 and CD23, the slides were then lightly counterstained with hematoxylin. For cardiac muscle and brain, the human β-2 microglobulin was first developed using nickel chloride as the chromagen and then was subjected to a secondary immunohistochemical staining for SERCA-2 (1:50 dilution) or glial fibrillary acid protein (1:100 dilution), respectively (both from Vector Laboratories), as described[25]. Secondary staining was developed using Vector VIP substrate kit (Vector Laboratories). No counterstaining was used on these double-stained slides.

For skeletal muscle frozen sections, sections 5 μm in thickness were collected on glass slides and stored at −20 °C. Slides were air-dried and incubated overnight at 4 °C or at 37 °C for 3 h with primary antibody: human dystrophin (clone DYS-2; 1:10 dilution), human myosin heavy chain, slow type (clone WB-MHCs; 1:100 dilution) or human myosin heavy chain, fast type (clone WB-MHCf; 1:100 dilution, all from Novocastra Laboratories). Slides were then incubated with secondary antibody and avidin–biotin complex as described above, except that the Vector alkaline phosphatase mouse IgG kit (PK-6102; Vector Laboratories) was used and washes were done in 0.1 M Tris-buffered saline, pH 7.5. The slides were developed using the Vector alkaline phosphatase substrate kit (SK-5200; Vector Laboratories). For double staining with β-2 microglobulin, slides were transferred to distilled water, then fixed for 30 min at room temperature in 1% neutral buffered formalin (Fisher Scientific) in PBS. They were blocked for 30 min at room temperature with 10% horse serum, followed by incubation with human β-2 microglobulin antibody as described above.

***In situ* hybridization.** For frozen skeletal muscle sections, slides were first stained with dystrophin or myosin antibodies and then developed as described above before the *in situ* hybridization. Slides were incubated for 5 min with 100 μg/ml proteinase K, then were post-fixed in 1% formalin in PBS. A fluorescein-conjugated human ALU probe (Innogenex, San Ramon, California) was applied and hybridization was done at 80 °C for 5 min, followed by 37 °C overnight. Slides were developed using the Innogenex *in situ* hybridization kit for fluorescein-labeled probes (SH-2009-06; Innogenex) according to the manufacturer's directions. After the horseradish peroxidase step, the Vector DAB substrate kit (SK-4100; Vector Laboratories) was used to develop the stain. For cardiac sections, *in situ* hybridization was done before staining with SERCA-2. Slides were deparaffinated, hydrated and 'microwave retrieved' as described above, then incubated for 20 min at 37 °C with 20 μg/ml proteinase K. The remainder of the staining was as for the frozen muscle sections except a 2× concentration of the human ALU probe was used (Innogenex).

RECEIVED 28 MARCH; ACCEPTED 22 SEPTEMBER 2000

1. Caplan, A.I. The mesengenic process. *Clin. Plastic Surg.* **21**, 429–435 (1994).
2. Prockop, D.J. Marrow stromal cells as stem cells for nonhematopoietic tissues. *Science* **276**, 71–74 (1997).
3. Pittenger, M.F., *et al.* Multilineage potential of adult human mesenchymal stem cells. *Science* **284**, 143–147 (1999).
4. Zanjani, E.D., Flake, A.W., Rice, H., Hedrick, M. & Tavassoli, M. Long-term repopulating ability of xenogeneic transplanted human fetal liver hematopoietic stem cells in sheep. *J. Clin. Invest.* **93**, 1051–1055 (1994).
5. Silverstein, A.M., Prendergast, R.A. & Kraner, K.L. Fetal response to antigenic stimulus IV. Rejection of skin homografts by the fetal lamb. *J. Exp. Med.* **119**, 955–964 (1964).
6. Flake, A.W., Harrison, M.R., Adzick, N.S. & Zanjani, E.D. Transplantation of fetal hematopoietic stem cells *in utero*: the creation of hematopoietic chimeras. *Science* **233**, 776–778 (1986).
7. Zanjani, E.D., Ascensao, J.L. & Tavassoli, M. Liver-derived fetal hematopoietic stem cells selectively and preferentially home to the fetal bone marrow. *Blood* **81**, 399–404 (1993).
8. Zanjani, E., Almeida-Porada, G., Ascensao, J., MacKintosh, F. & Flake, A. Transplantation of hematopoietic stem cells *in utero*. *Stem Cells* **15**, 79–93 (1997).
9. Zanjani, E.D., Almeida-Porada, G. & Flake, A.W. The human/sheep xenograft model: a large animal model of human hematopoiesis. *Int. J. Hematol.* **63**, 179–192 (1996).
10. Zanjani, E.D., Almeida-Porada, G., Livingston, A.G., Flake, A.W. & Ogawa, M. Human bone marrow CD34- cells engraft *in vivo* and undergo multilineage expression that includes giving rise to CD34+ cells. *Exp. Hematol.* **26**, 353–360 (1998).
11. Fourcade, C. *et al.* Expression of CD23 by human bone marrow stromal cells. *Eur. Cytokine Network* **3**, 539–543 (1992).
12. Schlossman, S., Bloumsell, L. & Gilks, W. In *Leukocyte Typing V: White Cell Differentiation Antigens.* (Oxford University Press, New York, 1995).
13. Sharp, A.H. *et al.* Differential immunohistochemical localization of inositol 1,4,5-trisphosphate- and ryanodine-sensitive Ca2+ release channels in rat brain. *J. Neurosci.* **13**, 3051–3063 (1993).
14. Nicholson, L.V. *et al.* Dystrophin or a "related protein" in Duchenne muscular dystrophy? *Acta. Neurol. Scand.* **86**, 8–14 (1992).
15. Keating, A. *et al.* Donor origin of the *in vitro* haematopoietic microenvironment after marrow transplantation in man. *Nature* **298**, 280–283 (1982).
16. Anklesaria, P. *et al.* Engraftment of a clonal bone marrow stromal cell line *in vivo* stimulates hematopoietic recovery from total body irradiation. *Proc. Natl. Acad. Sci. USA* **84**, 7681–7685 (1987).
17. Ferrari, G. *et al.* Muscle regeneration by bone marrow-derived myogenic progenitors. *Science* **279**, 1528–1530 (1998).
18. Horwitz, E.M. *et al.* Transplantability and therapeutic effects of bone marrow-derived mesenchymal cells in children with osteogenesis imperfecta. *Nature Med.* **5**, 309–313 (1999).
19. Hou, Z. *et al.* Osteoblast-specific gene expression after transplantation of marrow cells: implications for skeletal gene therapy. *Proc. Natl. Acad. Sci. USA* **96**, 7294–7299 (1999).
20. Gussoni, E. *et al.* Dystrophin expression in the mdx mouse restored by stem cell transplantation. *Nature* **401**, 390–394 (1999).
21. Pereira, R.F. *et al.* Cultured adherent cells from marrow can serve as long-lasting precursor cells for bone, cartilage, and lung in irradiated mice. *Proc. Natl. Acad. Sci. USA* **92**, 4857–4861 (1995).
22. Pereira, R.F. *et al.* Marrow stromal cells as a source of progenitor cells for nonhematopoietic tissues in transgenic mice with a phenotype of osteogenesis imperfecta. *Proc. Natl. Acad. Sci. USA* **95**, 1142–1147 (1998).
23. Culling, C.F.A. In *Handbook of Histopathological and Histochemical Techniques* (Butterworth and Co., London, 1974).
24. Gilliland, G., Perrin, S., Blanchard, K. & Bunn, F. Analysis of cytokine mRNA and DNA: detection and quantification by competetive polymerase chain reaction. *Proc. Natl. Acad. Sci. USA* **87**, 2725–2729 (1990).
25. Van Der Loos, C.M., Becker, A.E. & Van Den Oord, J.J. Practical suggestions for successful immunoenzyme double-staining experiments. *Histochem. J.* **25**, 1–11 (1993).

Rationale for Stem Cell Based Pacemaker

Natural pacemaker:

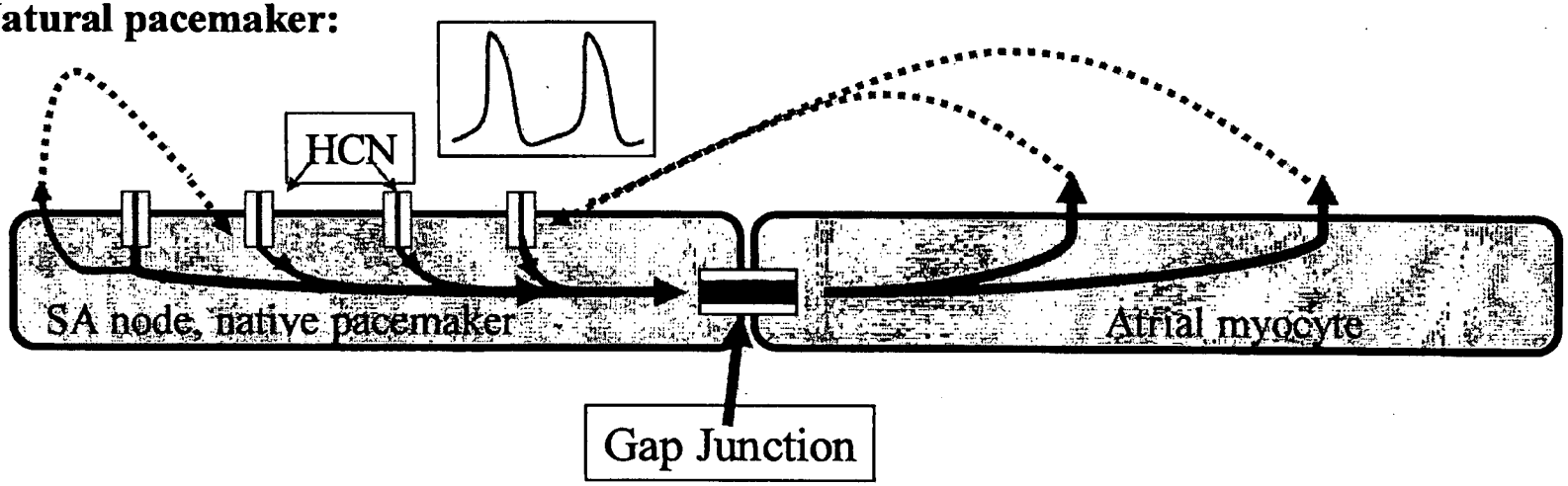

A genetically engineered stem cell coupled to a heart cell can serve as a biological pacemaker.

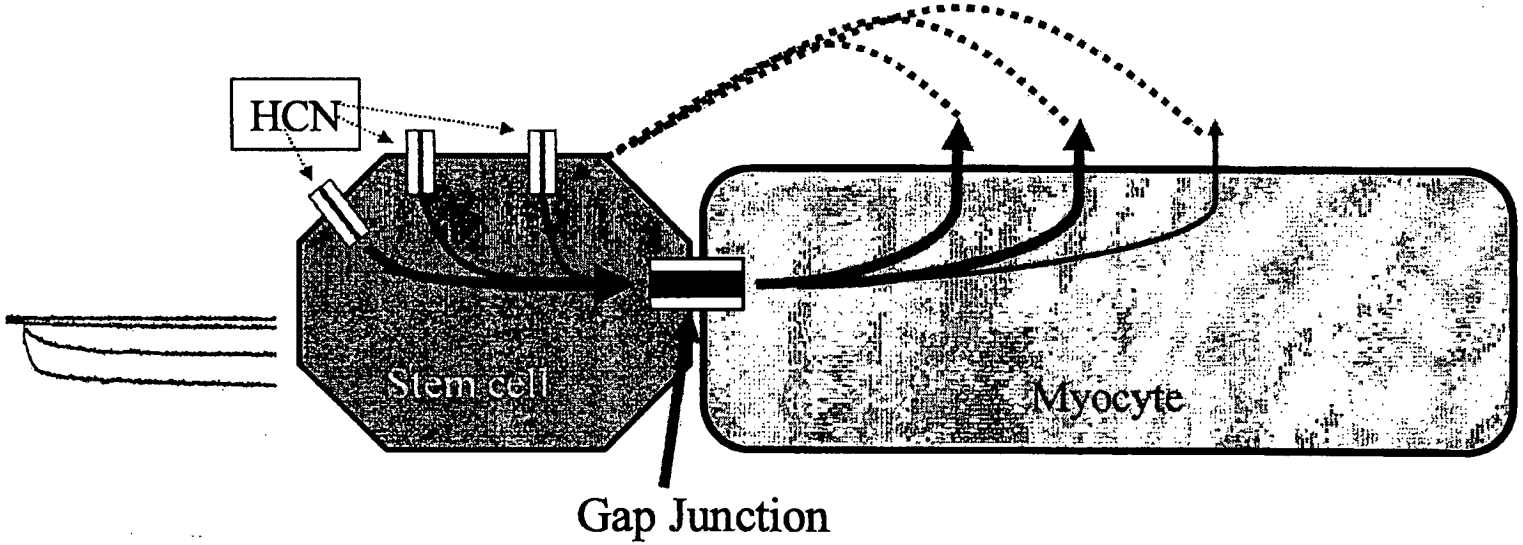

Frontiers in physiology

Scandinavian Physiological Society

American Physiological Society

JOINT MEETING, STOCKHOLM, SWEDEN

August 16-19, 2000

WORLD'S FIRST HUMAN MYOBLAST TRANSFER INTO THE HEART

Authors:
Law P, Weinstein J, Ben Hain S, Williams S, Fang Q, Hall T, Brown F, Addison J, Goodwin T.

Address of presenting author:
Cell Therapy Research Foundation. 1770 Moriah Woods Blvd. Suite 18, Memphis, TN. 38117 USA

Email:

Telephone:

Text of abstract:
Heart muscle degeneration associated with aging, cardiomyopathy, infarcts and congestive heart failure is the leading cause of debilitation and death in humans. Being terminally differentiated, cardiomyocytes do not divide significantly to regenerate the myocardium. Stem cells transplant posts ethical issues of abortion and technical uncertainties as to whether these pluripotent cells will absolutely differentiate into cardiomyocytes and not osteoblasts, chondrocytes or others. Myoblasts are myogenic cells similar to cardiomyocytes at early differentiation. Recent animal studies suggest that implanted myoblasts might be "differentiated" into cardiomyocytes within the heart milieu. We present the first successful endovascular transfer of human myoblasts into the porcine myocardium. Porcine hearts highly resemble those of humans and are more prompt to fibrillate upon minor injury.

Following IACAC guidelines. A 100-lb juvenile female pig was anesthetized. Access was obtained via the right femoral artery using cutdown technique. Catheter advance into the left ventricle through the aorta was guided with fluoroscopy followed by endomyocardial mapping with the electromagnetic NOGA system (Johnson & Johnson). Approximately $1*10^9$ human myoblasts were injected through a needle timed to protrude 6mm from the tip of the catheter into the myocardium. Twenty injections were made at different locations within 40 minutes, having volumes of 0, 1, 0.2, 0.3, 0.5, 1.0 ml, and cell concentration of $100X10^6$ /ml. Heart rate, electrocardiogram and temperature were continuously monitored. Other than transient short runs of ventricular ectopy, the pig remained in stable condition throughout the injection period. There was no significant change in the parameters monitored. Vital dye staining of the myoblasts before versus after the procedure showed no significant difference in cell viability. Furthermore, cell passage through the injection catheter showed less than 5% of cell death. At the completion of the procedure, the pig was sacrificed and the heart processed for histological examination. Transmyocardial perforation was not observed. Numerous prominent round and mononucleated human myoblasts were found widely and evenly distributed throughout the apex and the lateral wall of the pig left ventricle where the myoblasts were injected.

Conclusions: This study provides the first direct evidence demonstrating the feasibility and safety of endovascular delivery of human myoblast into the porcine heart using the NOGA catheter injection system. Considering about 2,600 donor hearts were available in 1999 to serve 7-million Americans that have heart attacks each year, we urge that research on human cardiac myoblast transfer be prioritized and expedited to prevent and treat heart dysfunction.

Keywords:

Stem Cell Center

TEXAS HEART® INSTITUTE
at St. Luke's Episcopal Hospital
STEM CELL CENTER

Back to previous page

Cardiovascular Anesthesiology
Cardiovascular Pathology
Cullen Cardiovascular Research Laboratories
Electrophysiology
Heart Assist Devices
Stem Cell and Heart Failure
Stem Cell Center
Transplant
Vulnerable Plaque
Wafic Said Molecular Cardiology & Gene Therapy Research Laboratory

Mission

The Stem Cell Center is dedicated to the study of adult stem cells and their role in treating cardiovascular disease. We have completed clinical trials (in human patients), as well as many preclinical studies (in the laboratory) using stem cells.

The primary mission of the Stem Cell Center is to help patients through the advancement of clinical stem cell research. Our research is in the area of autologous adult stem cells, which means we use the patient's own stem cells to

Does the Stem Cell Center study all forms of Heart Failure?

No. Heart Failure may be caused by many different diseases. The Stem Cell Center is only studying Heart Failure caused by a lack of blood flow to the heart. For example, the Stem Cell Center is not studying Diastolic Heart Failure.

How does stem cell therapy work?

It is unclear how stem cells interact with the tissue they are placed in.

They may differentiate into the cells that surround them (a stem cell placed in the heart may become another heart cell), they may release hormones that help the surrounding tissue function more efficiently, or they may wake up the dormant stem cells in the tissue. Even though we do not fully understand how stem cells work, one of the goals of our research at the Stem Cell Center is to further our knowledge in this area.

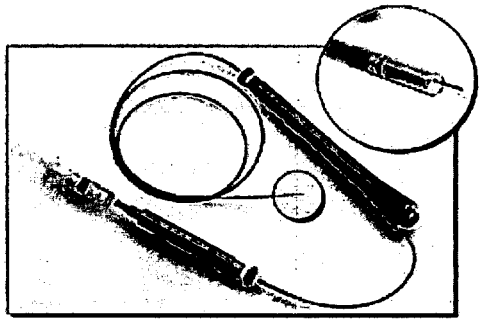

Picture of a Myostar™ Injection Catheter.*

How do you place the stem cells in the heart?

Ongoing studies at the Stem Cell Center inject the stem cells directly into the muscle of the heart from inside the heart chamber. This is performed with a catheter that is inserted in the groin. The exact area of disease is located through a sophisticated mapping system known as the NOGA® Cardiac Navigation System and the cells are injected using a Myostar™ Injection Catheter*.

**The Myostar™ Injection Catheter is not yet available for sale in the United States and is currently in use in IND (Investigational Device) studies.*

Does the Stem Cell Center research therapy using Embryonic Stem Cells?

Note: Performing your original search, ***NOGA catheter***, in PubMed will retrieve *32* citations.

1: Catheter Cardiovasc Interv. 2001 Mar;52(3):400-6. Related Articles, Links

Assessment of NOGA catheter stability during the entire cardiac cycle by means of a special needle-tipped catheter.

Lessick J, Kornowski R, Fuchs S, Ben-Haim SA.

Department of Cardiology, Rambam Medical Center, Haifa, Israel.

The NOGA system maps regional myocardial function and delivers local catheter-based therapeutics, requiring stability and precise localization of the catheter tip throughout the cardiac cycle. A special catheter having a retractable needle at its tip was used to compare tip stability with and without needle insertion into the myocardium, assuming this prevents catheter slippage. For multiple sites in seven pig left ventricles, we recorded sets of three consecutive point locations: pre-, post-, and during needle insertion. In-point location stability (LocStab), defined as the mean displacement between catheter tip trajectories of two consecutive cardiac cycles at a specific point, did not differ among the three groups of points (mean, 1.33 +/- 0.61 mm; P = 0.37 by ANOVA), indicating that trajectories are equally stable and repeatable with or without needle insertion. Between-point LocStab(p1,p2), i.e., displacement between the trajectories of two different points (p1 and p2) at the same location, was not increased when p1 = a needle insertion point and p2 = a noninsertion point, compared to both p1,p2 = noninsertion points, suggesting that slippage of noninsertion points is negligible. In conclusion, catheter tip trajectories at any location are highly stable throughout the cardiac cycle.

PMID: 11246261 [PubMed - indexed for MEDLINE]

Catheter-based delivery of cells to the heart

Warren Sherman*, Timothy P Martens, Juan F Viles-Gonzalez and Tomasz Siminiak

SUMMARY

Clinical trials have begun to assess the feasibility, safety, and efficacy of administering progenitor cells to the heart in order to repair or perhaps reverse the effects of myocardial ischemia and injury. In contrast to surgical-based injections, which are often coupled with coronary bypass surgery, catheter-based injections are less invasive and make it possible to evaluate cell products used as sole interventions. The two methods that have been tested in humans are injecting cells directly into the ventricular wall with catheter systems dedicated to that purpose and infusing cells into coronary arteries with standard balloon angioplasty catheters. The catheters described in this article have been shown in both animal and clinical studies to be effective in cell delivery and to be safe. They are well-designed and user-friendly devices, but require further investigation to identify means for optimizing cell retention and to address other limitations. Randomized, placebo-controlled trials utilizing catheters for cell implantation are under way, and others are soon to follow. The results of these studies will help to shape the direction of future investigations, both clinical and basic. The spectrum of cardiac diseases, the variety of catheters for cell delivery, and the wide array of progenitor cell types open up this young field to creative discoveries.

KEYWORDS catheters, cell delivery, intramyocardial, intracoronary, progenitor cells

W Sherman is the Director of Cardiac Cell-Based Endovascular Therapies, at The Center for Interventional Vascular Therapy, Columbia University Medical Center, and Adjunct Assistant Professor, Mount Sinai School of Medicine, New York, NY, USA. TP Martens is a Research Fellow, in the Department of Surgery, Columbia University Medical Center, New York, NY, USA. JF Viles-Gonzalez is a Research Associate, at the Cardiovascular Institute, Mount Sinai School of Medicine, New York, NY, USA. T Siminiak is Professor of Cardiology at the University School of Medical Sciences, Department of Cardiology and Internal Medicine, District Hospital, Poznán, Poland.

Correspondence
*Cardiac Cell-Based Endovascular Therapies, The Center for Interventional Vascular Therapy, Columbia University Medical Center, 161 Fort Washington Avenue, IP-519, New York, NY 10032, USA
wsherman@crf.org

Received 6 September 2005 **Accepted** 19 November 2005
www.nature.com/clinicalpractice
doi:10.1038/ncpcardio0446

INTRODUCTION

An unfortunate characteristic of the adult mammalian heart is its ineffective use of programs for repair and regeneration, especially after acute coronary occlusion and ST-elevation myocardial infarction (STEMI). Experimental studies have explored ways to overcome this limitation by introducing progenitor cells into the myocardium.[1] The choice of cells and of methods for isolating them are described in other papers in this issue of *Nature Clinical Practice Cardiovascular Medicine*.[2–10] The administration of progenitor cells to humans with cardiac disease has been recently described.[11–16] This article reviews methods for cell delivery that utilize percutaneous catheter technology.

Because the field of cardiac cell-based therapy is at a very early stage, many questions remain unanswered, including those relating to our basic understanding of the biologic effects of such therapy. Similarly, aspects of cell delivery, such as effective dose and timing of administration, are still largely undefined. Therefore, what follows is a synopsis of an evolving field, intended to provide a basic understanding of catheter-delivery systems and their functional capabilities.

CURRENT DELIVERY METHODS

Percutaneous transplantation of progenitor cells into the heart, performed as a sole therapy, allows the evaluation of the cells' effects independently of revascularization or other interventions.[17] Furthermore, multiple administrations over time would be more easily justified with a low-risk percutaneous procedure. Two catheter-based methods have been used in clinical trials to deliver cells to the heart: direct intramyocardial injection and intracoronary infusion. Though substantially different techniques, they share the common goal of seeding progenitor cells into specific histoanatomic locations, specifically into the perivascular, interstitial space surrounding injured or ischemic myocardium. In doing so,

Table 1 Devices for intramyocardial delivery of cells.

Device	Core needle			Support			Notes
	OD (mm)	Length (cm)	Composition; configuration	Size (Fr[a])	Length (cm)	Configuration	
Helix™,[39]	0.51	124	Stainless steel; helical	8	110	Deflectable guide catheter	Guide catheter (Morph™) is FDA approved
MyoCath™,[b]	0.51	122	Stainless steel; straight	8	115	Integrated; multiple curves	
Myostar™,[24]	0.41	123	Nitinol; straight	8	115	Integrated; multiple curves	NOGA-guided;[c] CE marked
Stiletto™,[35,36]	0.46	133	Nitinol; straight; spring loaded	9, 7	100, 125	Two guide catheters	
TransAccess Delivery System™,[25]	0.41	177	Nitinol; curved; injection catheter	6.2, 10	125, 80	Guide catheter; transvenous	IVUS-guided; Peripheral device (Pioneer™) FDA and CE approved

[a]French size. [b]Sherman W *et al.* Results of the MYOHEART study, a phase I skeletal myoblast study for congestive heart failure. Presented at the 2005 scientific sessions of Transcatheter Cardiovascular Therapeutics, Washington DC, USA, October, 2005. [c]NOGA, an electromagnetic mapping system (Biologics Delivery Systems, Diamond Bar, CA, USA).
CE, European Community (European Union); IVUS, intravascular ultrasound; OD, outer diameter.

it is hoped that cells so placed will find conditions suitable for their survival and retention, thereby giving them their best chance to effect repair or regeneration.

Direct intramyocardial injection

As in the development of other biotherapeutics, early studies in cardiac cell therapy were conducted in animal models—in this case, open-chest models—in which techniques of controlled myocardial injury and administration of specific agents are well established. In large animals, surgical exposure of the beating heart permits myocardial injections, tagged for subsequent analysis, to be localized to segments diseased by coronary occlusion. With these techniques, the regenerative potential of many cell types has been studied.[1,18] Such studies became the foundation for the first injections of autologous skeletal myoblasts[19] and bone marrow-derived cells[20] in humans during coronary artery bypass surgery.

Catheter-based direct intramyocardial methods attempt to simulate surgical injection techniques,[21] by approaching the myocardium from either its epicardial or its endocardial surface. The demands of this task have led to the development of devices constructed of multiple components. One component (the core element) is dedicated solely to the transport of cells. It is small in caliber and terminates in a beveled injection needle distally. The core catheter is advanced and retracted within the outer elements of the device. The other components (support catheters) are multifunctional, serving to protect the core and to direct it toward the region(s) of myocardium to be injected. However, while it is believed that the capacity to deliver cells by catheter-based methods is similar to that obtained with open surgical procedures, there are few data comparing the two delivery methods.[22] Moreover, certain aspects of the surgical technique described above are not feasible with current catheter systems.

Five intramyocardial catheter-based delivery systems have been used in clinical trials (Table 1). All share the multicomponent design features just described. However, they differ in their anatomic approach to the myocardium, in specific design aspects and materials, and in ancillary imaging modalities.

The first four devices listed (the Helix™ [BioCardia Inc., South San Francisco, CA, USA], the MyoCath™ [Bioheart Inc., Sunrise, FL, USA], the Myostar™ [Biologics Delivery Systems, Diamond Bar, CA, USA], and the Stiletto™ [Boston Scientific, Natick, MA, USA]) approach the myocardium from within the left ventricular chamber (the 'transendocardial approach'), which is accessed crossing the aortic valve in a retrograde fashion, much as is done during routine left heart catheterizations.

Two of these transendocardial devices—the MyoCath™ (Figure 1) and the Myostar™ (Figure 2)—are so-called integrated systems, in which the core and support catheters are joined to form a single unit. These two devices are manipulated through a combination of axial rotation and deflection of the distal aspect (the latter under a separate control mechanism capable of inducing up to 180° of flexion). With the tip of the device in contact with the endocardium, the core catheter is advanced, forcing a straight needle to a controlled intramyocardial depth (3–8 mm). The integrated design provides a relatively simple mechanism for navigation and repeated injections. However, there is no guide-wire lumen in either and they must be advanced from the femoral artery and across the aortic valve using the same navigation mechanisms that guide the device within the ventricular chamber.

The other two transendocardial devices—the Helix™ (Figure 3) and the Stiletto™ (Figure 4)—are not integrated: the core catheter is a physically separate device that can be inserted and removed in its full length separately from the support catheters. The latter are constructed, and approved, for use as vascular guiding catheters. Directional control within the left ventricle is effected by manipulation of a single, deflectable catheter (the Helix™) or of two preshaped support catheters (the Stiletto™). Two features are unique to these two devices: the ability to insert the support catheters into the ventricle over a guide wire, and the configuration of the injection needles, which in one case is helical and in the other is spring loaded. The helical design, based on pacemaker lead technology, may be advantageous with regard to stability of the needle tip during injection. The spring-loaded needle of the Stiletto™ device is set to a fixed depth (3.5 mm) and may be more able to penetrate fibrotic tissue. As with integrated devices, the coordinated movement of support catheters and core elements enables multiple, topographically distinct injections throughout the left ventricle.

The fifth catheter listed in Table 1, the TransAccess Delivery System™ (Medtronic Vascular, Santa Rosa, CA, USA) (Figure 5) is unique among the intramyocardial devices in approaching the myocardium through the epicardial surface. To achieve this, a support catheter is positioned in specific branches of the cardiac venous system, by way of the femoral vein. An intravascular ultrasound probe contained within the support catheter makes it possible to localize the adjacent coronary artery and pericardium. With these structures used as landmarks, the coronary vein is punctured with a small-caliber needle, and

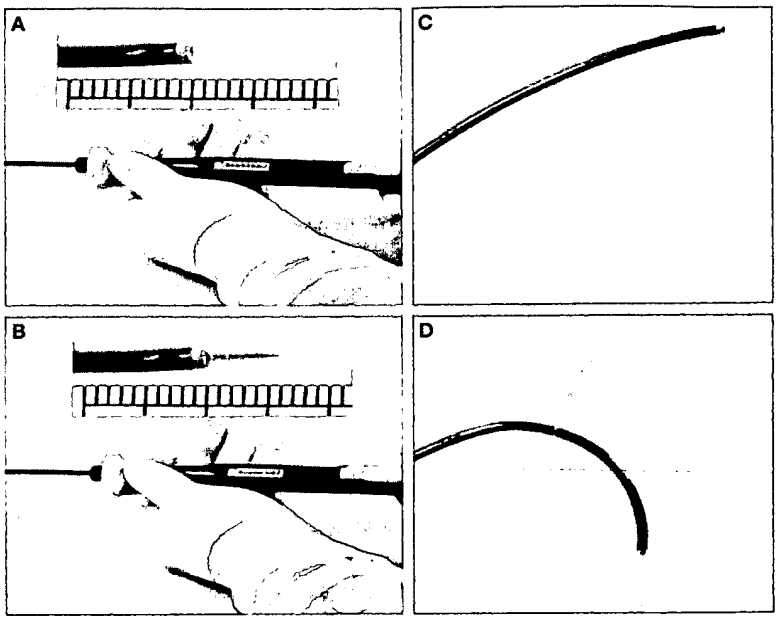

Figure 1 MyoCath™ catheter for intramyocardial delivery of cells. An integrated-device with control mechanisms for needle movement from withdrawn (**A**) to extended (**B**) position, as well as for tip movement from straight (**C**) to deflected (**D**) position. Image courtesy of Bioheart Inc., Sunrise, FL, USA.

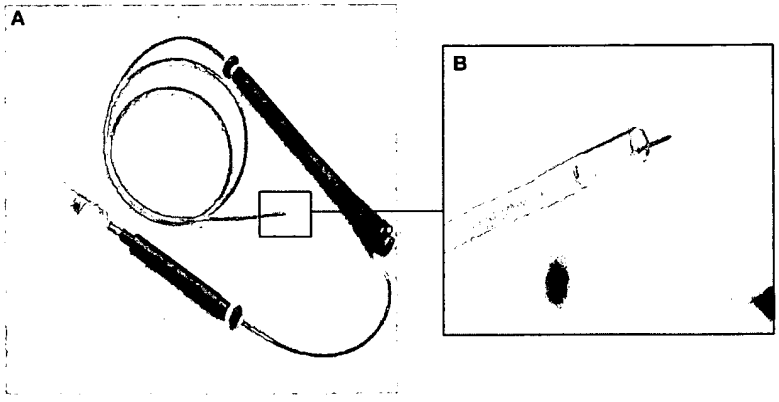

Figure 2 Myostar™ catheter for intramyocardial delivery of cells. An integrated-device with similar control mechanisms (**A**) as noted in Figure 1, but with endocardial (NOGA) mapping capability. The sensor is contained within the distal tip of the catheter (**B**), through which the injection needle is extended. Image courtesy of Biologics Delivery Systems, Diamond Bar, CA, USA.

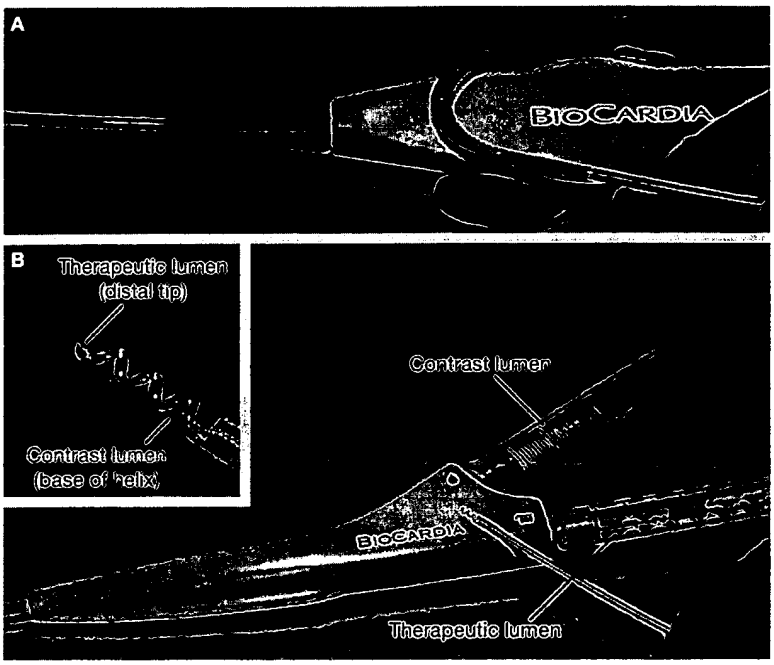

Figure 3 The Helix™ catheter for intramyocardial delivery of cells. A non-integrated system with an independent deflectable guide catheter (**A**) and removable helical-shaped-needle injection catheter (**B**). Image courtesy of BioCardia Inc., South San Francisco, CA, USA.

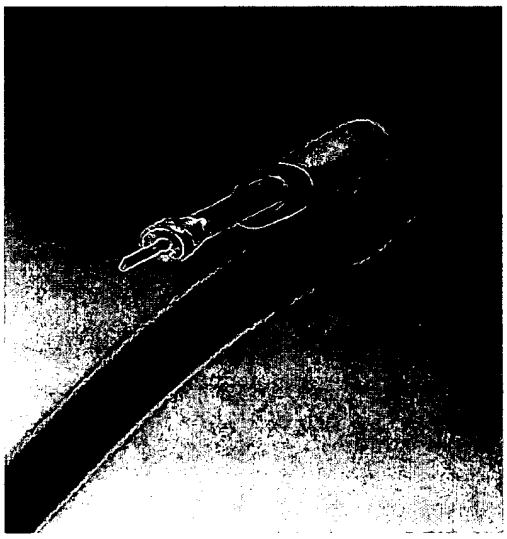

Figure 4 The Stiletto™ catheter for intramyocardial delivery of cells. A nonintegrated system with two independently configured guide catheters and a removable spring-loaded needle. As shown here, the needle is extended beyond the flat surface of the core injection component. Image courtesy of Boston Scientific, Natick, MA, USA.

through this an injection catheter is passed into the ventricular wall through its epicardial surface. The injection catheter can be advanced for several centimetres along a trajectory within the wall. In this respect it more closely resembles surgical injection techniques than do other intramyocardial devices.

Adjunctive imaging for catheter guidance is incorporated into the Myostar™ system.[11] Using electromechanical signal detection, a baseline 3-dimensional endocardial map (NOGA™, Biologics Delivery Systems) can be created; this map is color-coded to delineate regions of viable, ischemic myocardium (for an example of such a map, see Opie *et al.*[23] in this issue). Target areas can be precisely identified and electronically marked with each injection. Extensive experience with this system has been accumulated in both preclinical and clinical studies.[24,25]

Other differences between the five devices relate to the needle composition (stainless steel or nitinol), and method of activation (i.e. manual or spring loaded). The relative merits of each design feature are not established.

Whether the ease of use of one-piece, integrated systems outweighs the versatility of independently controlled systems, whether the level of precision provided by devices with enhanced guidance mechanisms is necessary for effective delivery, and whether specific needle designs facilitate delivery and augment retention of cells are questions still open to debate. In the future, the selection of intramyocardial device may well be found to depend on the underlying myocardial disease. We are presently conducting studies to address this question.

In the US, all the devices listed in Table 1 are classified as having investigational status for intramyocardial injection; one (Myostar™) has CE marking (certifying conformity with the standards of the European Union and the European Free Trade Association) for this purpose. One of the guide catheters (Morph™, BioCardia) and a transvenous access catheter, similar to the TransAccess Delivery System™ but larger in caliber (Pioneer™, Medtronic Vascular, Santa Rosa, CA, USA) are approved by the FDA for use in treating peripheral vascular disease.

Intracoronary infusion

The other method by which cells have been administered in clinical trials is intracoronary infusion. The underlying rationale is both

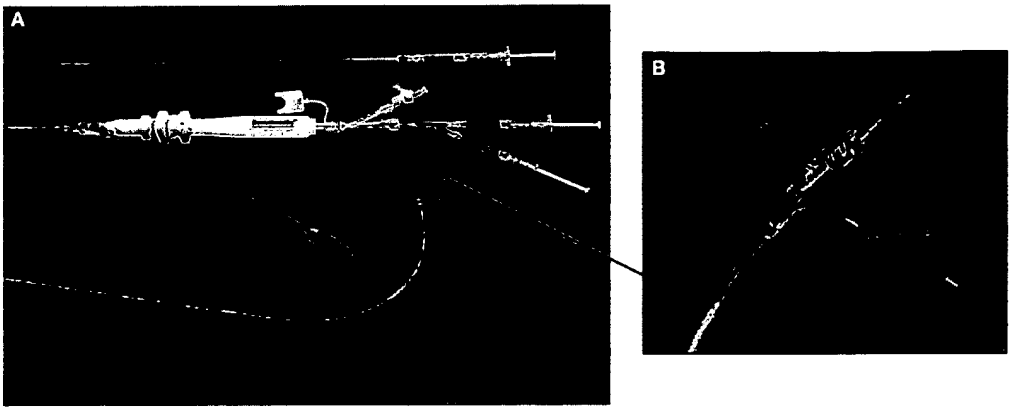

Figure 5 TransAccess Delivery System™ catheter for intramyocardial delivery of cells. A nonintegrated system. **(A)** The full system with the proximal connection for the intravascular ultrasound component (IVUS, colored black). **(B)** The distal catheter tip, with the internal intravascular ultrasound imaging element (IVUS) and the extended needle and injection catheter (core). Image courtesy of Medtronic Vascular Systems, Santa Rosa, CA, USA.

biologic and pragmatic. The biologic goal is to amplify cell trafficking to ischemic myocardium, raising it above the levels known to occur after both acute and chronic coronary occlusion.

Acute coronary occlusion and STEMI lead to immediate, irreversible effects on myocardial function within the distribution of the infarct-related artery. Further deterioration of myocardial function can extend beyond the borders of the infarction, observed weeks or months after the acute event, in a process known as remodeling. The clinical consequences of remodeling are profound, leading to further deterioration of left ventricular function and congestive heart failure. Remodeling is believed to be due, in part, to 'demand' myocardial ischemia and myocyte apoptosis of the peri-infarction regions. Immediately after acute coronary occlusion, vascular progenitor cells are released from bone marrow, enter the peripheral circulation, and home to the site of myocardial injury,[26] where they promote the development of neovasculature and are incorporated into it. However, the scale of this process appears to be small in the clinical setting of STEMI.[27] Interventions that increase the level of neovascularization, such as through the administration of vascular progenitor cells, might mitigate the remodelling process.[28]

Patients with chronic coronary occlusions, myocardial ischemia, and refractory angina are also underserved by intrinsic levels of angiogenesis. They have been the focus of numerous trials of gene therapy[29] and other novel therapies[30] and may benefit from increased levels of vascular progenitor cells in regions of chronic ischemia.[29]

There are also pragmatic reasons for intracoronary cell administration. Because diseased myocardial tissue retains a blood supply, irrespective of the nature or extent of disease, vascular pathways are identifiable by angiography. Cells injected into proximal coronary segments can be distributed to large regions of myocardium. Alternatively, infusion into specific branch vessels, such as infarct-related arteries, could utilize methods common to percutaneous coronary interventions (PCI) and familiar to interventional cardiologists.

From the preceding discussion, it follows that the efficacy of intracoronary administration depends on specific properties of the cell preparation and on coronary anatomy. Cells used for intracoronary infusion must be capable of transendothelial migration to perivascular spaces, as noted previously. Cell preparations that are viscous or in which the cell diameters are large may not be suitable for intracoronary infusion, due to the risk of microvascular obstruction and myocardial ischemia.[31] Additionally, myocardial targets must be supplied by well-defined vascular channels readily accessed by delivery catheters. While these requirements are ideally suited to patients with post-PCI STEMI, they may not be met in patients with chronic occlusive coronary

Table 2 Some published clinical trials using over-the-wire balloon catheters.

Reference	Disease	Cells injected		Catheter (supplier)	Infusion regimen[a] (min)
		Number	Type		
Assmus *et al.*[13]	STEMI	2.4×10^8 10×10^6	BMMC, CPC	OpenSail™ (Guidant Corp., Indianapolis, IN, USA	3×3
Wollert *et al.*[14]	STEMI	2.5×10^9	BMMC	Concerto™ (Occam International BV, Eindhoven, the Netherlands)	5×2.5–4
Bartunek *et al.*[41]	STEMI	12.4×10^6	BM-derived $CD133^+$	Maverick™ (Boston Scientific, Natick, MA, USA)	3×2–3
Janssens *et al.*[b]	STEMI	3×10^8	BMMC	Maverick™ (Boston Scientific)	3×2–3

[a]Number of infusions × duration of each infusion. [b]Janssens S *et al.* Intracoronary autologous bone marrow cell transfer after myocardial infarction: a double-blind, randomized, and placebo-controlled clinical trial. Presented at the 2005 Scientific Sessions of the American College of Cardiology 2005, Orlando, FL, USA, March, 2005. BM, bone marrow; BMMC, bone marrow mononuclear cells; CPC, circulating progenitor cells; STEMI, ST-elevation myocardial infarction.

disease, in whom ischemic areas are fed solely by collateral vessels, often arising from arteries afflicted with obstructive disease.

Clinical trials that have delivered cells by intracoronary infusion have done so through coronary balloon angioplasty catheters. Such catheters are well suited for this purpose, given the ease with which they can be positioned into selected coronary branches. The two features of balloon-dilating catheters that bear on their utility in delivering cells are the central (core) lumen and the expandable balloon. In 'over-the-wire' devices, unlike 'monorail' devices, the central wire extends the full length of the catheter. After positioning of the catheter, the guide wire can be withdrawn from the lumen, leaving it to function as a conduit for injection into the distal coronary bed. Furthermore, to prevent cell washout by antegrade blood flow and to increase the dwell time (the time during which the injected cells remain undisturbed by the resumption of blood flow), occlusive balloon inflation is initiated just before distal injection of the cell suspension and continued for up to 5 min or until the onset of clinically important ischemia. So far, catheters that lack the ability to obstruct coronary flow proximal to the site of cell injection have not been used in clinical trials.

Several commercially available over-the-wire balloons have been used in this way in clinical trials (Table 2). It is important to note that no balloon angioplasty catheter has received regulatory approval specifically for cell infusion, even though all are made of biologically inert materials and are unlikely to adversely affect cell survival or function.

COMPARISON OF DELIVERY TECHNIQUES

The intramyocardial and intracoronary delivery techniques each have their own distinct advantages and limitations. Intracoronary procedures are performed extensively for the treatment of coronary artery disease, and any modifications specific to cell infusions would be easily integrated into such procedures. Intramyocardial procedures would require additional operational training, albeit with devices that are not complex. Moreover, the facility with which cells reach the extravascular compartment from an intracoronary injection may differ considerably from one cell population to another. Intramyocardial administration overcomes this problem by circumventing the vascular barrier.

Early studies have compared the two techniques, either directly or with surgically applied injections.[32] The retention of cells is poor by either route of administration,[32,33] with fewer than 10% of the injected cells detectable after 24 h. These studies were conducted in normal[32,33] or recently infarcted[34] myocardium, and their applicability to myocardium with chronic fibrosis is questionable. Retention of cellular or other biologic agents is low by every implantation method thus far tested, including surgical implantation. Solutions to this problem may be found in products that combine cells with agents more adhesive to resident tissue.[35]

CONCLUSION

The field of cell-based therapy for cardiovascular disease is at an early stage. The catheters described in this article are well-designed, user-friendly devices that have demonstrated their

capability of delivering cells to the heart. In both animal and clinical studies, their safety profiles have been excellent—an especially noteworthy achievement for the intramyocardial devices, which are complex to construct and require needle puncture for access to the ventricular wall.

Important questions remain regarding catheter-based cell delivery; the catheter systems described here require further characterization. Balloon-dilating catheters were not designed (and have not been approved) for the administration of therapeutic agents. Though unlikely to pose significant problems to cell function and viability, each should undergo preclinical testing before use in clinical studies. Direct intramyocardial delivery catheters, on the other hand, were essentially developed in parallel with cell products[36,37] and consequently have had to undergo extensive biocompatibility testing. Despite the poor retention of cells injected by either route of administration, both compare favourably with the cell retention obtained by direct transepicardial implantation at surgery.

Standards have not been developed for testing and comparing the physical attributes of delivery catheters, or for their efficacy in delivering cells. We feel it important to conduct such evaluations in order to define their respective performance ranges. Our group is analyzing certain of these characteristics, as well as the physical properties of diseased myocardium, and believe the results will be pertinent to the design, conduct, and interpretation of future clinical studies.

Catheters used in clinical trials are sophisticated and, from the standpoint of cell delivery, early-generation devices. Whether by refining current designs, or by combining them in novel ways with other technologies,[38] or by developing techniques that pursue entirely new approaches,[39,40] significant advances in the efficacy of cell delivery will be made in the coming years.

References

1 Marelli D *et al.* (1992) Cell transplantation for myocardial repair: an experimental approach. *Cell Transplant* **1:** 383–390
2 Torella D *et al.* (2006) Resident human cardiac stem cells: role in cardiac cellular homeostasis and potential for myocardial regeneration. *Nat Clin Pract Cardiovasc Med* **3 (Suppl 1):** S8–S13
3 Fraidenraich D and Benezra R (2006) Embryonic stem cells prevent developmental cardiac defects in mice. *Nat Clin Pract Cardiovasc Med* **3 (Suppl 1):** S14–S17
4 Martens TP *et al.* (2006) Mesenchymal lineage precursor cells induce vascular network formation in ischemic myocardium. *Nat Clin Pract Cardiovasc Med* **3 (Suppl 1):** S18–S22
5 Schächinger V *et al.* (2006) Bone-marrow-derived progenitor cell therapy in need of proof of concept: design of the REPAIR-AMI trial. *Nat Clin Pract Cardiovasc Med* **3 (Suppl 1):** S23–S28
6 Fraser JK *et al.* (2006) Plasticity of human adipose stem cells towards endothelial cells and cardiomyocytes. *Nat Clin Pract Cardiovasc Med* **3 (Suppl 1):** S33–S37
7 Siminiak T *et al.* (2006) Postinfarction heart failure: surgical and trans-coronary-venous transplantation of autologous myoblasts. *Nat Clin Pract Cardiovasc Med* **3 (Suppl 1):** S46–S51
8 Bartunek J *et al.* (2006) Timing of intracoronary bone-marrow-derived stem-cell transplantation following ST-elevation MI. *Nat Clin Pract Cardiovasc Med* **3 (Suppl 1):** S52–S56
9 Behfar A and Terzic A (2006) Derivation of a cardiopoietic population from human mesenchymal stem cells yields cardiac progeny. *Nat Clin Pract Cardiovasc Med* **3 (Suppl 1):** S78–S82
10 Shintani S *et al.* (2006) Synergistic effect of combined intramyocardial CD34$^+$ cells and VEGF2 gene therapy after myocardial infarction. *Nat Clin Pract Cardiovasc Med* **3 (Suppl 1):** S123–S128
11 Smits PC *et al.* (2003) Catheter-based intramyocardial injection of autologous skeletal myoblasts as a primary treatment of ischemic heart failure: clinical experience with six-month follow-up. *J Am Coll Cardiol* **42:** 2063–2069
12 Strauer BE *et al.* (2002) Repair of infarcted myocardium by autologous intracoronary mononuclear bone marrow cell transplantation in humans. *Circulation* **106:** 1913–1918
13 Assmus B *et al.* (2002) Transplantation of progenitor cells and regeneration enhancement in acute myocardial infarction (TOPCARE-AMI). *Circulation* **106:** 3009–3017
14 Wollert KC *et al.* (2004) Intracoronary autologous bone-marrow cell transfer after myocardial infarction: the BOOST randomised controlled clinical trial. *Lancet* **364:** 141–148
15 Fernández-Avilés F *et al.* (2004) Experimental and clinical regenerative capability of human bone marrow cells after myocardial infarction. *Circ Res* **95:** 742–748
16 Menasché P *et al.* (2003) Autologous skeletal myoblast transplantation for severe postinfarction left ventricular dysfunction. *J Am Coll Cardiol* **41:** 1078–1083
17 Siminiak T *et al.* (2003) Myocardial replacement therapy. *Circulation* **108:** 1167–1171
18 Taylor DA *et al.* (1998) Regenerating functional myocardium: improved performance after skeletal myoblast transplantation. *Nat Med* **4:** 929–933
19 Menasché P *et al.* (2001) Myoblast transplantation for heart failure. *Lancet* **357:** 279–280
20 Stamm C *et al.* (2003) Autologous bone-marrow stem-cell transplantation for myocardial regeneration. *Lancet* **361:** 45–46
21 Sherman W (2003) Cellular therapy for chronic myocardial disease: nonsurgical approaches. *Basic Appl Myol* **13:** 11–14
22 Grossman PM *et al.* (2002) Incomplete retention after direct myocardial injection. *Catheter Cardiovasc Interv* **55:** 392–397
23 Opie SR and Dib N (2006) Surgical and catheter delivery of autologous myoblasts in patients with congestive heart failure. *Nat Clin Pract Cardiovasc Med* **3 (Suppl 1):** S42–S45

Acknowledgments
We are grateful to V Fuster, of the Zena and Michael A Wiener Cardiovascular Institute and the Marie-Josée and Henry R Kravis Center for Cardiovascular Health, Mount Sinai School of Medicine, New York, NY, USA, and to MB Leon, of the Cardiovascular Research Foundation and of the Center for Interventional Vascular Therapy, Columbia University Medical Center, for their guidance in preparing this paper.

Competing interests
The authors declared they have no competing interests.

24 Vale PR *et al.* (2000) Left ventricular electromechanical mapping to assess efficacy of phVEGF(165) gene transfer for therapeutic angiogenesis in chronic myocardial ischemia. *Circulation* **102:** 965–974
25 Losordo DW *et al.* (1998) Gene therapy for myocardial angiogenesis: initial clinical results with direct myocardial injection of phVEGF165 as sole therapy for myocardial ischemia. *Circulation* **98:** 2800–2804
26 Asahara T *et al.* (1997) Isolation of putative progenitor endothelial cells for angiogenesis. *Science* **275:** 964–967
27 Shintani S *et al.* (2001) Mobilization of endothelial progenitor cells in patients with acute myocardial infarction. *Circulation* **103:** 2776–2779
28 Kocher AA *et al.* (2001) Neovascularization of ischemic myocardium by human bone-marrow-derived angioblasts prevents cardiomyocyte apoptosis, reduces remodeling and improves cardiac function. *Nat Med* **7:** 430–436
29 Losordo DW and Dimmeler S (2004) Therapeutic angiogenesis and vasculogenesis for ischemic disease: part II: cell-based therapies. *Circulation* **109:** 2692–2697
30 Leon MB *et al.* (2005) A blinded, randomized, placebo-controlled trial of percutaneous laser myocardial revascularization to improve angina symptoms in patients with severe coronary disease. *J Am Coll Cardiol* **46:** 1812–1819
31 Vulliet PR *et al.* (2004) Intra-coronary arterial injection of mesenchymal stromal cells and microinfarction in dogs. *Lancet* **363:** 783–784
32 Hou D *et al.* (2005) Radiolabeled cell distribution after intramyocardial, intracoronary, and interstitial retrograde coronary venous delivery: implications for current clinical trials. *Circulation* **112 (Suppl 9):** I-150–I-156
33 Smits PC *et al.* (2002) Efficacy of percutaneous intramyocardial injections using a nonfluoroscopic 3-D mapping based catheter system. *Cardiovasc Drugs Ther* **16:** 527–533
34 Hill JM *et al.* (2003) Serial cardiac magnetic resonance imaging of injected mesenchymal stem cells. *Circulation* **108:** 1009–1014
35 Christman KL *et al.* (2004) Injectable fibrin scaffold improves cell transplant survival, reduces infarct expansion, and induces neovasculature formation in ischemic myocardium. *J Am Coll Cardiol* **44:** 654–660
36 Naimark WA *et al.* (2003) Adenovirus-catheter compatibility increases gene expression after delivery to porcine myocardium. *Hum Gene Ther* **14:** 161–166
37 Marshall DJ *et al.* (2000) Biocompatibility of cardiovascular gene delivery catheters with adenovirus vectors: an important determinant of the efficiency of cardiovascular gene transfer. *Mol Ther* **1:** 423–429
38 Corti R *et al.* (2005) Real time magnetic resonance guided endomyocardial local delivery. *Heart* **91:** 348–353
39 Fearon WF *et al.* (2004) Evaluation of high-pressure retrograde coronary venous delivery of FGF-2 protein. *Catheter Cardiovasc Interv* **61:** 422–428
40 Ikeno F *et al.* (2004) Novel percutaneous adventitial drug delivery system for regional vascular treatment. *Catheter Cardiovasc Interv* **63:** 222–230
41 Bartunek J *et al.* (2005) Intracoronary injection of CD133-positive enriched bone marrow progenitor cells promotes cardiac recovery after recent myocardial infarction: feasibility and safety. *Circulation* **112 (Suppl 9):** I-178–I-183

www.nature.com/clinicalpractice/cardio

Methods of stem cell delivery in cardiac diseases

Emerson C Perin* and Javier López

SUMMARY

There are several strategies for cell delivery in cardiac stem cell therapy. The cells can be delivered through coronary arteries, coronary veins, or peripheral veins. Alternatively, direct intramyocardial injection can be performed, using a surgical, transendocardial, or transvenous approach. In this article, we describe the most important conceptual aspects and the evidence for the use of these techniques, with emphasis on intramyocardial injections.

KEYWORDS cardiac stem cell therapy, delivery technique, intramyocardial injection

EC Perin is Director of New Cardiovascular Interventional Technology in the Department of Adult Cardiology, Texas Heart Institute at St Luke's Episcopal Hospital, Houston, TX, USA. J López is a Clinical Cardiologist at the Instituto de Ciencias del Corazón (ICICOR), Hospital Clínico de Valladolid, Valladolid, Spain.

Correspondence
*New Cardiovascular Interventional Technology, Department of Adult Cardiology, Texas Heart Institute, St Luke's Episcopal Hospital, 6624 Fannin, Suite 2220, Houston, TX 77030, USA
eperin@crescentb.net

Received 25 September 2005 **Accepted** 7 November 2005
www.nature.com/clinicalpractice
doi:10.1038/ncpcardio0447

INTRODUCTION

The main objective of any mode of stem cell delivery is to achieve the ideal concentration of cells needed to repair the injured myocardial region with the lowest risk to patients. Therefore, cell-delivery strategies must take into account the clinical setting and local milieu, because stem cells may perform differently according to local signaling. The cardiac environment may also help to determine the degree of cell retention.

Stem cells can be delivered through coronary arteries, coronary veins, or peripheral veins. Alternatively, direct intramyocardial injection can be performed using a surgical, transendocardial, or transvenous approach. A delivery strategy may involve mobilization of stem cells from the bone marrow using cytokine therapy, with or without peripheral harvesting. Here, we briefly review the main delivery strategies, with particular emphasis on intramyocardial injection, which we believe to be the most promising technique.

STEM CELL MOBILIZATION

In humans, mobilization of progenitor cells from the bone marrow occurs after acute myocardial infarction (AMI), suggesting a natural attempt at cardiac repair.[1,2] Therapeutic mobilization of bone marrow progenitor cells after AMI would, in theory, amplify the existing healing response. Mobilization of these progenitors is an attractive strategy because it is simple and would obviate the need for invasive harvesting or delivery procedures. However, safety concerns have been raised about 'off label' application (e.g. in severe chronic ischemic heart disease),[3] because of the possibility of adverse events in a different patient population, as well as a theoretical concern about tumorigenesis. Additionally, in one clinical trial of bone-marrow-cell transfer after AMI,[4] an increase in the rate of re-stenosis was observed, which may have been related to the increased availability of inflammatory cells to a recently injured, still-healing coronary artery.

TRANSVASCULAR CELL DELIVERY

Peripheral (intravenous) infusion of stem cells, as performed in bone marrow transplants, would be a convenient way of delivering cells. A study in a mouse model has confirmed that, when infused into the peripheral circulation, human bone marrow cells home to peri-infarct areas.[5] However, only a few cells reach the affected area,[6] and the technique would be most applicable only after AMI, because it would rely on physiologic homing signals alone. Moreover, peripherally infused stem cells home to infarcted areas only when injected within a few days of AMI, so this delivery strategy is less useful for treating chronic myocardial ischemia. The major drawback of intravenous cell delivery would be failure to reach the desired destination due to trapping of the cells in the microvasculature of the lungs, liver, and lymphoid tissues.

Infusion of stem cells through the coronary venous system (coronary sinus) under high pressure has been achieved in experimental models.[7] In this procedure, the coronary sinus is cannulated and an angioplasty balloon is advanced into the great cardiac vein. The balloon is positioned in the selected cardiac vein, depending on the territory to be treated. After balloon inflation, with consequent flow interruption in the coronary venous system, the cell infusate is delivered under high pressure through the lumen of the balloon catheter. This delivery mode supposedly provides a broad and uniform distribution of cells. Its limitations include the lack of specific targeting of a myocardial area (when such targeting is desirable) and the variability and tortuosity of the coronary venous system, which can make accessing certain myocardial veins difficult or impossible.

Intracoronary infusion is the most popular mode of cell delivery in the clinical setting, especially after AMI.[4,8–11] Stem cells delivered 4–9 days after AMI are associated with a good safety profile. The technique is similar to that used for coronary angioplasty, which involves OVER-THE-WIRE POSITIONING of an angioplasty balloon in one of the coronary arteries. The coronary blood flow is then stopped for approximately 2–4 min while the stem cells are infused under pressure. This maximizes contact between stem cells and the microcirculation of the infarct-related artery, thereby optimizing 'homing time'. Again, this delivery technique would be suitable only in the setting of acute ischemia after adhesion molecules and cytokine signaling are temporarily upregulated. Although intracoronary infusion is widely used, this method of delivery lacks a strong experimental background with regard to safety and efficacy.

INTRAMYOCARDIAL INJECTION

Intramyocardial injection, which can be carried out through the epicardium, endocardium, or coronary vein, is performed in chronic myocardial ischemia.[12–22] In this technique, a preparation of cells is introduced into the myocardium under pressure using a hollow needle. This is the preferred delivery route in patients with chronic total occlusion of coronary arteries and in clinical settings that involve weaker homing signals, such as chronic congestive heart failure. In theory, it should be the most suitable route for delivering larger cells, such as skeletal myoblasts and mesenchymal stem cells, which can plug capillaries.

Transepicardial injection

Transepicardial delivery of stem cells is the most commonly used technique in cardiac stem cell therapy. It has been performed during open-surgical revascularization procedures in which cells are injected into infarct border zones or areas of infarcted or scarred myocardium under direct visualization.[12–15] This approach requires sternotomy and, being highly invasive, is associated with significant surgical morbidity. However, in a planned open-heart procedure, the ancillary delivery of cell therapy in this fashion can be easily justified. One important advantage of this technique is that it can provide a high level of cells per unit area injected. Nonetheless, not all areas of the myocardium (e.g. the septum) can be reached using a direct external approach.[16] The safety of direct injection in AMI has not been tested.

Transendocardial injection

Transendocardial injection is performed using a percutaneous femoral approach. Once an injection-needle catheter has been advanced in retrograde fashion across the aortic valve and positioned against the endocardial surface, cells can be injected directly into any area of the left ventricular wall. Two catheter systems are currently available for transendocardial cell delivery: the Stiletto™ (Boston Scientific, Natick, MA, USA) and the Myostar™ (Cordis Corp., Warren, NJ, USA).

The Stiletto™ catheter (see Sherman *et al.*[23] [Figure 4] in this issue) is guided fluoroscopically,

GLOSSARY

OVER-THE-WIRE POSITIONING
Technique in which the angioplasty balloon passes over the whole length of the guide wire, which enters at the distal orifice of the catheter and exits at the proximal one

GLOSSARY

GATED
In the case of the NOGA system, conected to or coordinated with a surface electrocardiogram so that all the points are acquired at the same point in the cardiac cycle

usually in two planes. It has the essential drawback of a 2-dimensional orientation and the inherent lack of precision associated with fluoroscopy. Another limitation is that it does not adequately show the underlying or target myocardium. It has been coupled, in preclinical experiments, with real-time cardiac magnetic resonance imaging, which permits 3-dimensional, online assessment of the full-thickness myocardium and perfusion. This technology is still under investigation; few preclinical studies have been performed,[17] and no safety data have been assessed in humans. Nevertheless, it is promising for use in association with other imaging technologies or when myocardial therapy does not need to be targeted.

The NOGA system (Cordis Corp.) is a catheter-based electromechanical system for intramyocardial navigation and mapping (for an example of such a map, see Opie and Dib[24] in this issue). This technique uses ultralow magnetic fields generated by a triangular magnetic pad positioned beneath the patient. The magnetic fields intersect with a location sensor proximal to the deflectable tip of the mapping catheter, which helps determine the real-time location and orientation of the catheter tip inside the left ventricle. The NOGA injection catheter (Myostar™) (see Sherman *et al.*[23] [Figure 2] in this issue) takes advantage of nonfluoroscopic magnetic guidance. Injections take place inside a 3-dimensional left ventricular electromechanical map, which represents the endocardial surface of the left ventricle. The map is constructed by acquiring a series of points at multiple locations on the endocardial surface, which are GATED to a surface electrocardiogram. The NOGA system uses an algorithm to calculate and analyse the movement of the catheter tip or the location of an endocardial point during systole and diastole. That movement is then compared with the movement of neighboring points in the area of interest. The resulting (linear local shortening [LLS]) value is expressed as a percentage and represents the degree of mechanical function of the left ventricular region at that endocardial point. Data are obtained only when the catheter tip is in stable contact with the endocardium; contact is determined automatically.

The mapping catheter also incorporates electrodes that measure endocardial electrical signals (unipolar or bipolar voltage). Voltage values are assigned to each point acquired during left ventricular mapping, and an electrical map is constructed concurrently with the mechanical map. Each data point has an LLS value and a voltage value. When the map is complete, all the data points are integrated by the NOGA workstation and presented in a 3-dimensional, color-coded reconstruction of the endocardial surface, as well as 9- and 12-segment bull's-eye views that show average values for the LLS and voltage data in each myocardial segment. These maps can be spatially manipulated in real time on a Silicon Graphics (Mountain View, CA, USA) workstation. The 3-dimensional representations acquired during the cardiac cycle can also be used to calculate left ventricular volumes and ejection fraction.

The electromechanical map thus provides a 3-dimensional platform in which the catheter can navigate the left ventricle and provide the necessary orientation for transendocardial injection, as well as a diagnostic platform that can distinguish between ischemic areas (with low LLS [<8%] values and preserved unipolar voltage [>6.9 mV] and areas of infarct (with low LLS (<8%) values and low unipolar voltage (<6.9 mV). Moreover, the Myostar™ catheter allows assessment of myocardial viability at each specific injection site, where the catheter touches the endocardial surface. The operator therefore has the ability to target therapy to viable tissue (e.g. in chronic ischemia, where neoangiogenesis may have an important role) or nonviable tissue (e.g. an area of scarred tissue). Because of the patchy nature of myocardial involvement in human ischemic heart disease, the ability to distinguish underlying tissue characteristics is important in cell delivery. This technology has been widely tested in both animals and humans and has an excellent safety profile.[16–19]

Trans-coronary-venous injection

Trans-coronary-venous injection is performed using a catheter system that is placed percutaneously into the coronary sinus. Initial studies have confirmed the feasibility and safety of this approach in porcine models.[16] This delivery method has also been used to deliver skeletal myoblasts to scarred myocardium in patients with cardiomyopathy.[21] It uses intravascular ultrasound guidance, which enables the operator to extend a catheter and needle away from the pericardial space and coronary artery into the adjacent myocardium. To date, feasibility studies have shown a good safety profile for this technique.[16]

Preliminary data suggest that the efficiency of acute retention (cells remaining in the myocardium in the first hours after injection) using this transvenous method with fluoroscopic guidance is superior to that of endoventricular approaches guided by electromechanical mapping.[22] The limitations of this technique are similar to those mentioned above, regarding the restrictions associated with the tortuosity of coronary veins and the lack of site-specific targeting, but also include the fact that this may be one of the more technically challenging delivery modes. Unlike the transendocardial approach, in which cells are injected perpendicularly into the left ventricular wall, the trans-coronary-venous approach allows parallel cell injection, which may result in greater cell retention.

CONCLUSION

There are various modalities for cell delivery in cardiac stem cell therapy. Cells may be delivered by means of direct surgical injection, intracoronary infusion, retrograde venous infusion, transendocardial injection, and peripheral infusion. Each technique has its own peculiarities, and so the choice of the modality should be based on the clinical scenario in which we find ourselves.

Competing interests
The authors declared they have no competing interests.

References

1 Leone AM *et al.* (2005) Mobilization of bone marrow-derived stem cells after myocardial infarction and left ventricular function. *Eur Heart J* **26:** 1196–1204
2 Shintani S *et al.* (2001) Mobilization of endothelial progenitor cells in patients with acute myocardial infarction. *Circulation* **103:** 2776–2779
3 Wang Y *et al.* (2005) Effect of mobilization of bone marrow stem cells by granulocyte colony stimulating factor on clinical symptoms, left ventricular perfusion and function in patients with severe chronic ischemic heart disease. *Int J Cardiol* **100:** 477–483
4 Wollert KC *et al.* (2004) Intracoronary autologous bone marrow cell transfer after myocardial infarction: the BOOST randomized controlled clinical trail. *Lancet* **364:** 141–148
5 Kocher AA *et al.* (2001) Neovascularization of ischemic myocardium by human bone-marrow derived angioblasts prevents cardiomyocyte apoptosis, reduces remodeling and improves cardiac function. *Nat Med* **7:** 430–436
6 Gao J *et al.* (2001) The dynamic *in vivo* distribution of bone marrow-derived mesenchymal stem cells after infusion. *Cells Tissues Organs* **169:** 12–20
7 Thompson CA *et al.* (2003) Percutaneous transvenous cellular cardiomyoplasty. A novel nonsurgical approach for myocardial cell transplantation. *J Am Coll Cardiol* **41:** 1964–1971
8 Fernández-Avilés F *et al.* (2004) Experimental and clinical regenerative capability of human bone marrow cells after myocardial infarction. *Circ Res* **95:** 742–748
9 Siminiak T *et al.* (2003) Autologous bone marrow stem cell transplantation in acute myocardial infarction—report on two cases. *Kardiol Pol* **59:** 502–510
10 Assmus B *et al.* (2002) Transplantation of progenitor cells and regeneration enhancement in acute myocardial infarction (TOPCARE-AMI). *Circulation* **106:** 3009–3017
11 Strauer BE *et al.* (2001) Intracoronary, human autologous stem cell transplantation for myocardial regeneration following myocardial infarction [in German]. *Dtsch Med Wochenschr* **126:** 932–938
12 Herreros J *et al.* (2003) Autologous intramyocardial injection of cultured skeletal muscle-derived stem cells in patients with non-acute myocardial infarction. *Eur Heart J* **24:** 2012–2020
13 Dib N *et al.* (2005) Safety and feasibility of autologous myoblast transplantation in patients with ischemic cardiomyopathy: four-year follow-up. *Circulation* **112:** 1748–1755
14 Siminiak T *et al.* (2004) Autologous skeletal myoblast transplantation for the treatment of postinfarction myocardial injury: phase I clinical study with 12 months of follow-up. *Am Heart J* **148:** 531–537
15 Pagani FD *et al.* (2003) Autologous skeletal myoblasts transplanted to ischemia-damaged myocardium in humans. Histological analysis of cell survival and differentiation. *J Am Coll Cardiol* **41:** 879–888
16 Thompson CA *et al.* (2003) Percutaneous transvenous cellular cardiomyoplasty: a novel nonsurgical approach for myocardial cell transplantation. *J Am Coll Cardiol* **41:** 1964–1971
17 Smits PC *et al.* (2003) Catheter-based intramyocardial injection of autologous skeletal myoblasts as a primary treatment of ischemic heart failure: clinical experience with six-month follow-up. *J Am Coll Cardiol* **42:** 2063–2069
18 Perin EC *et al.* (2003) Transendocardial, autologous bone marrow cell transplantation for severe, chronic ischemic heart failure. *Circulation* **107:** 2294–2302
19 Kawamoto A *et al.* (2003) Intramyocardial transplantation of autologous endothelial progenitor cells for therapeutic neovascularization of myocardial ischemia. *Circulation* **107:** 461–468
20 Amado L *et al.* (2005) Cardiac repair with intramyocardial injection of allogenic mesenchymal stem cells after myocardial infarction. *Proc Natl Acad Sci USA* **102:** 11474–11479
21 Siminiak T *et al.* (2004) Percutaneous transvenous transplantation of autologous myoblasts in the treatment of postinfarction heart failure: the POZNAN trial. *Eur Heart J* **25 (Suppl):** 264
22 Smits P *et al.* (2002) Efficiency and retention of a percutaneous transendomyocardial injection of VEGF165 by a fluoroscopy guided transendomyocardial injection catheter. In *XIVth World Congress of Cardiology.* Sydney, NSW
23 Sherman W *et al.* (2006) Catheter-based delivery of cells to the heart. *Nat Clin Pract Cardiovasc Med* **3 (Suppl 1):** S57–S64
24 Opie SR and Dib N (2006) Surgical and catheter delivery of autologous myoblasts in patients with congestive heart failure. *Nat Clin Pract Cardiovasc Med* **3 (Suppl 1):** S42–S45

Journal of the American College of Cardiology
© 2003 by the American College of Cardiology Foundation
Published by Elsevier Inc.

Vol. 42, No. 12, 2003
ISSN 0735-1097/03/$30.00
doi:10.1016/j.jacc.2003.06.017

Cell Transplantation

Catheter-Based Intramyocardial Injection of Autologous Skeletal Myoblasts as a Primary Treatment of Ischemic Heart Failure

Clinical Experience With Six-Month Follow-Up

Pieter C. Smits, MD, PHD,* Robert-Jan M. van Geuns, MD, PHD,† Don Poldermans, MD, PHD,* Manolis Bountioukos, MD,* Emile E. M. Onderwater,* Chi Hang Lee, MD,* Alex P. W. M. Maat, MD,* Patrick W. Serruys, MD, PHD*

Rotterdam, The Netherlands

OBJECTIVES We report on the procedural and six-month results of the first percutaneous and stand-alone study on myocardial repair with autologous skeletal myoblasts.

BACKGROUND Preclinical studies have shown that skeletal myoblast transplantation to injured myocardium can partially restore left ventricular (LV) function.

METHODS In a pilot safety and feasibility study of five patients with symptomatic heart failure (HF) after an anterior wall infarction, autologous skeletal myoblasts were obtained from the quadriceps muscle and cultured in vitro for cell expansion. After a culturing process, 296 ± 199 million cells were harvested (positive desmin staining 55 ± 30%). With a NOGA-guided catheter system (Biosense-Webster, Waterloo, Belgium), 196 ± 105 million cells were transendocardially injected into the infarcted area. Electrocardiographic and LV function assessment was done by Holter monitoring, LV angiography, nuclear radiography, dobutamine stress echocardiography, and magnetic resonance imaging (MRI).

RESULTS All cell transplantation procedures were uneventful, and no serious adverse events occurred during follow-up. One patient received an implantable cardioverter-defibrillator after transplantation because of asymptomatic runs of nonsustained ventricular tachycardia. Compared with baseline, the LV ejection fraction increased from 36 ± 11% to 41 ± 9% (3 months, $p = 0.009$) and 45 ± 8% (6 months, $p = 0.23$). Regional wall analysis by MRI showed significantly increased wall thickening at the target areas and less wall thickening in remote areas (wall thickening at target areas vs. 3 months follow-up: 0.9 ± 2.3 mm vs. 1.8 ± 2.4 mm, $p = 0.008$).

CONCLUSIONS This pilot study is the first to demonstrate the potential and feasibility of percutaneous skeletal myoblast delivery as a stand-alone procedure for myocardial repair in patients with post-infarction HF. More data are needed to confirm its safety. (J Am Coll Cardiol 2003; 42:2063–9) © 2003 by the American College of Cardiology Foundation

Cell transplantation is emerging as a potential novel therapeutic approach for the treatment of heart failure (HF). Initial studies with different cell types have shown promising results of cell transplantation in ischemic animal models.

See page 2070

Most preclinical experience has been reported on transplantation of skeletal myoblasts in infarcted myocardium. These studies demonstrated that transplanted skeletal myoblasts in damaged myocardium are capable of cellular engraftment, myotube formation, expression of the slow fiber marker beta-myosin heavy chain, long-term graft survival, and augmentation of ventricular function (1–6). As a result of the outcomes of these animal studies, a pilot safety and feasibility study on percutaneous transplantation of autologous skeletal myoblasts by transendocardial injection as a stand-alone procedure in five patients with ischemic HF was completed. We report on the procedural and six-month follow-up results.

From the *Department of Cardiology, Thorax Center; and the †Department of Radiology, Erasmus Medical Center, Rotterdam, The Netherlands. This study was partly financially supported by Bioheart Inc., Weston, Florida.
Manuscript received April 16, 2003; accepted June 4, 2003.

PROCEDURE

Objectives. The primary objectives of this pilot study are feasibility and safety at six months. The secondary objective was to assess improvement of the left ventricular (LV) function by iterative investigations at baseline and one, three, and six months. The protocol was approved by the local medical ethics committee, and written, informed consent was obtained from all patients.

Patient selection. Only symptomatic patients with New York Heart Association functional class ≥II under optimal medical therapy were selected. All patients were known to have a previous anterior wall myocardial infarction and depressed LV function (left ventricular ejection fraction

JACC Vol. 42, No. 12, 2003
December 17, 2003:2063–9

Abbreviations and Acronyms

DSE = dobutamine stress echocardiography
ECG = electrocardiogram
HF = heart failure
ICD = implantable cardioverter-defibrillator
LAO = left anterior oblique
LV = left ventricle/ventricular
LVEF = left ventricular ejection fraction
MRI = magnetic resonance imaging
NSVT = non-sustained ventricular tachycardia
RAO = right anterior oblique
TDI = tissue Doppler imaging

[LVEF] between 20% and 45% by radionuclide radiography). Myocardial infarction had to be >4 weeks old at the time of implantation. The presence and location of a myocardial scar were defined by: akinesia or dyskinesia at rest during echocardiography, LV angiography, and magnetic resonance imaging (MRI); no contractile reserve during dobutamine stress echocardiography (DSE); and hyperenhancement by gadolinium on the MRI scan. Exclusion criteria for myoblast injections were: target region wall thickness <5 mm by echocardiography or MRI; a history of syncope or sustained ventricular tachycardia or fibrillation or (potential candidate for) implantable cardioverter-defibrillator (ICD) placement; and positive serologic test results for human immunodeficiency virus, hepatitis B or C, or syphilis.

Muscle biopsy. Biopsy of the quadriceps muscle was done under local anesthesia. On average, 8.4 g (range 5 to 13 g) of muscle biopsy was excised through a 10-cm-long surgical incision. All five biopsy procedures were uneventful and done on an outpatient basis. Biopsies were placed in a bottle containing a proprietary solution designed to preserve the biopsy during controlled shipment. The bottle was put in an insulated thermobox with frozen and refrigerated gel packs to maintain temperatures between 2°C and 8°C during transit. The transport conditions were monitored by the use of a programmable temperature monitor (Sensitech, Beverly, Massachusetts). The container was sent to clinical Good Manufacture Practice (BioWhittaker, Cambrex Corp., Walkersville, Maryland) for myoblast cell isolation and expansion. The average transit duration was 41 h (range 35 to 50 h); no temperature excursions were noted.

Cell-culturing process. On receipt at the culturing facility, the biopsies were processed according to the Myocell protocols by Bioheart Inc. The biopsy was minced finely and then dissociated using digestive enzymes. The dissociated tissue was washed several times and filtered until a single-cell suspension was achieved. The expansion culture was initiated when the cells were plated into sterile tissue culture flasks in growth media for skeletal muscle myoblasts. The media were changed at regular intervals; the cells were harvested and replated according to cell confluence parameters. Final harvest was done after three to five passages. Myoblasts were identified using an immunohistochemical marker specific for desmin (DAKO) to identify cells committed to a myogenic differentiation. Specific cell lot release specifications (cell viability, cell identity, and sterility tests) were established before the start of the trial, which, if not met, would result in a re-biopsy of the patient and re-initiation of the culture process. In three patients a re-biopsy was required due to the desmin staining results falling below the lot release criteria. In these patients, a prestimulation procedure was performed using multiple needle punctures of the muscle three days before the biopsy procedure to increase the percentage of myoblast cells in the muscle biopsy (7).

After a culturing period of 17 days (range 14 to 19 days), the harvested cells were formulated in a specially designed transport/injectate media and transferred into a sterile 30-ml bag and sent to our hospital. Shipment was done under the same controlled conditions as after biopsy. The transit time averaged 62 h (range 24 to 96 h), and no temperature excursions were noted. The cells have been validated for having a 96-h shelf life under controlled conditions.

Transplantation procedure. The transplantation procedure was scheduled the day after arrival of the cells. Cell transplantation was done in the cardiac catheterization laboratory. Access was obtained through the femoral artery, and 100 IU/kg heparin was given. The target activated clotting time was between 250 s and 300 s and was regularly checked every half hour. After a coronary and biplane LV angiogram (left anterior oblique [LAO] 60° and right anterior oblique [RAO] 30°) was obtained, an outline of the LV chamber was drawn on transparent tabloids that were taped to the fluoroscopy monitors. Then an electromechanical NOGA map (8) of the LV was obtained using a 7F NOGASTAR catheter (F-curve) connected to the NOGA console (Biosense-Webster, Waterloo, Belgium). Areas exhibiting low voltages and linear local shortening (unipolar voltage <4 mV and linear local shortening <4%) on the NOGA map were considered as the target areas of treatment if these areas were geographically concordant with the scar areas assessed by the preprocedural DSE, MRI, and LV angiogram. We refrained from transendocardial injections into areas with a known wall thickness <5 mm by MRI. With an 8F MYOSTAR (Biosense-Webster) injection catheter, 16 ± 4 (mean ± SD; range 9 to 19) transendocardial injections were made. The catheter has nitinol tubing that ends in a 27-gauge retractable needle. Depending on the average wall thickness of the target region, the needle length was set at 4.5 to 6.0 mm when the catheter tip had a 90° curve. By connecting a 1-ml Luer-Lok syringe to the injection port, the catheter was preloaded with the skeletal myoblast solution. After establishing stable endomyocardial contact on the NOGA map and fluoroscopy, the needle was advanced manually, which often caused ventricular extra beats. Whenever a regular electrocardiographic (ECG) rhythm resumed with persisting, stable endomyocardial contact, injections of 0.3 ml (16.6 million cells) were

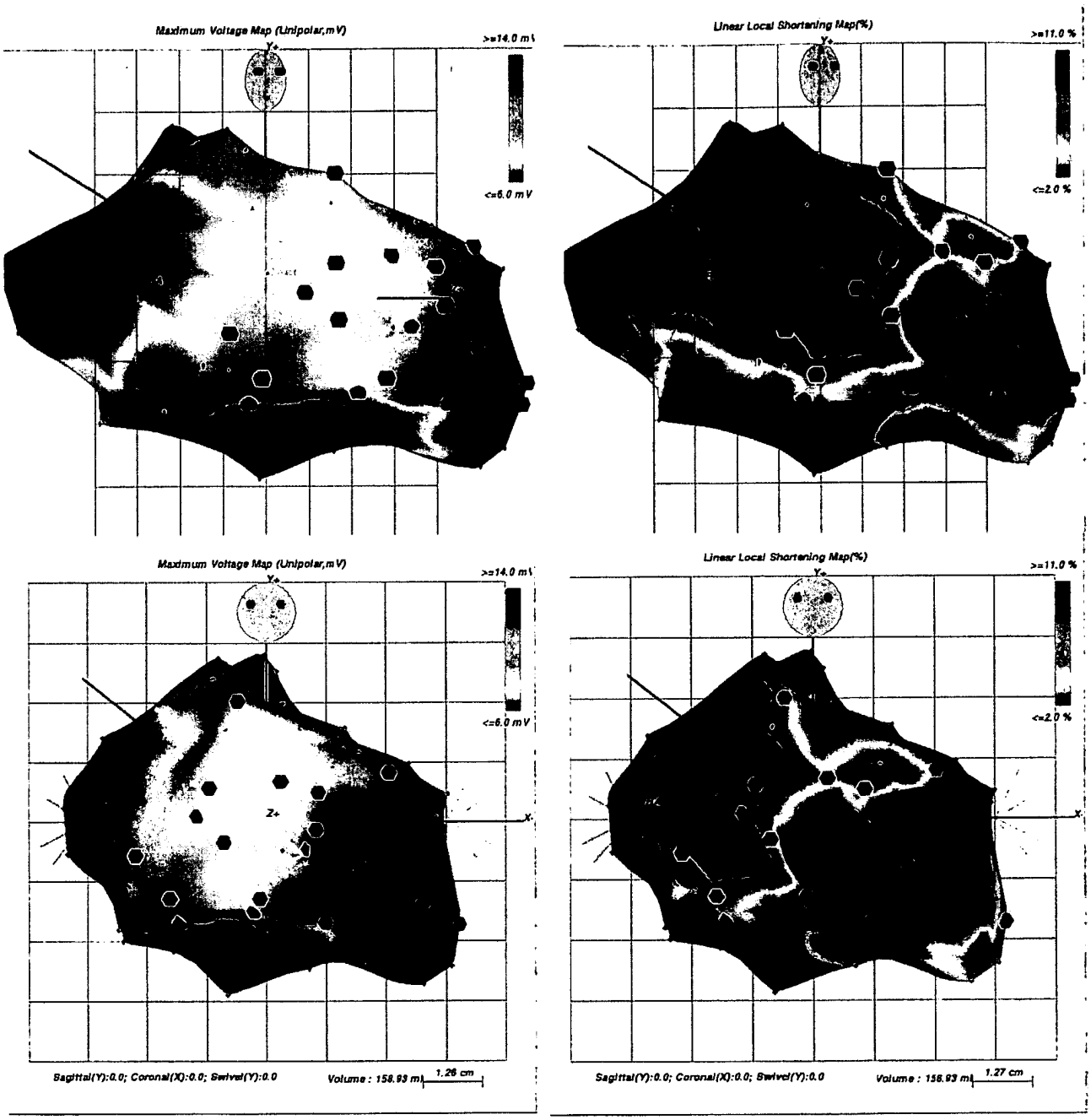

Figure 1. NOGA maps (**left** = unipolar voltage maps; **right** = linear local shortening maps) in the right anterior oblique **(top)** and anteroposterior **(bottom)** views of Patient no. 2 after 19 injections with autologous skeletal myoblasts in the anteroseptal and anterior myocardial scar and border zone. The myocardial scar is indicated in **red** on the unipolar voltage map (<6 mV) and on the local linear shortening map (<2%). The **black dots** indicate the transendocardial injection sites.

made. Only the first patient received 0.1-ml injections (2.5 million cells) because of the limited volume of myoblast solution. Injection sites were marked on the NOGA map (Fig. 1) and the transparent tabloids. Spacing between injection sites was approximately 1.0 cm apart. After the injection procedure, a control biplane LV angiogram was obtained. Afterward, patients were ECG monitored for 18 h, and cardiac enzymes were checked twice at 6- to 8-h intervals. In all five cases, the in-hospital stay was uneventful, and the patients were discharged within 24 h after the procedure.

Methods of assessment. At baseline and one, three, and six months of follow-up, 24-h ambulant ECG monitoring and DSE with pulsed-wave tissue Doppler imaging (TDI) were done. The DSE and TDI procedures were performed with a Hewlett-Packard Sonos 5500 (Andover, Massachu-

Table 1. Patient and Cell Culture Characteristics

Pt. No.	Gender, Age (yrs)	Previous Anterior AMI (years ago)	NYHA Class	Patent LAD	Known Arrythmias	Cells at Harvest × 10^6	Cells Injected × 10^6	Desmin Staining (%)	Cell Viability (%)	Potency (%)
1	F, 78	6	III	Yes	PAT runs	25	25	85	98	90
2	M, 53	3	II/III	Yes	PAT runs	544	293	12	97	20–40
3	M, 55	11	III/IV	No*	PAF, NSVT runs†	183	183	54	95	70
4	M, 59	7	III	Yes	No	211	211	80	95	100
5	M, 49	2	III	Yes	No	382	270	44	98	40

*LAD filled by collateral channels. †Asymptomatic, 8 complexes.
AMI = acute myocardial infarction; LAD = left anterior descending coronary artery; NSVT = non-sustained ventricular tachycardia runs; NYHA = New York Heart Association; PAF = paroxymal atrial fibrillation; PAT = paroxymal atrial tachycardia.

setts) imaging system equipped with second harmonic imaging to optimize endocardial border detection and performed as previously described (9,10). In short, after baseline echocardiography, dobutamine was infused at a starting dose of 5 μg/kg/min for 5 min, followed by 10 μg/kg/min for 5 min (low-dose stage). Dobutamine was then increased by 10 μg/kg/min every 3 min up to a maximum dose of 40 μg/kg/min. Atropine (1 to 2 mg) was added at the end of the last stage if the target heart rate had not been achieved. Images were acquired continuously and recorded on tape at the end of every dose step. In addition, the baseline, low-dose, peak stress, and recovery images (standard apical and short-axis views) were displayed in a cine loop format. Wall motion was scored according to the criteria of the American Society of Echocardiography by two experienced reviewers blinded to the MRI data for systolic wall thickening. Pulsed-wave TDI was performed with a Hewlett-Packard Sonos 5500, and a transducer operating at frequencies of 1.8 or 2.1 MHz with a pulse repetition frequency of 45 to 60 kHz was used. Using a six-segment model, pulsed-wave TDI was performed close to the mitral annulus in the apical four-chamber, apical two-chamber, and apical three-chamber views with high temporal resolution (4 ± 3 ms; range 1 to 7). The depth of the sample volume was kept constant in each patient during DSE. A sample volume with a fixed length of 4 mm was used. The ECG and phonocardiogram were simultaneously recorded with the pulsed-wave TDI velocity profile and stored on videotape. The peak pulsed-wave TDI velocity amplitude of the ejection phase and early and late diastole were measured off-line using a computer-assisted drawing system, and the values were expressed in cm/s (10). Five consecutive beats were analyzed, and the mean velocity values were calculated to minimize the measurement variability determined by respiration. The E/A ratio was also calculated. Cardiac cycles with extrasystolic or postextrasystolic beats or any disturbance of the rhythm were excluded. Recordings and measurements were repeated at baseline and at a low-dose (10 μg/kg/min) dobutamine infusion rate.

Furthermore, at baseline and three and six months of follow-up, the LV volume and LVEF were assessed by biplane LV angiography and technetium-99m–labeled erythrocyte radionuclide scintigraphy. Biplane LV angiography was done in the LAO 60° and RAO 30° projections with 100-ml sphere calibration in the isocenter. Quantitative analysis was performed using CAAS II software (Pie Medical, Maastricht, The Netherlands). Also, at baseline and three-month follow-up, a MRI scan of the heart was obtained. The studies were performed on a 1.5-T whole-body MRI system (Sonata, Siemens, Erlangen, Germany). Patients were placed in a supine position with a four-channel quadrature body phased-array coil placed over the thorax. For quantitative analysis, multiple parallel short-axis slices covering the heart from base to apex were obtained using a ECG-triggered breath-hold cine gradient-echo sequence. Imaging parameters were: repetition time of 3.2 ms, echo time of 1.6 ms, and flip angle 65°, which resulted in a temporal resolution of 47 ms. Quantitative analysis was performed using standardized software (Argus Siemens, Erlangen, Germany). Endocardial and epicardial contours were traced using semi-automatic software to calculate the LV volumes and LVEF. Each short-axis image was divided into eight segments of 45°, which resulted in 64 to 80 segments per patient, depending on the number of short-axis slices covering the heart from base to apex. Regional wall thickening was calculated for each segment by subtracting the end-diastolic wall thickness from the end-systolic wall thickness. Delayed contrast-elucidated MRI images were used to identify transmural and nontransmural infarcts using a three-dimensional inversion-recovered gradient echo sequence 15 min after injection of 0.1 mmol gadolinium-based contrast agent.

RESULTS

Baseline patient characteristics and cell-culturing results are summarized in Table 1. No procedural complications occurred. Only in one patient (Patient no. 5) was minor elevation of creatine kinase and its MB fraction (<2 times upper level) and troponin T (0.16 μg/l) noted after the procedure.

During follow-up, Patient no. 3 needed to be hospitalized at six weeks after the procedure due to progressive HF and long asymptomatic runs of non-sustained ventricular tachycardia (NSVT) on Holter monitoring. After recompensation, telemetry still showed NSVT, and an ICD was implanted prophylactically. In the other four patients, no adverse events or ventricular arrhythmias were observed.

Table 2. Global Left Ventricular Function Results

Pt. No.	Baseline			3-Month Follow-Up			6-Month Follow-Up	
	LVEF (%) by Angiography (EDV/ESV)	LVEF (%) by Nuclear Radiography	LVEF (%) by MRI (EDV/ESV)	LVEF (%) by Angiography (EDV/ESV)	LVEF (%) by Nuclear Radiography	LVEF (%) by MRI (EDV/ESV)	LVEF (%) by Angiography (EDV/ESV)	LVEF (%) by Nuclear Radiography
1	43 (187/107)	39	36 (189/120)	47 (203/108)	42	41 (190/113)	54 (200/93)	56
2	40 (135/82)	45	43 (167/96)	42 (150/87)	40	37 (166/104)	49 (156/80)	39
3	18 (153/126)	32	22 (169/132)	26 (148/109)	26	25 (166/125)	46 (150/82)	42
4	40 (201/120)	36	26 (206/152)	44 (195/110)	31	24 (202/154)	33 (211/141)	32
5	42 (141/83)	37	35 (125/82)	47 (119/64)	40	37 (132/82)	43 (129/43)	57
Average	36 ± 11 (163 ± 29/103 ± 21)	38 ± 5	32 ± 8 (171 ± 30/116 ± 28)	41 ± 9* (163 ± 35/95 ± 20)	36 ± 7	33 ± 8 (171 ± 27/116 ± 26)	45 ±8 (169 ± 35/94 ± 27)	45 ± 11

*p = 0.009.
EDV and ESV = end-diastolic and end-systolic volume, respectively; LVEF = left ventricular ejection fraction; MRI = magnetic resonance imaging.

Global LV function results at three- and six-month follow-up are summarized in Table 2. Compared with baseline, angiographic LVEF at three months increased from 36 ± 11% to 41 ± 9% (p = 0.009). This increase in LVEF, however, was not observed by nuclear or MRI assessment at three-month follow-up. At six-month follow-up, both angiographic and nuclear LVEF assessments showed a trend toward increased LVEF (36 ± 11% to 45 ± 8% [p = 0.23] and 38 ± 8% to 45 ± 11% [p = 0.07], respectively).

The MRI analysis of regional wall thickening showed a descriptive shift toward more regional wall thickening in the target segments and less regional wall thickening in the remote hyperkinetic segments (Figs. 2 and 3). By comparing the marked injection sites on the NOGA map and the fluoroscopy sheets with the MRI segments, 87 of the 304 MRI segments (all 5 patients) were identified as injected segments. Paired analysis of these injected segments showed significantly increased wall thickening at follow-up (0.9 ± 2.3 mm at baseline vs. 1.8 ± 2.4 mm at 3-month follow-up, p = 0.008).

In all five patients at baseline, DSE showed no signs of ischemia or ventricular tachycardias. Compared with baseline, the TDI results of the target anteroseptal and anterior wall showed a trend toward increased contraction velocity at six-month follow-up (anteroseptal wall: 5.4 ± 1.9 cm/s vs. 6.1 ± 0.8 cm/s at rest and 8.8 ± 3.4 cm/s vs. 9.1 ± 2.5 cm/s at low-dose dobutamine; anterior wall: 5.2 ± 1.9 cm/s vs. 5.9 ± 0.7 cm/s at rest and 6.7 ± 1.7 vs. 7.5 ± 1.6 cm/s at low-dose dobutamine).

DISCUSSION

Treatment of ischemic HF remains a problem. A significant proportion of patients with congestive HF remain symptomatic despite maximal medication. Alternative therapies, including surgical cardiomyoplasty, resynchronization therapy, LV assist device, and cardiac transplantation, have their own indications and limitations. Cell transplantation has emerged as a potential new treatment strategy. Different cell types have been used for transplantation in initial preclinical experiments, but to date, most experience has been accumulated with skeletal myoblasts. There are several features that make skeletal myoblasts an attractive cell type for cardiac cell transplantation. Skeletal myoblasts can easily be obtained in sufficient quantity directly from the patient (autologous), negating the problems of organ shortage, ethical concerns, and immunosuppressive therapy. Skeletal myoblasts are relatively more resistant to ischemia than cardiomyocytes, thus favoring cellular engraftment within the ischemic or infarcted myocardium. Furthermore, the capillary density of infarcted myocardium resembles the environment in which normal skeletal muscle is obtained. The biopsy procedure is mildly invasive, and patients can be discharged within 1 h after the procedure. Although skeletal myoblasts are not cardiomyocytes, in vitro studies and in vivo observations have shown that these cells can transform

JACC Vol. 42, No. 12, 2003
December 17, 2003:2063–9

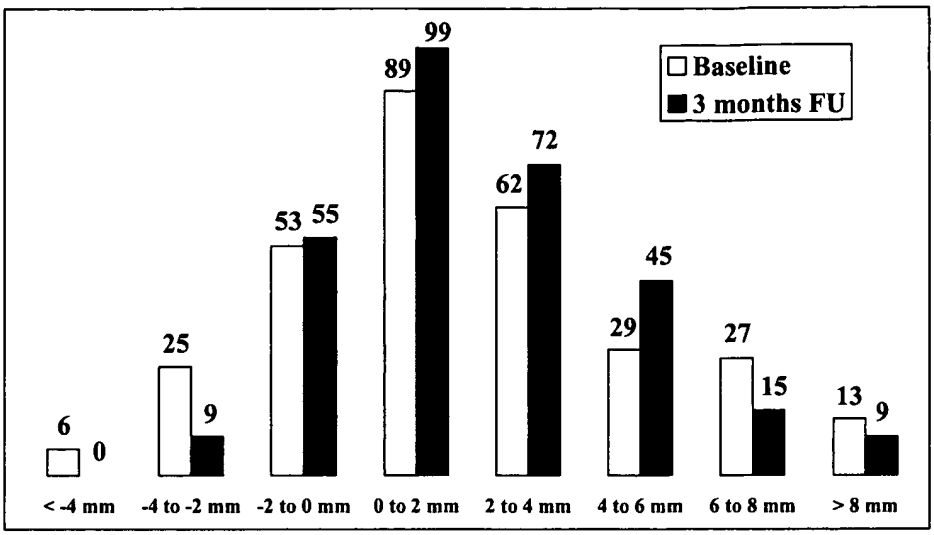

Figure 2. Changes in regional wall thickening for all 304 magnetic resonance imaging segments. The **open and solid bars** indicate the number of segments with wall thickening at baseline and three-month follow-up (FU), respectively. Compared with baseline, less segments showed thinning and more segments showed moderate thickening at three-month follow-up, and less segments with greater wall thickening were observed at that point.

into contractile cells with expression of beta-myosin heavy chain, like cardiomyocytes (6,11). The major limitation, however, is the lack of evidence of electromechanical coupling between the grafted myoblasts and the native cardiomyocytes in vivo (11), as well as the potential danger of inducing a reentry circuit for ventricular arrhythmias by the formed grafted myotubes in the scarred myocardium. It is known that skeletal myoblasts lose their capability to express major adhesion and gap junction proteins like N-cadherin and connexin-43, which are essential for electromechanical coupling, when the cells differentiate into myotubes (11).

We report on the first five percutaneous and stand-alone cellular cardiomyoplasty procedures as a potential new treatment modality for ischemic HF. In post-myocardial infarction patients with LVEF <45% and symptoms of HF, autologous skeletal myoblasts were injected into the scarred myocardium by an injection catheter. No periprocedural complications occurred, and during a 3- to 12-month follow-up period, in one case, an ICD was implanted at 2 months based on a prophylactic indication because of asymptomatic NSVT runs. At three-month follow-up, in all five patients, a significant moderate increase in global LV function by LV angiography was noted. This angiographic LVEF improvement, however, was not consistently observed in all patients by nuclear or MRI assessment. Because MRI and, to a lesser extent, radionuclide angiography have

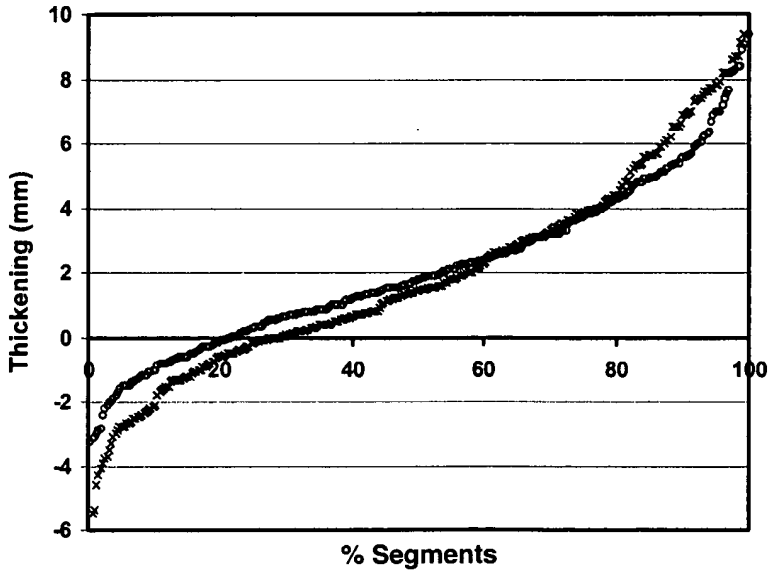

Figure 3. Cumulative distribution of regional wall thickening segments by magnetic resonance imaging at baseline **(open circles)** and three-month follow-up (×). At follow-up, there was a descriptive shift toward less thinning and moderate thickening in the target regions and less thickening in the normokinetic and hyperkinetic remote areas, indicating a kind of left ventricular remodeling.

been recently recognized as the most reliable and accurate methods for assessment of LV dimensions and function (12,13), cellular cardiomyoplasty efficacy studies focusing on change in LVEF should incorporate one or both of these techniques.

Regional analysis by MRI showed a significant increase in wall thickening at the target areas at three-month follow-up in all five patients. This paradox between equal global and improved regional LV function is probably explained by the remodeling of the LV, in which regional improvement of injected dyskinetic and akinetic segments is counterbalanced by less thickening of the hypercontractile remote segments, as seen by MRI. Potentially, less neurohormonal stimulation after treatment may also have occurred, resulting in less vigorous contraction of normal segments and less dyskinesia of infarcted segments. One of the limitations in our functional assessment is the missing information on the pulse-pressure double product at the different assessment time points. Pressure-volume loop and neurohormonal marker measurements in future may overcome this limitation.

Feasibility and safety. We cannot draw firm conclusions from this initial experience, but we believe that catheter-based cell transplantation in HF patients is feasible and that the transendocardial catheter-based cell delivery technique is safe from a procedural point of view. An important question about potential arrhythmogenic properties of skeletal myoblast transplantation is still unanswered. Although no syncope or malignant arrhythmias were observed in our pilot study, we have observed in two consecutive follow-up studies on catheter-based autologous skeletal myoblast transplantation in eight patients, two sudden deaths and three ventricular arrhythmias (one symptomatic and two asymptomatic) within three months after the procedure (unpublished data, P. C. Smits, 2003). These serious adverse events necessitated elementary changes in the protocols of the consecutive studies. Currently, both phase 1 follow-up studies have restarted with enrollment of patients with ICDs and rigorous rhythm monitoring before and after the procedure.

Also, Menasché et al. (14) have reported four ICD implantations within one month after the procedure in a phase 1 trial involving transepicardial autologous skeletal myoblast injections during bypass surgery in 10 post-myocardial infarction patients with an average baseline LVEF of 23%. However, the arrhythmogenic incidents observed in this study and in other skeletal myoblast cell transplantation studies may also reflect the natural course of this high-risk population for arrhythmias. Furthermore, the likelihood of finding a non-sustained ventricular arrhythmia recording on serial Holter monitoring is 40% in patients with HF (15). Therefore, the question remains unanswered whether skeletal myoblast transplantation is arrythmogenic and safe.

From this initial experience, we conclude that catheter-based cell transplantation with autologous skeletal myoblasts for the treatment of ischemic HF is feasible and promising. However, extensive pre- and post-procedural monitoring studies for arrhythmias and well-defined functional parameters are needed to evaluate the safety and efficacy of cellular cardiomyoplasty procedures in the near future.

Acknowledgments

The help and support of Warren Sherman, MD, Howard B. Haines, PhD, and John M. Harvey, MPH, in this study are greatly appreciated.

Reprint requests and correspondence: Dr. Pieter C. Smits, Department of Cardiology, Thorax Center, Room Bd 412, Erasmus Medical Center Rotterdam, Dr. Molewaterplein 40, 3015 GD Rotterdam, The Netherlands. E-mail: p.c.smits@erasmusmc.nl.

REFERENCES

1. Chiu RC-J, Zibatis A, Kao RL. Cellular cardiomyoplasty: myocardial regeneration with satellite cell implantation. Ann Thorac Surg 1995; 60:12–8.
2. Taylor DA, Atkins BZ, Hungspreugs P, et al. Regenerating functional myocardium: improved performance after skeletal myoblast transplantation. Nat Med 1998;4:929–33.
3. Pouzet B, Vilquin JT, Messas E, et al. Factors affecting functional outcome following myoblast cell transplantation. Ann Thorac Surg 2001;71:844–51.
4. Murry CE, Wiseman RW, Schwartz SM, et al. Skeletal myoblast transplantation for repair of myocardial necrosis. J Clin Invest 1996; 98:2512–23.
5. Jain M, DerSimonian H, Brenner DA, et al. Cell therapy attenuates deleterious ventricular remodeling and improves cardiac performance after myocardial infarction. Circulation 2001;103:1920–7.
6. Ghostine S, Carrion C, Souza LCG, et al. Long-term efficacy of myoblast transplantation on regional structure and function after myocardial repair. Circulation 2002;106 Suppl I:I131–6.
7. Law PK. Myoblast transfer: gene therapy for muscular dystrophy. In: Medical Intelligence Unit. Austin, TX: R. G. Landes Company, 1994.
8. Ben-Haim SA, Osadchy D, Schuster I, et al. Nonfluoroscopic, in vivo navigation and mapping technology. Nat Med 1996;2:1393–5.
9. Elhendy A, van Domburg RT, Bax JJ, et al. Optimal criteria for the diagnosis of coronary artery disease by dobutamine stress echocardiography. Am J Cardiol 1998;82:1339–44.
10. Rambaldi R, Poldermans D, Bax JJ, et al. Doppler tissue velocity sampling improves diagnostic accuracy during dobutamine stress echocardiography for the assessment of viable myocardium in patients with severe left ventricular dysfunction. Eur Heart J 2000;21:1091–8.
11. Reinecke H, MacDonald GH, Hauschka SD, et al. Electromechanical coupling between skeletal and cardiac muscle: implications for infarct repair. J Cell Biol 2000;149:731–40.
12. Matheijssen NA, Baur LH, Reiber JH, et al. Assessment of left ventricular volume and mass by cine magnetic resonance imaging in patients with anterior myocardial infarction intra-observer and inter-observer variability on contour detection. Int J Card Imaging 1996;12: 11–9.
13. Bax JJ, Lamb H, Dibbets P, et al. Comparison of gated single-photon emission computed tomography with magnetic resonance imaging for evaluation of left ventricle function in ischemic cardiomyopathy. Am J Cardiol 2000;86:1299–305.
14. Menasché P, Hagege AA, Vilquin JT, et al. Autologous skeletal myoblast transplantation for severe postinfarction left ventricular dysfunction. J Am Coll Cardiol 2003;41:1078–83.
15. Cleland JGF, Chattopaddhyay S, Khand A, Houghton T, Kaye GC. Prevalence and incidence of arrhythmias and sudden death in heart failure. Heart Fail Rev 2002;7:229–42.

Electrophysiological properties of human mesenchymal stem cells

Jürgen F. Heubach[1], Eva M. Graf[1], Judith Leutheuser[1], Manja Bock[1], Bartosz Balana[1], Ihor Zahanich[1], Torsten Christ[1], Sabine Boxberger[2], Erich Wettwer[1] and Ursula Ravens[1]

[1]*Institut für Pharmakologie und Toxikologie, and* [2]*Medizinische Klinik und Poliklinik I, Medizinische Fakultät Carl Gustav Carus der TU Dresden, D-01307 Dresden, Germany*

Human mesenchymal stem cells (hMSC) have gained considerable interest due to their potential use for cell replacement therapy and tissue engineering. One strategy is to differentiate these bone marrow stem cells *in vitro* into cardiomyocytes prior to implantation. In this context ion channels can be important functional markers of cardiac differentiation. At present there is little information about the electrophysiological behaviour of the undifferentiated hMSC. We therefore investigated mRNA expression of 26 ion channel subunits using semiquantitative RT-PCR and recorded transmembrane ion currents with the whole-cell voltage clamp technique. Bone marrow hMSC were obtained from healthy donors. The cells revealed a distinct pattern of ion channel mRNA with high expression levels for some channel subunits (e.g. Kv4.2, Kv4.3, MaxiK, HCN2, and α1C of the L-type calcium channel). Outward currents were recorded in almost all cells. The most abundant outward current rapidly activated at potentials positive to +20 mV. This current was identified as a large-conductance voltage- and Ca^{2+}-activated K^+ current, conducted by MaxiK channels, due to its high sensitivity to tetraethylammonium (IC_{50} = 340 μM) and its inhibition by 100 nM iberiotoxin. A large fraction of cells also demonstrated a more slowly activating current at potentials positive to –30 mV. This current was selectively inhibited by clofilium (IC_{50} = 0.8 μM). Ba^{2+} inward currents, stimulated by 1 μM BayK 8644 were found in a few cells, indicating the expression of functional L-type Ca^{2+} channels. Other inward currents such as sodium currents or inward rectifier currents were absent. We conclude that undifferentiated hMSC express a distinct pattern of ion channel mRNA and functional ion channels that might contribute to physiological cell function.

(Resubmitted 25 September 2003; accepted after revision 23 October 2003; first published online 24 October 2003)
Corresponding author U. Ravens: Institut für Pharmakologie und Toxikologie, Medizinische Fakultät Carl Gustav Carus der TU Dresden, Fetscherstrasse 74, D-01307 Dresden, Germany. Email: ravens@rcs.urz.tu-dresden.de

The bone marrow stem cell pool is a rich source of undifferentiated cells that may play a role in physiological tissue restoration (Caplan, 1991; Orlic *et al.* 2002). Two subpopulations of stem cells can be distinguished, the haematopoietic and stromal (mesenchymal) stem cells. The adult bone marrow stem cells have gained much interest as starting material for tissue engineering and cell therapy. Aspiration and defined processing of human bone marrow allows the expansion of a multipotent cell population, the human mesenchymal stem cells (hMSC; Pittenger *et al.* 1999). The cells can be used for *in vitro* studies, where differentiation into osteogenic (Haynesworth *et al.* 1992), chondrogenic (Mackay *et al.* 1998; Winter *et al.* 2003) and adipogenic (Janderova *et al.* 2003) lineage can be readily achieved.

There is evidence that hMSC can also obtain the characteristics of excitable cells. hMSC have the capability of differentiating into cells with a neurone-like phenotype both *in vitro* (Kim *et al.* 2002) and *in vivo* (Zhao *et al.* 2002), and implantation into the ischaemic brain of rats improved functional performance of the apoplectic animals (Zhao *et al.* 2002). In addition, hMSC might be a suitable cell source for cardiac tissue repair in patients with myocardial infarction or heart failure. It has been shown that hMSC injected into the ventricles of immunodeficient mice engrafted into the myocardium and appeared to differentiate into cardiomyocytes, albeit with low frequency (Toma *et al.* 2002). In a swine myocardial infarction model injection of hMSC into the region of myocardial infarction reduced the extent of wall thinning and improved contractile dysfunction (Shake

DOI: 10.1113/jphysiol.2003.055806

et al. 2002). Based on these findings it was proposed that hMSC would be useful for cardiomyoplasty (Cahill *et al.* 2003).

Meanwhile, cell therapy for the treatment of ischaemic heart disease has advanced to early clinical studies. In patients with myocardial infarction, bone marrow cells were obtained and injected into the infarct-related coronary artery using a balloon catheter (Assmus *et al.* 2002; Strauer *et al.* 2002). Other groups implanted the cells into ischaemic myocardium by means of a catheter-directed intramural injection (Tse *et al.* 2003) or directly injected cells into the infarct border zone during open heart surgery (Stamm *et al.* 2003). All four studies report an improvement of myocardial perfusion or functional parameters. With the exception of one study (Stamm *et al.* 2003), the mononuclear bone marrow cell suspension employed for cardiac injection was highly heterogeneous, and the used cell populations varied greatly among these clinical studies.

Up to now, enhanced incidence of arrhythmias in patients who received cardiac implantation of bone marrow stem cells has not been noted, although such risk cannot be excluded (Al-Radi *et al.* 2003). Cardiomyocytes derived from human embryonic stem cells have the potential to generate arrhythmic action potentials under some conditions (Zhang *et al.* 2002). At present there is little information about the electrophysiological properties of human bone marrow stem cells. We therefore studied the population of hMSC isolated in our laboratory from bone marrow samples. Commercially available hMSC were used for comparison. We investigated whether undifferentiated hMSC express ion channel mRNA and whether the cells have functional ion currents.

Methods

Isolation of hMSC and cell culture conditions

All parts of this study, especially isolation of human mesenchymal stem cells (hMS) were performed according to the Declaration of Helsinki. The study was approved by the local ethics committee and written informal consent was obtained from donors of bone marrow and cardiac samples. Bone marrow samples were collected from 16 healthy donors at the Mildred Scheel Bone Marrow Transplantation Center of the University Clinics, Dresden hMSC were isolated and cultured according to modifications of previously reported methods (Haynesworth *et al.* 1992; Pittenger *et al.* 1999). Briefly, an aliquot from bone marrow aspirate diluted with PBS–0.5% human serum albumin (HSA) was layered over a Percoll solution (d = 1.073 g ml^{-1}, Biochrom, Germany) and centrifuged at 900 *g* for 30 min. Mononuclear cells at the interface were recovered, washed twice in PBS–HSA and seeded into 75 cm^2 flasks containing Dulbecco's modified Eagle's medium (DMEM, low glucose) supplemented with 2 mM GlutaMAX, 10 U ml^{-1} penicillin, 100 $\mu g\ ml^{-1}$ streptomycin (all from Gibco Invitrogen, UK) and 10% fetal calf serum (Biochrom). The medium was completely changed after 24 h. After automatic counting cells were maintained in a humidified atmosphere at 5% CO_2 and 37°C until reaching 90% confluency. For subcultivation the cells were replated at a density of 5000 cells cm^{-2} (Bruder *et al.* 1997). Aliquots of different passages were used for flow-cytometric characterization of the cells (FACS calibor 3CS, Becton Dickinson).

In addition to hMSC isolated in our laboratory we investigated commercially available hMSC (Poietics, BioWhittaker, San Diego, CA, USA) for comparison. These hMSC originated from three Caucasian female donors aged 18, 19 and 26 years (lot numbers 0F2014, 1F0658 and 1F1061). The cells were obtained from the supplier in the 1st or 2nd passage and were certified by the following surface markers: $CD29^+$, $CD44^+$, $CD105^+$, $CD166^+$ (each > 95%) and $CD14^-$, $CD34^-$, $CD45^-$ (each < 1%). hMSC from BioWhittaker were cultured with the respective mesenchymal stem cell growth medium (hMSCGM; BioWhittaker). mRNA was extracted from subconfluent 4th passages and patch clamp experiments were performed on cells from the 3rd to 6th passage.

Electrophysiological recordings

Membrane currents were measured in the whole cell configuration of the patch clamp technique at 21–23°C (Hamill *et al.* 1981). Initially, we tried to record currents of hMSC attached to glass cover slips. However, electrophysiological analysis was not feasible under these conditions. We therefore detached subconfluent hMSC from small culture flasks (T25, Greiner, Frickenhausen, Germany) using trypsin–EDTA. After centrifugation at 88 *g* for 5 min cells were recovered in culture medium. The suspension was stored at room temperature and used within 6 h.

For electrophysiological recordings the cells were transferred to a small chamber (Warner Instruments, Hamden, CT, USA) and allowed to attach to the glass bottom for 15 min. Subsequently, the bath was perfused continuously at a rate of 1.8 ml min^{-1}. Ion channel blockers were applied with the use of a magnet valve or with a rapid solution exchanger (DAD-12 superfusion system, ALA Scientific Instruments,

Table 1. Primer pairs and conditions for PCR

Gene	Acc. no.	Forward primer sequence (5′–3′)	Reverse primer sequence (5′–3′)	Binding position	Length (bp)	Cycle no.	Reference
α1C	L29534	TGA GAC CGA GTC CGT CAA A	GAA AAT CAC CAG CCA GTA GAA GA	1333–1522	190	30	Grammer *et al.* 2000
α1D	M83566	GCA AGA TGA CGA GCC TGA G	ATG GTT ATG ATG GTT ATG ACA C	5164–5407	244	30	
α1G	AF134986	ATG GCC ATG GAG CAC TAC C	CGA GGC GTT GAC CTC GAT T	4882–5100	219	30	Huang *et al.* 2000
α1H	AF051946	CAC TCA TTC TAC AAC TTC ATC	CTC TCC CGC TGC TTC GTC	1250–1368	190	30	
α1S	L33798	GGT GGA GGC TGC GAT GGA	ATG GCT GTT GCT ATG GTT GCT	4989–5262	274	30	Barry, 2000
GAPDH	J02642	AAC AGC GAC ACC CAC TCC TC	GGA GGG GAG ATT CAG TGT GGT	869–1126	258	29	
HCN1	AF064876	TTG TCG TCT TTA CTC ACT TTC	CTC CTG ATT GTT GAA AAC AC	1311–1491	181	30	
HCN2	AJ012582	GCC TGA TCC GCT ACA TCC A	TGC GAA GGA GTA CAG TTC AC	1078–1304	227	30	Ludwig *et al.* 1999
HCN4	AJ132429	CGC CTC ATT CGA TAT ATT CAC	CGC GTA GGA GTA CTG CTT C	1743–1970	228	30	Ludwig *et al.* 1999
Kir2.1	L36069	GAC CTG GAG ACG GAC GAC	AGC CTG GAG TCT GTC AAA GTC	910–1302	393	30	Wang *et al.* 1998*b*
Kir2.2	U16861	TTG AGT AAA CAG GAC ATT GAC	CTG GTT GTG AAG GTC TAT G	1171–1560	390	30	Wang *et al.* 1998*b*
Kir2.3	S72503	TAT GGC ATG GGC AAG GAG	AGC TGC CTC CTC CTC CAT C	912–1274	363	30	Wang *et al.* 1998*b*
Kir3.1	U50964	TCC CCT TGA CCA ACT TGA ACT	ACG ACA TGA GAA GCA TTT CCT C	928–1301	374	30	
Kir3.4	U52154	TTT TCC AAC AAC GCA GTC A	CAC AAC TTC AAA CTC TTC C	983–1285	303	30	
Kv1.1	L02750	CCA TCA TTC CTT ATT TCA TCA C	CTC TTC CCC CTC AGT TTC TC	782–1269	488	30	
Kv1.4	L02751	GAG AGA AGA GGA AGA CAG GGC	TGG GGT GCT GAA GTA TCA TTC	828–1073	246	34	Ohya *et al.* 1997
Kv1.5	M83254	CAT TGC CCT GCC TGT GCC	TGC TCC CGC TGA CCT TCC	1677–1834	158	34	
Kv2.1	L02840	TAC TGG GGC ATC GAC GAG A	GAC TGG CCG AAC TCA TCG A	547–854	308	34	Schultz *et al.* 2001
Kv3.1	S56770	AGG ACG AGC TGG AGA TGA CC	AAG AAG AGG GAA GCG AAG G	505–664	160	35	Wulfsen *et al.* 2000
Kv4.2	AJ010969	ATC TTC CGC CAC ATC CTG AA	GAT CCG CAC GGC ACT GTT TC	700–1061	362	34	Postma *et al.* 2000
Kv4.3	AF205857	GAT GAG CAG ATG TTT GAG CAG	AGC AGG TGG TAG TGA GGC C	1534–1639	106	28	
Kv7.1	U89364	CAT CAT CGA CCT CAT CGT GG	TTC TCG GCA GCA TAG CAC CT	399–959	561	30	Lai *et al.* 1999
Kv7.2	AF033348	GGA CTC GCT TTC AGG AAG G	CCC TTC CCC TTG GCA G	1331–1494	164	35	
Kv7.3	AF033347	GGA GAG GAG ATG AAA GAG GAG	TGA AGA AAG GAA AAG AGA CGA C	736–1093	358	35	
MaxiK	U11058	ACA ACA TCT CCC CCA ACC	TCA TCA CCT TCT TTC CAA TTC	1222–1531	310	35	
SCN5A	M77235	CCT AAT CAT CTT CCG CAT CC	TGT TCA TCT CTC TGT CCT CAT C	2814–3022	208	35	
Twik1	U336321	TCC TGC TTC TTC TTC ATC	AGG CTC ATT TTG CTT CTG GTC	759–1143	385	30	Wang *et al.* 1998*b*

The table specifies forward and reverse primers used for semi-quantitative RT-PCR of various ion channels and the primers for the housekeeping gene glyceraldehyde-3-phosphate dehydrogenase (GAPDH). Primers were constructed with HUSAR program package (Senger *et al.* 1998) or modified using published sequences. Annealing temperature (T_A) was 60°C for all primers except for Kv7.2 (54°C) and Kv7.3 (58°C). After initial denaturation at 94°C for 5 min, cycling conditions were 94°C for 30 s, T_A for 30 s and 72°C for 30 s for all primers except for Kv7.1 (94°C for 60 s, T_A for 60 s and 72°C for 60 s) and Kv7.3 (94°C for 30 s, T_A for 30 s and 72°C for 60 s). Numbers of cycles are indicated for each primer pair. For a final extension reaction mixes were heated at 72°C for 7 min.

Westbury, NY, USA). Membrane currents were measured with a List EPC-7 amplifier (List Medical Instruments, Darmstadt, Germany) under the control of pCLAMP 5.5 software (Axon Instruments, Foster City, CA, USA). Patch electrodes were pulled with a horizontal puller (Zeitz, München, Germany) from filamented borosilicate glass. The tip resistance was 1.5–4.0 MΩ, when filled with electrode solution. Membrane capacitance was measured with fast depolarizing ramp pulses (from –55 to –50 mV, duration 5 ms) at the beginning of each experiment as previously described (Heubach *et al.* 1999). Series resistance was routinely checked and compensated by 50–70%. Membrane currents were low-pass filtered at 2 kHz.

Outward currents were recorded with the following bath solution (mM): NaCl 150, KCl 5.4, $CaCl_2$ 2, $MgCl_2$ 2, glucose 11, Hepes 10 (pH 7.4 adjusted with NaOH). The pipette solution included (mM): NaCl 8, KCl 40, potassium aspartate 100, Tris-GTP 0.1, Mg-ATP 5, $CaCl_2$ 2, EGTA 5 (pH adjusted to 7.3 with KOH) resulting in a calculated free Ca^{2+} and Mg^{2+} concentration of 64 nM and 587 μM, respectively (Fabiato & Fabiato, 1979). Solutions containing different concentrations of tetraethylammonium chloride were prepared by mixing bath solution as described above with a bath solution in which 20 mM NaCl was replaced by 20 mM tetraethylammonium chloride, in order to keep osmolarity constant. All membrane potentials were corrected for a calculated liquid junction potential of 12.5 mV (JPCalc version 2.2; Barry, 1994). The stimulation frequency was 0.25 Hz. Current amplitude was determined at the end of individual depolarizing steps.

The presence of functional Ca^{2+} channels was assessed with Na^+-free external solution supplemented with 2 mM Ca^{2+} or 10 mM Ba^{2+} under conditions previously described (Heubach *et al.* 2000). Inward rectifier currents were measured in 20 mM K^+ solution with ramp pulses from −100 mV to +40 mV of 1250 ms duration from a holding potential of –80 mV as used for the recording of inward rectifier currents in human atrial myocytes (Dobrev *et al.* 2000). In order to enhance the ATP-sensitive potassium current ($I_{K,ATP}$), if present, the intrapipette Mg-ATP concentration was reduced to 0.1 μM. The presence of hyperpolarization-activated currents was investigated as described for mouse ventricular myocytes (Graf *et al.* 2001). Membrane potential was hyperpolarized for 2 s by steps to –140 mV from a holding potential of –40 mV.

Isolation of RNA and polymerase chain reaction experiments

Total RNA (0.5 μg) isolated by the guanidinium method (Chomczynski & Sacchi, 1987) was reverse transcribed in a 21 μl reaction mixture that contained 75 mM KCl, 50 mM Tris-HCl (pH 8.3), 3 mM $MgCl_2$, 0.5 mM of each dATP, dCTP, dGTP, dTTP, 600 ng of random hexamer primers, 10 mM DTT, 2 U of RNase inhibitor and 10 U of Superscript RNase H^- (Invitrogen, Karlsruhe, Germany) according to the manufacturer's instructions. For PCR experiments 3 μl aliquots of total cDNA were amplified (Master Cycler, Eppendorf, Hamburg, Germany) in a 25 μl reaction mixture containing 50 mM KCl, 10 mM Tris-HCl (pH 8.3), 1.5 mM $MgCl_2$, 0.2 mM of each dATP, dCTP, dGTP, dTTP, 25 pmol of each forward and reverse primer and 1.25 U of *Taq* polymerase (Applied Biosystems, Weiterstadt, Germany; for primers and reaction conditions see

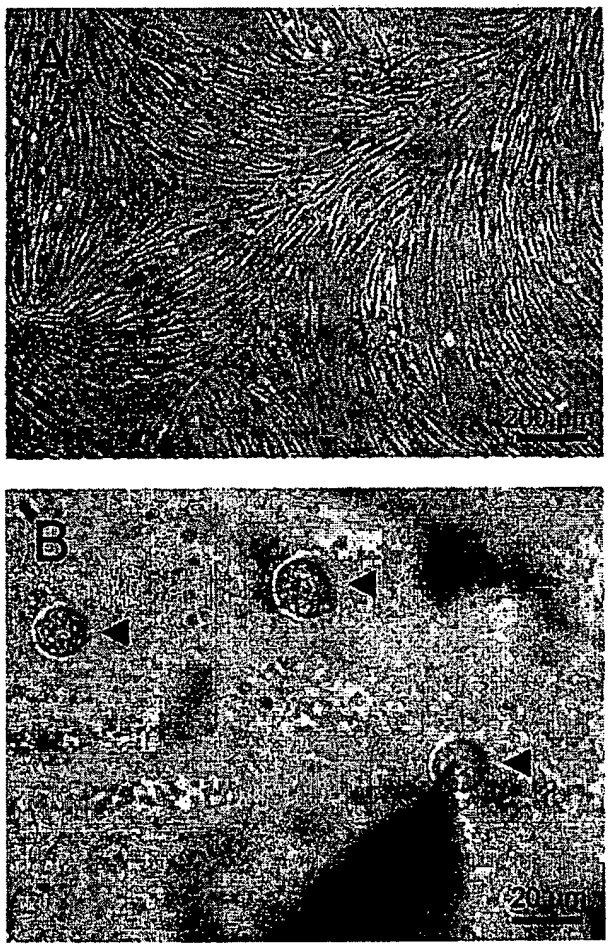

Figure 1. Morphology of human mesenchymal stem cells (hMSC)
A, subconfluent culture with characteristic morphology of adherent cells. *B*, ball-shaped cells after detachment from culture-flasks by trypsin–EDTA treatment and 15 min attachment to the glass bottom of the patch-clamp chamber. Three hMSC are indicated by arrowheads. The right cell was used for electrophysiological recordings (note the patch-electrode).

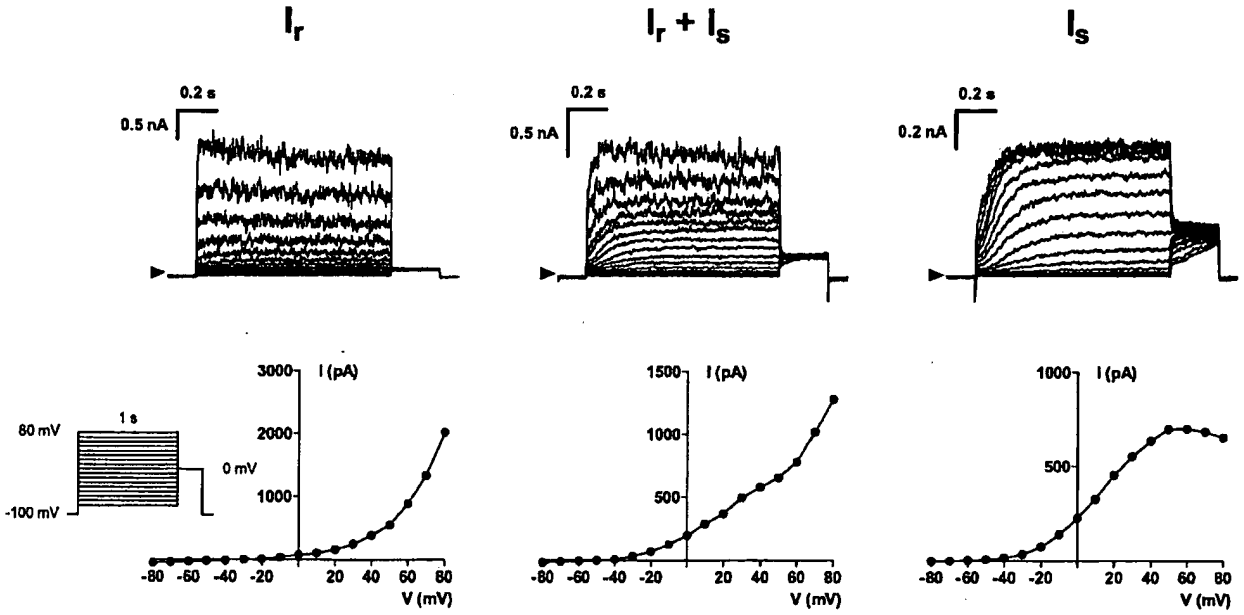

Figure 2. Different patterns of outward currents in hMSC
The top row demonstrates examples of original current traces recorded in three different hMSC, respective current–voltage relations are depicted below. Most of the cells demonstrated a rapidly activating current I_r with noisy current traces at potentials positive to +20 mV (left, a hMSC from 6th passage). The occurrence of a pure slowly activating current I_s was a rare event (right, 5th passage). This current activated at potentials positive to −30 mV and demonstrated saturation at strongly depolarized potentials. In many cells the two currents coexisted (middle, 6th passage) and the ratio between I_r and I_s was highly variable.

Table 1). The same single-stranded cDNA product was used to analyse the expression of all genes described. To ensure that amplification was in the exponential range, the progress of PCR was determined by amplifying identical reaction mixtures for ascending numbers of cycles. After the cited number of PCR cycles amplification rate was sufficient without reaching saturation for any of the amplicons. PCR products were analysed by agarose gel electrophoresis (2% agarose) and ethidium bromide staining. Bands imaged by a CCD camera (Biostep,

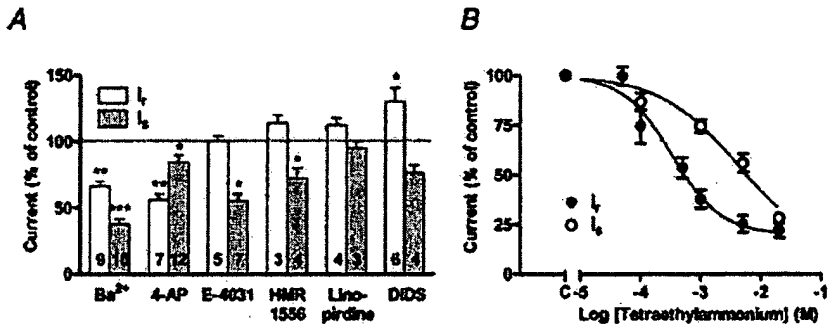

Figure 3. Pharmacological characterization of the two outward currents I_r and I_s
I_r was analysed at the potential +70 mV, whereas I_s was tested at +20 mV to avoid contamination by I_r (see Methods). *A*, effects of the K^+ channel blockers Ba^{2+} (1 mM), 4-aminopyridine (4-AP, 3 mM), E-4031 (5 μM), HMR1556 (1 μM), linopirdine (10 μM) and of the chloride channel blocker DIDS (200 μM). Outward current amplitudes in the presence of blockers were normalized to predrug amplitudes. Numbers in columns give the number of cells tested. *B*, effects of tetraethylammonium on outward current amplitudes. The effects of all compounds were reversible upon washout. $^*P < 0.05$, $^{**}P < 0.01$, $^{***}P < 0.001$; Student's paired *t* test.

Jahnsdorf, Germany) were analysed via optic densitometry with Phoretix 1D software (Biostep).

Chemicals

All chemicals used were of analytical grade and were purchased from commercial suppliers (Sigma, Deisenhofen, Germany, and VWR, Darmstadt, Germany). 4-Aminopyridine, BayK 8644, tetraethylammonium chloride, linopirdine and 4,4′-diisothiocyanatostilbene-2,2′-disulphonic acid (DIDS) were ordered from Sigma. Clofilium tosylate was from Lilly (Indianapolis, IN, USA), E-4031 was from Eisai Co. (Ibaraki, Japan), and HMR1556 was from Aventis (Frankfurt, Germany). Recombinant iberiotoxin was obtained from Calbiochem (San Diego, CA, USA) and recombinant ergtoxin was ordered from Alomone Laboratories (Jerusalem, Israel). Hanatoxin was a kind gift from Dr Kenton J. Swartz (National Institute of Neurological Disorders and Stroke, NIH Bethesda, MA, USA). Solutions containing peptide

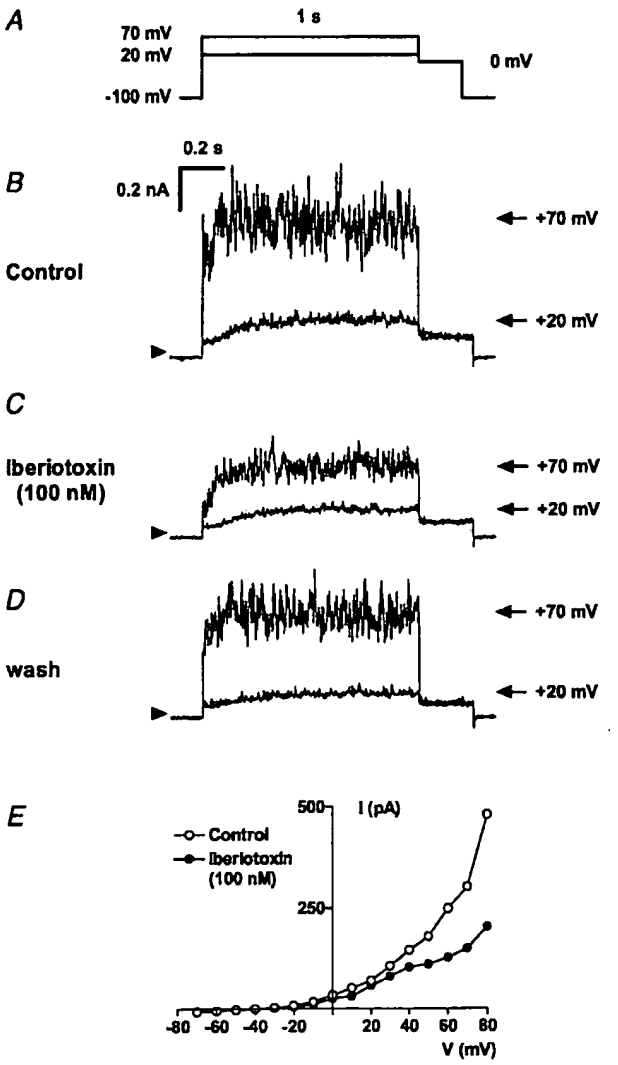

Figure 4. Reversible inhibition of I_r by 100 nm iberiotoxin, a blocker of Ca^{2+}-activated K^+ channels of large conductance
A, voltage protocol. Current traces are shown at +20 mV (I_s) and at +70 mV ($I_r + I_s$) under control conditions (*B*), in the presence of 100 nM iberiotoxin (*C*) and after washout (*D*). The current–voltage relation in the absence and presence of iberiotoxin shows selective inhibition of I_r without major block of I_s (*E*; hMSC from 4th passage).

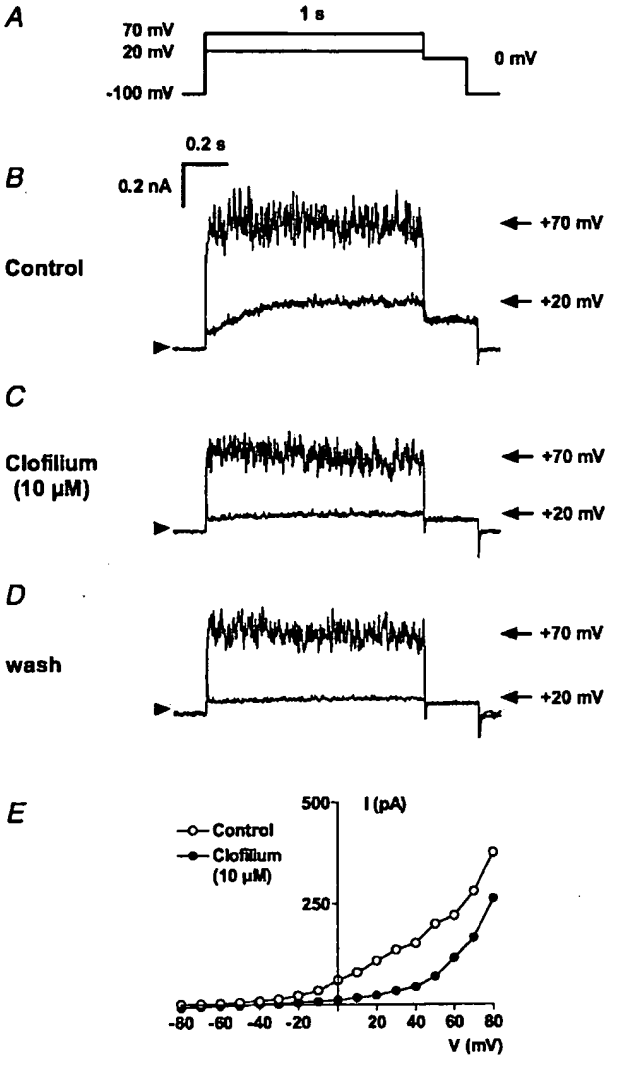

Figure 5. Irreversible block of I_s by 10 μm clofilium, a non-selective blocker of K^+ currents
A, voltage protocol. Current traces are shown at +20 mV (I_s) and at +70 mV ($I_r + I_s$) under control conditions (*B*), in the presence of 10 μM clofilium (*C*) and after washout (*D*). The current–voltage relation in the absence and presence of clofilium shows selective inhibition of I_s without major block of I_r (*E*; hMSC from the 4th passage).

toxins were supplemented with 0.1% bovine serum albumin.

Data analysis and statistics

As shown below we detected two different outward currents (I_t and I_s) in hMSC which variably contributed to total outward current. Differences in voltage dependence of the two currents allowed the classification of hMSC in cells with exclusive occurrence of I_t, I_s or a mixture of both currents. We defined hMSC with exclusive prevalence of I_t current as cells where the ratio between current measured at +20 mV (I_{20}) and current measured at +70 mV (I_{70}) was below 0.25 (compare Fig. 1). A ratio of I_{20} and I_{70} of 0.25–0.5 defined cells with coexistence of both currents and I_{20}/I_{70} above 0.5 defined cells with exclusive occurrence of I_s. Significance of differences between means was tested using Student's paired or unpaired t test with a level of $P < 0.05$ taken to be statistically significant. ANOVA followed by Bonferroni's *post hoc* test was applied in most cases when several groups were compared.

Results

Characterization of hMSC

Human mesenchymal stem cells (hMSC) isolated by our group were characterized by means of flow cytometry. Cells from passages 0 and 1 were positive for CD29 (93 ± 2%), CD105 (92 ± 3%), and CD166 (95 ± 1%), and were negative for CD34 (0%), and CD45 (2 ± 1%) ($n = 3$–6 different donors). These levels remained constant during repeated subcultivation up to the last passage (5th) investigated by flow cytometry. The cultures demonstrated a characteristic growth pattern (Fig. 1*A*) of a homogeneous cell phenotype. Electrophysiological recordings were performed using ball-shaped cells (Fig. 1*B*) obtained after trypsin–EDTA treatment of the cultures shown in Fig. 1*A*.

Outward currents of hMSC

Almost all human mesenchymal stem cells (hMSC) investigated demonstrated outward currents (102 out of 118 cells). Distribution of current patterns and current amplitudes were independent of hMSC source (isolated by our group, $n = 25$ cells *versus* commercial supplier, $n = 77$ cells) and of passage number. Therefore, the pooling of the results for further analysis appeared to be justified.

The most frequently observed current was a rapidly activating outward current which we named I_t (Fig. 2, left). This current activated at potentials positive to +20 mV and only slightly inactivated at positive potentials during prolonged pulses of 1 s duration. Activation of I_t was associated with an increased noise of the current recordings (Fig. 2, left and middle). Tail currents were absent at 0 mV (Fig. 2, left) and also at more negative potentials (data not shown). Mean current density was 16.1 ± 1.8 pA pF^{-1} at +70 mV in 44 cells that exclusively demonstrated I_t. Forty-nine cells demonstrated an additional current (Fig. 2, middle) that activated at more negative potentials and with slower kinetics. This current is referred to as I_s. Only nine cells exclusively demonstrated this I_s current (Fig. 2, right). I_s did not inactivate and saturated at +50 mV. Mean current density in these nine hMSC was 11.4 ± 1.8 pA pF^{-1} at +70 mV. Cell capacitance as a measure of cell size was similar in hMSC that

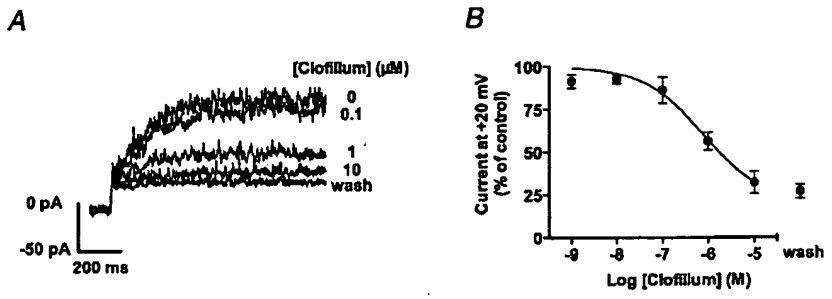

Figure 6. Concentration-dependent block of I_s by clofilium
A, representative current traces at voltage steps from −100 mV to +20 mV in the absence and presence of different clofilium concentrations. The inhibition of I_s was not reversible after washout of the drug. *B*, summary of effects. Inhibition by clofilium was analysed at +20 mV to avoid interference from I_t. Up to three increasing concentrations were tested in one cell ($n = 2$–4 cells per concentration).

exclusively demonstrated I_r (54.1 ± 2.9 pF, $n = 44$) or I_s (54.8 ± 6.7 pF, $n = 9$) or the coexistence of both currents (55.2 ± 3.6 pF, $n = 49$). Membrane potential, however, was significantly more negative in cells demonstrating I_s current as compared to cells lacking I_s (–35.2 ± 1.6 mV, $n = 29$, *versus* –28.9 ± 2.1 mV, $n = 17$; $P < 0.05$).

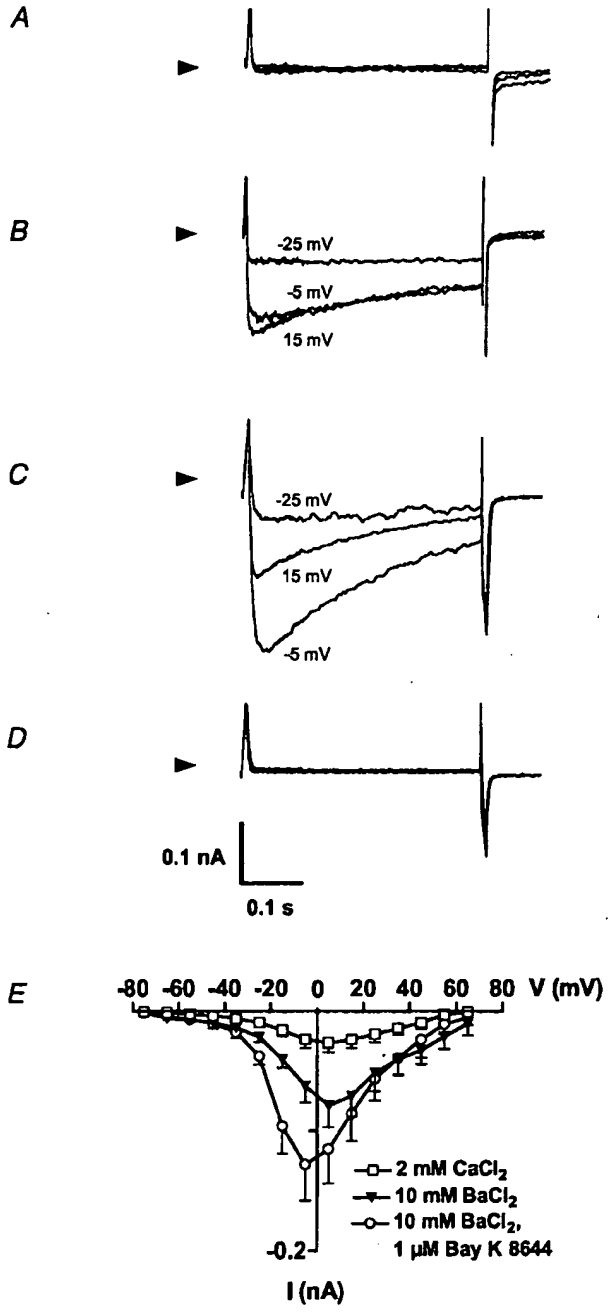

Figure 7. Ca^{2+} and Ba^{2+} currents of hMSC
Original current traces of a representative cell are shown at –25 mV, –5 mV and 15 mV in the presence of 2 mM Ca^{2+} (*A*), 10 mM Ba^{2+} (*B*), 10 mM Ba^{2+} plus 1 µM BayK 8644 (*C*) and 100 µM Cd^{2+} (*D*). Currents were elicited during 400 ms step depolarizations from a holding potential of –95 mV. Arrowheads indicate zero current.
Current–voltage relations of the Cd^{2+}-sensitive currents are shown in (*E*) for $n = 10$ cells.

Characterization of I_r and I_s

Characterization of the two currents depended on their appropriate separation. Investigation of I_r with pharmacological tools was performed on cells that exclusively demonstrated I_r and currents were analysed at a potential of +70 mV (compare Fig. 2, left). However, at +70 mV I_s was contaminated by I_r in most cells (Fig. 2, middle). We therefore analysed I_s at +20 mV, a potential where I_s amplitude was indeed not at maximum, but free of I_r.

Ba^{2+} significantly blocked both currents, with 1 mM Ba^{2+} having a larger effect on I_s than on I_r (Fig. 3*A*). 4-Aminopyridine, an unselective blocker of K^+ currents (3 mM), reduced I_r to approximately 50% but only slightly inhibited I_s. The selective blocker of cardiac delayed rectifier I_{Kr}, E-4031 (5 µM; Sanguinetti & Jurkiewicz, 1990) had no effect on I_r, whereas I_s was reduced by 50%. The highly selective HERG channel blocker ergtoxin (100 nM; Gurrola *et al.* 1999) did not inhibit I_s in three hMSC investigated (101 ± 4% of control; data not shown).

A possible relationship of I_s to cardiac delayed rectifier I_{Ks} was tested with HMR1556 (1 µM; Gögelein *et al.* 2000). There was only a slight block of I_s without modulation of I_r (Fig. 3*A*). Linopirdine (10 µM), which blocks K^+ channels Kv7.2 and Kv7.3 (i.e. KCNQ2 and 3; Wang *et al.* 1998*a*), had no effect on I_r and I_s. Hanatoxin, a spider toxin that blocks Kv2.1 channels (Swartz & MacKinnon, 1995) did not block I_s in two cells investigated (data not shown). In addition we investigated the effects of DIDS, a specific inhibitor of cellular anion permeability including Cl^- conductance (200 µM; Hume *et al.* 2000). This compound significantly stimulated I_r, but had no effect on I_s (Fig. 3*A*).

Application of tetraethylammonium chloride markedly reduced the amplitudes of both currents (Fig. 3*B*). I_s was blocked by tetraethylammonium with half-maximum inhibition at a concentration of 4.1 mM. I_r was found to be more sensitive to this blocker ($IC_{50} = 0.34$ mM), and this, together with other characteristics, suggested that I_r was conducted by voltage- and Ca^{2+}-activated K^+ channels of large conductance (MaxiK).

To identify the channel molecule responsible for I_r we applied iberiotoxin, a selective blocker of MaxiK channels (Galvez *et al.* 1990; Fig. 4). Iberiotoxin (100 nM) inhibited current measured at +70 mV to 51 ± 1% of control amplitude in four cells and the extent of noise, typical for

I_r, was clearly reduced. I_s measured at +20 mV was largely unaffected by iberiotoxin. However, I_s current at +20 mV was irreversibly blocked by clofilium (Castle, 1991) with little effect on I_r (Fig. 5). The IC_{50} value for the inhibition of I_s by clofilium was 0.79 μM, as shown in Fig. 6.

Inward currents of hMSC

The conditions applied for recording outward currents were also suitable for detecting sodium inward currents, but sodium currents were absent in all cells investigated. In addition we tested for the presence of functional Ca^{2+} channels. At 2 mM external Ca^{2+} it was hard to identify clearly any inward current (Fig. 7*A*). However, after switching to 10 mM Ba^{2+}, 10 out of 70 cells demonstrated inward currents that were stimulated by 1 μM BayK 8644 and completely blocked by 100 μM Cd^{2+} (Fig. 7*B–D*). The currents activated around –35 mV and peaked at –5 to 5 mV (Fig. 7*E*), consistent with Ba^{2+} currents conducted by L-type Ca^{2+} channels of other cell types. The capacitance of cells with Ba^{2+} currents (116 ± 17 pF) was significantly larger than the capacitance of cells where Ba^{2+} currents were below the limit of detection or absent (67.6 ± 3.8 pF; $P < 0.05$).

Inward rectifier currents were assessed with high external K^+ solution (20 mM, see Methods) to increase K^+ reversal potential and thereby to emphasize the inward branch of these currents (Dobrev *et al.* 2000). Inward currents were small in amplitude and could hardly be distinguished from putative small leak currents (n = 11 cells, data not shown). There were no effects of 1 mM Ba^{2+}, a non-selective blocker of inward rectifier currents. Carbachol (2 μM) did not stimulate inward currents, indicating a lack of muscarinic receptors and/or a lack of the acetylcholine-stimulated inward rectifier current $I_{K,ACh}$. Furthermore, the $I_{K,ATP}$ channel opener rilmakalim (10 μM) and the $I_{K,ATP}$ channel blocker glibenclamide (10 μM) did not modulate inward currents in these 11 cells. The hyperpolarization-activated inward current I_f was absent in five hMSC investigated (data not shown).

mRNA expression of ion channel subunits in hMSC

Finally, we investigated the expression pattern for ion channel isoform mRNA in undifferentiated hMSC. Samples from human atrium and ventricle were taken as control tissues for comparison. hMSC isolated by our group and hMSC obtained from the commercial source exhibited a consistent pattern of ion channel mRNA. Figure 8 demonstrates mRNA expression for ion channel subunits associated with outward currents. There was clear mRNA amplification for Kv4.2 and Kv4.3, two ion channel subunits responsible for transitory outward currents, but

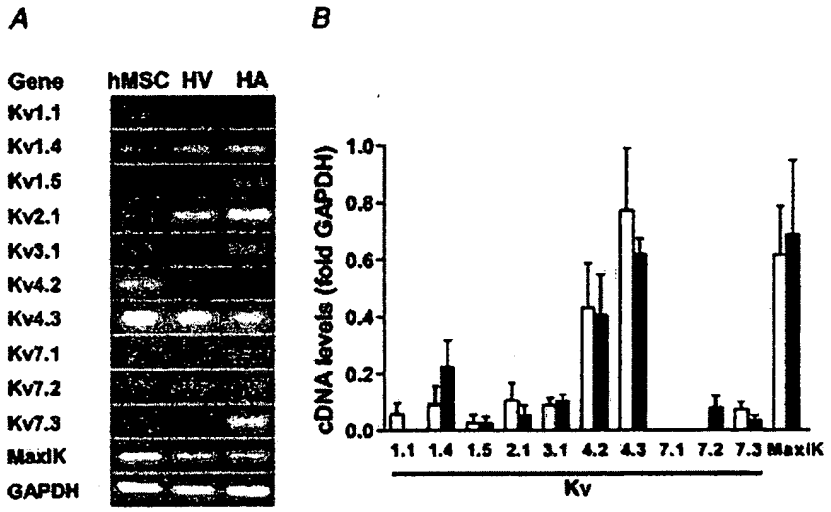

Figure 8. Amplification of mRNA of ion channel subunits related to outward currents by RT-PCR
A, original gels demonstrating amplification of ion channel subunit transcripts in hMSC, human ventricle (HV) and human atrium (HA). *B*, summary of amplification with hMSC samples isolated by our group (open bars, n = 3–5 donors) and with commercially available hMSC (filled bars, n = 3 donors). High mRNA expression levels were detected for channels that conduct transitory outward currents (Kv4.2 and Kv4.3). In addition, MaxiK channels, responsible for large-conductance Ca^{2+}-activated K^+ currents, were strongly expressed. Please note, that despite the absence of, for instance, Kv1.5 in this hMSC sample (*A*) others did express this channel leading to a small mean value.

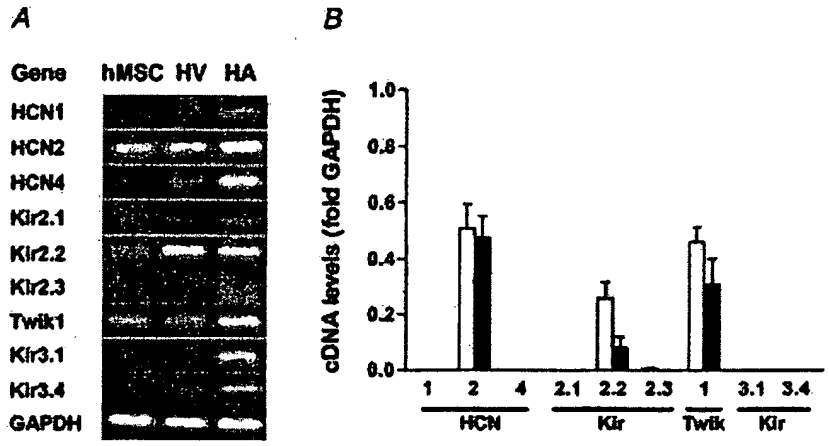

Figure 9. Amplification of mRNA of ion channel subunits related to hyperpolarization-activated inward currents and inward rectifier currents by RT-PCR
A, original gels. *B*, summary of mean values from hMSC samples isolated by our group (open bars, $n = 4$ donors) and from commercially available hMSC (filled bars, $n = 3$ donors). We found strong amplification of cDNA derived from mRNA for the hyperpolarization-activated and cyclic nucleotide-gated channel (HCN) isoform 2 (HCN2), but no amplification for HCN1 and HCN4. High mRNA levels were deteted for the two inward rectifier (Kir) subunits Kir2.2 and Twik1, whereas mRNA for the two inward rectifier channels Kir3.1 and Kir3.4 associated with cardiac $I_{K,ACh}$ was absent or below the detection limit.

transient outward currents were not observed in hMSC. However, the high levels of MaxiK mRNA were in line with the detection of an iberiotoxin-sensitive outward current (I_t) in most of the hMSC investigated. In addition we detected low levels of mRNA for Kv1.1, Kv1.4, Kv1.5, Kv2.1, Kv3.1, Kv7.2 and Kv7.3.

mRNA expression levels of channel subunits conducting hyperpolarization-activated currents and inward rectifier currents are shown in Fig. 9. There was strong expression of mRNA for the hyperpolarization-activated and cyclic nucleotide-gated ion channel isoform 2 (HCN2) in all samples of hMSC, but the respective current I_f was not observed (see above). Similarly, there were high levels of mRNA for two channel subunits associated with the inward rectifier current I_{K1}, Kir2.2 and Twik1, but inward rectifier currents were absent. There was no mRNA expression for Kir3.1 and Kir3.4, responsible for the cardiac acetylcholine-stimulated inward rectifier current $I_{K,ACh}$.

RT-PCR results for Na^+ and Ca^{2+} channel subunits are shown in Fig. 10. mRNA for the Na^+ channel isoform SCN5A was only detected in one sample. However, there was strong expression of the L-type Ca^{2+} channel α1C subunit in all hMSC samples, whereas mRNA levels for other α1 subunits of the L-type Ca^{2+} channel (α1D, α1S) or T-type Ca^{2+} channel (α1G, α1H) were low or undetectable. As shown in the original gels of Figs 8–10, expression levels for several ion channels were in the same order of magnitude as in tissue samples from human heart. The expression patterns were similar in hMSC isolated by our group and in hMSC obtained from the commercial source.

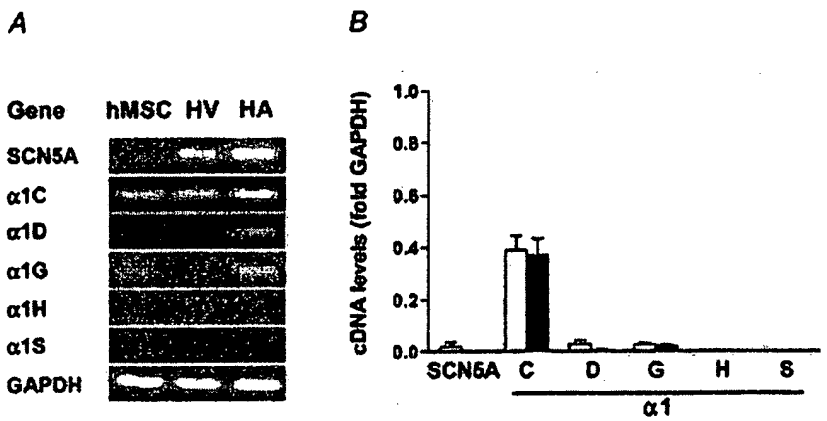

Figure 10. Amplification of mRNA of ion channel subunits related to Na^+ or Ca^{2+} inward currents by RT-PCR
A, original gels. *B*, summary of mean values from hMSC samples isolated by our group (open bars, $n = 4$–5 donors) and from commercially available hMSC (filled bars, $n = 3$ donors). High expression levels were only found for the α1C subunit of L-type Ca^{2+} channels.

Discussion

In the context of *in vivo* and *in vitro* differentiation of human mesenchymal stem cells (hMSC) into excitable cells we describe the electrophysiological properties of undifferentiated hMSC. We recorded two distinct outward currents, present either alone or in combination, in almost all cells investigated. A small fraction of cells demonstrated functional Ca^{2+} channels. Semi-quantitative RT-PCR from mRNA of cultured hMSC revealed a consistent expression pattern of ion channel subunits.

Identification of outward currents

Most hMSC demonstrated outward currents that were inhibited by K^+ channel blockers such as Ba^{2+} and 4-aminopyridine, but were not blocked by DIDS, a blocker of Cl^- currents. This general finding suggests that both currents I_f and I_s are carried by K^+.

The most prevalent outward current of hMSC was I_f, a rapidly activating current which hardly demonstrated any inactivation. One clue towards the identification of its molecular nature is provided by the high sensitivity to tetraethylammonium. There are only a few K^+ channels that are blocked with IC_{50} values around 0.3 mM, namely the Kv1.1 channel, channels of the Kv3 family, Kv7.2 channels and the voltage- and Ca^{2+}-activated K^+ channels of large conductance MaxiK (Rudy & McBain, 2001).

The electrophysiological properties and the pharmacological profiles of Kv1.1, Kv3, and Kv7.2 channels are incongruous with those of I_f current (Coetzee *et al.* 1999). We positively identified I_f as the large-conductance Ca^{2+}-activated K^+ current due to the following additional findings: (i) typical electrophysiological properties, (ii) noisy current traces, which we interpret to be due to large-conductance single channel openings, (iii) sensitivity to iberiotoxin, a specific blocker of MaxiK channels, and finally (iv) high expression levels of MaxiK mRNA in hMSC. MaxiK channels are expressed in many cells and tissues, including neurones, smooth muscle cells and secretory glands (Wallner *et al.* 1999). Moreover, Ca^{2+}-activated K^+ channels were found in osteoblasts (Westkamp *et al.* 2000), adipocytes (Pershadsingh *et al.* 1986), endothelial cells (Wiecha *et al.* 1998) and fibroblasts (Estacion, 1991), i.e. cell types that can be derived from undifferentiated hMSC.

Identification of I_s based on a comparison of its electrophysiological and pharmacological properties with those of known channels is difficult. Slow kinetics of activation suggested some relation to cardiac delayed rectifier I_{Kr}, which is associated with HERG channels, and I_{Ks}, related to KCNQ1/minK. However, the I_{Kr} blocker E-4031 blocked I_s to a lower extent than expected for the relatively high concentration of 5 μM. In addition, the peptide blocker of I_{Kr}, ergtoxin, had no effect, suggesting that I_s does not flow through HERG channels. The blocker of cardiac I_{Ks}, HMR1556, only affected I_s to a moderate extent. Based on slow activation kinetics and other electrophysiological parameters, Kv2.1, Kv7.2 and Kv7.3 were further candidate molecules for I_s, but hanatoxin and linopirdine did not block this current. It was found that clofilium inhibited I_s with relatively high potency and high selectivity over I_f, and hence can be used in functional experiments for selective suppression of I_s.

Our failure to identify the molecular nature of I_s could be due to the presence of β subunits. The number of possible potassium channel constructs is extended by the presence of β subunits that associate with several pore-forming potassium channel subunits. This association often results in a profound modification of electrophysiological or pharmacological behaviour of the respective current (Nerbonne, 2000). The involvement of one or more β subunits in I_s of hMSC is possible and renders the attribution to known potassium channel subunits even more difficult.

Ion channel mRNA, though expressed at high levels, is not necessarily translated into functionally active channel molecules. The discrepancy between the presence of mRNA but lack of the respective current is most striking for the channel subunits Kv4.2 and Kv4.3, associated with transient outward current I_{to}, but also for the hyperpolarization-activated and cyclic nucleotide-gated channel isoform 2 (HCN2), responsible for the I_f inward current. The reason for the lack of functional channel molecules remains unclear.

Functional role and heterogeneity of ion currents in hMSC

MaxiK channels are sensors of intracellular Ca^{2+}. By this property they regulate membrane potential in a Ca^{2+}-dependent manner (Kawano *et al.* 2003). The activity of MaxiK channels is modulated by phosphorylation via specific receptor-dependent signalling cascades, as recently shown for pathways involving the cellular proto-oncogene pp60 (c-Src; Alioua *et al.* 2002). The large-conductance Ca^{2+}-activated K^+ current could therefore be an effector of trophic factors within the body fluids or cell culture medium.

The functional role of the unidentified I_s current is even more obscure. I_s activates at much more negative

potentials than the large-conductance Ca^{2+}-activated K^+ current. The presence of I_s should therefore shift the membrane potential of hMSC to more negative potentials. In fact this was observed: hMSC with I_s current had a significantly more negative membrane potential than hMSC without I_s.

Regulation of intracellular calcium in hMSC depends on several mechanisms, and voltage-operated Ca^{2+} currents do not contribute much (Kawano *et al.* 2002; Kawano *et al.* 2003). Only 15% of hMSC demonstrated a small dihydropyridine-sensitive calcium current in the presence of a high external calcium concentration (Kawano *et al.* 2002). This dihydropyridine-sensitive Ca^{2+} current was probably due to the cardiac isoform of the L-type calcium channel, since we found high levels of mRNA for the pore-forming α1C subunit in hMSC. Our electrophysiological observations confirm the low frequency of hMSC with functional L-type Ca^{2+} channels. Ca^{2+} and Ba^{2+} currents were observed in cells that were significantly larger than cells without these currents. Given a fixed current density, the small current amplitudes would be more easily detectable in large cells. However, this does not completely explain the heterogeneity of Ca^{2+} and Ba^{2+} currents. Heterogeneity was also observed with outward currents, where currents of individual hMSC were not consistent, i.e. some of the cells exclusively showed the large-conductance Ca^{2+}-activated K^+ current, others expressed I_s current or a mixture of both. Why do individual cells express different currents? There are several possible reasons. Despite the presence of consistent marker proteins on the cell surface and homogeneous morphology of the cultivated cells, the cells investigated possibly did not come from an absolutely homogeneous population of hMSC, but also included fractions of more or less committed progenitor cells (Minguell *et al.* 2001; Muraglia *et al.* 2000). These cell populations could slightly differ in their ion current patterns. Another possible reason is the dependence of ion current expression on cell function. For example, there is evidence that current expression varies at different phases of the cell cycle (Ouadid-Ahidouch *et al.* 2001; Chittajallu *et al.* 2002). Nevertheless, there is only a limited number of different currents observed in undifferentiated hMSC. The modification of present currents and the occurrence of new currents could be suitable markers of *in vitro* hMSC differentiation.

Consequences and perspectives

Preliminary clinical studies have shown that the injection of undifferentiated bone marrow stem cells into the infarcted heart can improve cardiac function. The fate of the implanted cells, whether they differentiate into cardiomyocytes, contribute to neoangiogenesis, or just perish, remains unclear. The injection transfers the undifferentiated cells, that can well include hMSC, directly into an electrically active environment. We have demonstrated that hMSC express a consistent pattern of ion channels and at least three different ion currents. Therefore, the cells have some bioelectrical activity, as also shown by others (Kawano *et al.* 2002, 2003). Based on our finding we cannot judge whether implantation of hMSC is safe or includes the risk of arrhythmia. However, careful monitoring of the patients will be necessary and will certainly be done, to rule out any pro-arrhythmogenic potential of the undifferentiated hMSC or of the hMSC-derived cardiomyocytes.

References

Alioua A, Mahajan A, Nishimaru K, Zarei MM, Stefani E & Toro L (2002). Coupling of c-Src to large conductance voltage-and Ca^{2+} activated K^+ channels as a new mechanism of agonist-induced vasoconstriction. *Proc Natl Acad Sci USA* **99**, 14560–14565.

Al-Radi OO, Rao V, Li RK, Yau T & Weisel RD (2003). Cardiac cell transplantation: closer to bedside. *Ann Thorac Surg* **75**, S674–S677.

Assmus B, Schächinger V, Teupe C, Britten M, Lehmann R, Döbert N, Grünwald F, Aicher A, Urbich C, Martin H, Hoelzer D, Dimmeler S & Zeiher A (2002). Transplantation of progenitor cells and regeneration enhancement in acute myocardial infarction (TOPCARE-AMI). *Circulation* **106**, 3009–3017.

Barry PH (1994). JPCalc, a software package for calculating liquid junction potential corrections in patch-clamp, intracellular, epithelial and bilayer measurements and for correcting junction potential measurements. *J Neurosci Meth* **51**, 107–116.

Barry EL (2000). Expression of mRNAs for the alpha 1 subunit of voltage-gated calcium channels in human osteoblast-like cell lines and in normal human osteoblasts. *Calcif Tissue Int* **66**, 145–150.

Bruder SP, Jaiswal N & Haynesworth SE (1997). Growth kinetics, self-renewal and the osteogenic potential of purified human mesenchymal stem cells during extensive subcultivation and following cryopreservation. *J Cell Biochem* **64**, 278–294.

Cahill KS, Toma C, Pittenger MF, Kessler PD & Byrne BJ (2003). Cell therapy in the heart: cell production, transplantation, and applications. *Meth Mol Biol* **219**, 73–81.

Caplan AI (1991). Mesenchymal stem cells. *J Orthopaed Res* **9**, 641–650.

Castle NA (1991). Selective inhibition of potassium currents in rat ventricle by clofilium and its tertiary homolog. *J Pharmacol Exp Ther* **257**, 342–350.

Chittajallu R, Chen Y, Wang H, Yuan X, Ghiani CA, Heckman T, McBain CJ & Gallo V (2002). Regulation of Kv1 subunit expression in oligodendrocyte progenitor cells and their role in G1/S phase progression of the cell cycle. *Proc Natl Acad Sci USA* **99**, 2350–2355.

Chomczynski P & Sacchi N (1987). Single-step method of RNA isolation by acid guanidinium thiocyanate-phenol-chloroform extraction. *Anal Biochem* **162**, 156–159.

Coetzee WA, Amarillo Y, Chiu J, Chow A, Lau D, McCormack T, Moreno H, Nadal MS, Ozaita A, Pountney D, Saganich M, Vega-Saenz de Miera E & Rudy B (1999). Molecular diversity of K^+ channels. *Ann NY Acad Sci* **868**, 233–285.

Dobrev D, Wettwer E, Himmel HM, Kortner A, Kuhlisch E, Schuler S, Siffert W & Ravens U (2000). G-protein β3-subunit 825T allele is associated with enhanced human atrial inward rectifier potassium currents. *Circulation* **102**, 692–697.

Estacion M (1991). Characterization of ion channels seen in subconfluent human dermal fibroblasts. *J Physiol* **436**, 579–601.

Fabiato A & Fabiato F (1979). Calculator programs for computing the composition of the solutions containing multiple metals and ligands used for experiments in skinned muscle cells. *J Physiol (Paris)* **75**, 463–505.

Galvez A, Gimenez-Gallego G, Reuben JP, Roy-Contancin L, Feigenbaum P, Kaczorowski GJ & Garcia ML (1990). Purification and characterization of a unique, potent, peptidyl probe for the high conductance calcium-activated potassium channel from venom of the scorpion *Buthus tamulus*. *J Biol Chem* **265**, 11083–11090.

Gögelein H, Bruggemann A, Gerlach U, Brendel J & Busch AE (2000). Inhibition of I_{Ks} channels by HMR1556. *Naunyn Schmiedebergs Arch Pharmacol* **362**, 480–488.

Graf EM, Heubach JF & Ravens U (2001). The hyperpolarization-activated current I_f in ventricular myocytes of non-transgenic and β_2-adrenoceptor overexpressing mice. *Naunyn-Schmiedbergs Arch Pharmacol* **364**, 131–139.

Grammer JB, Bosch RF, Kühlkamp V & Seipel L (2000). Molecular and electrophysiological evidence for 'remodeling' of the L-type Ca^{2+} channel in persistent atrial fibrillation in humans. *Z Kardiol* (Suppl. 4) **89**, IV/23–IV/29.

Gurrola GB, Rosati B, Rocchetti M, Pimienta G, Zaza A, Arcangeli A, Olivotto M, Possani LD & Wanke E (1999). A toxin to nervous, cardiac, and endocrine ERG K^+ channels isolated from *Centruroides noxius* scorpion venom. *FASEB J* **13**, 953–962.

Hamill OP, Marty A, Neher E, Sakmann B & Sigworth FJ (1981). Improved patch clamp technique for high resolution current recording from cells and cell-free membrane patches. *Pflugers Arch* **391**, 85–100.

Haynesworth SE, Goshima J, Goldberg VM & Caplan AI (1992). Characterization of cells with osteogenic potential from human marrow. *Bone* **13**, 81–88.

Heubach JF, Köhler A, Wettwer E & Ravens U (2000). T-type and tetrodotoxin-sensitive Ca^{2+} currents coexist in guinea pig ventricular myocytes and are both blocked by mibefradil. *Circ Res* **86**, 628–635.

Heubach JF, Trebeβ I, Wettwer E, Himmel HM, Michel MC, Kaumann AJ, Koch WJ, Harding SE & Ravens U (1999). L-type calcium current and contractility in ventricular myocytes from mice overexpressing the cardiac β_2-adrenoceptor. *Cardiovasc Res* **42**, 173–182.

Huang B, Qin D, Deng L, Boutjdir M & El-Sherif N (2000). Reexpression of L-type Ca^{2+} channel gene and current in post-infarction remodeled left rat ventricle. *Cardiovasc Res* **46**, 442–449.

Hume JR, Duan D, Collier ML, Yamazaki J & Horowitz B (2000). Anion transport in heart. *Physiol Rev* **80**, 31–81.

Janderova L, McNeil M, Murrell AN, Mynatt RL & Smith SR (2003). Human mesenchymal stem cells as an in vitro model for human adipogenesis. *Obes Res* **11**, 65–74.

Kawano S, Otsu K, Shoji S, Yamagata K & Hiraoka M (2003). Ca^{2+} oscillations regulated by Na^+-Ca^{2+} exchanger and plasma membrane Ca^{2+} pump induce fluctuations of membrane currents and potentials in human mesenchymal stem cells. *Cell Calcium* **34**, 145–156.

Kawano S, Shoji S, Ichinose S, Yamagata K, Tagami M & Hiraoka M (2002). Characterization of Ca^{2+} signalling pathways in human mesenchymal stem cells. *Cell Calcium* **32**, 165–174.

Kim BJ, Seo JH, Bubien JK & Oh YS (2002). Differentiation of adult bone marrow stem cells into neuroprogenitor cells in vitro. *Neuroreport* **13**, 1185–1188.

Lai L-P, Su M-J, Lin J-L, Lin F-Y, Tsai C-H, Chen Y-S, Tseng Y-Z, Lien W-P & Huang SKS (1999). Changes in the mRNA levels of delayed rectifier potassium channels in human atrial fibrillation. *Cardiology* **92**, 248–255.

Ludwig A, Zong X, Stieber J, Hullin R, Hofmann F & Biel M (1999). Two pacemaker channels from human heart with profoundly different activation kinetics. *EMBO J* **18**, 2323–2329.

Mackay AM, Beck SC, Murphy JM, Barry FP, Chichester CO & Pittenger MF (1998). Chondrogenic differentiation of cultured human mesenchymal stem cells from marrow. *Tissue Eng* **4**, 415–428.

Minguell JJ, Erices A & Conget P (2001). Mesenchymal stem cells. *Exp Biol Med* **226**, 507–520.

Muraglia A, Cancedda R & Quarto R (2000). Clonal mesenchymal progenitors from human bone marrow differentiate in vitro according to a hierarchical model. *J Cell Sci* **113**, 1161–1166.

Nerbonne JM (2000). Molecular basis of functional voltage-gated K^+ channel diversity in the mammalian myocardium. *J Physiol* **525**, 285–298.

Ohya S, Tanaka M, Oku T, Asai Y, Watanabe M, Giles WR & Imaizumi Y (1997). Molecular cloning and tissue distribution of an alternatively spliced variant of an A-type K^+ channel α-subunit, Kv4.3 in the rat. *FEBS Lett* **420**, 47–53.

Orlic D, Hill JM & Arai AE (2002). Stem cells for myocardial regeneration. *Circ Res* **91**, 1092–1102.

Ouadid-Ahidouch H, Le Bourhis X, Roudbaraki M, Toillon RA, Delcourt P & Prevarskaya N (2001). Changes in the K^+ current-density of MCF-7 cells during progression through the cell cycle: possible involvement of a h-ether.a-gogo K^+ channel. *Receptor Channel* **7**, 345–356.

Pershadsingh HA, Gale RD, Delfert DM & McDonald JM (1986). A calmodulin dependent Ca^{2+} activated K^+ channel in the adipocyte plasma membrane. *Biochem Biophys Res Commun* **135**, 934–941.

Pittenger MF, Mackay AM & Beck SC (1999). Multilineage potential of adult human mesenchymal stem cells. *Science* **284**, 143–147.

Postma AV, Bezzina CR, de Vries JF, Wilde AAM, Moorman AFM & Mannens MMAM (2000). Genomic organisation and chromosomal localisation of two members of the KCND ion channel family, KCND2 and KCND3. *Hum Genet* **106**, 614–619.

Rudy B & McBain CJ (2001). Kv3 channels: voltage-gated K^+ channels designed for high-frequency repetitive firing. *Trends Neurosci* **24**, 517–526.

Sanguinetti MC & Jurkiewicz NK (1990). Two components of cardiac delayed rectifier K^+ current. Differential sensitivity to block by class III antiarrhythmic agents. *J General Physiol* **96**, 195–215.

Schultz J-H, Volk T & Ehmke H (2001). Heterogeneity of Kv2.1 mRNA expression and delayed rectifier current in single isolated myocytes from rat left ventricle. *Circ Res* **88**, 483–490.

Senger M, Flores T, Glatting K, Ernst P, Hotz-Wagenblatt A & Suhai S (1998). W2H:WWW interface to the GCG sequence analysis package. *Bioinformatics* **14**, 452–457.

Shake JG, Gruber PJ, Baumgartner WA, Senechal G, Meyers J, Redmond JM, Pittenger MF & Martin BJ (2002). Mesenchymal stem cell implantation in a swine myocardial infarct model: engraftment and functional effects. *Ann Thorac Surg* **73**, 1919–1925.

Stamm C, Westphal B, Kleine HD, Petzsch M, Kittner C, Klinge H, Schumichen C, Nienaber CA, Freund M & Steinhoff G (2003). Autologous bone-marrow stem-cell transplantation for myocardial regeneration. *Lancet* **361**, 45–46.

Strauer BE, Brehm M, Zeus T, Köstering M, Hernandez A, Sorg RV, Kögler G & Wernet P (2002). Repair of infarcted myocardium by autologous intracoronary mononuclear bone marrow cell transplantation in humans. *Circulation* **106**, 1913–1918.

Swartz KJ & MacKinnon R (1995). An inhibitor of the Kv2.1 potassium channel isolated from the venom of a Chilean tarantula. *Neuron* **15**, 941–949.

Toma C, Pittenger MF, Cahill KS, Byrne BJ & Kessler PD (2002). Human mesenchymal stem cells differentiate to a cardiomyocyte phenotype in the adult murine heart. *Circulation* **105**, 93–98.

Tse HF, Kwong YL, Chan JKF, Lo G, Ho CL & Lau CP (2003). Angiogenesis in ischaemic myocardium by intramyocardial autologous bone marrow mononuclear cell implantation. *Lancet* **361**, 47–49.

Wallner M, Meera P & Toro L (1999). Molecular basis of fast inactivation in voltage and Ca^{2+}-activated K^+ channels: a transmembrane beta-subunit homolog. *Proc Natl Acad Sci USA* **96**, 4137–4142.

Wang HS, Pan Z, Shi W, Brown BS, Wymore RS, Cohen IS, Dixon JE & McKinnon D (1998*a*). KCNQ2 and KCNQ3 potassium channel subunits: Molecular correlates of the M-channel. *Science* **282**, 1890–1893.

Wang Z, Yue L, White M, Pelletier G & Nattel S (1998*b*). Differential distribution of inward rectifier potassium channel transcripts in human atrium versus ventricle. *Circulation* **98**, 2422–2428.

Westkamp M, Seidl W & Grissmer S (2000). Characterization of the increase in $[Ca^{2+}]_{(i)}$ during hypotonic shock and the involvement of Ca^{2+}-activated K^+ channels in the regulatory volume decrease in human osteoblast-like cells. *J Membr Biol* **178**, 11–20.

Wiecha J, Munz B, Wu Y, Noll T, Tillmanns H & Waldecker B (1998). Blockade of Ca^{2+}-activated K^+ channels inhibits proliferation of human endothelial cells induced by basic fibroblast growth factor. *J Vasc Res* **35**, 363–371.

Winter A, Breit S, Parsch D, Benz K, Steck E, Hauner H, Weber RM, Ewerbeck V & Richter W (2003). Cartilage-like gene expression in differentiated human stem cell spheroids: a comparison of bone marrow-derived and adipose tissue-derived stromal cells. *Arthritis Rheum* **48**, 418–429.

Wulfsen I, Hauber H-P, Schiemann C, Bauer CK & Schwarz JR (2000). Expression of mRNA for voltage-dependent and inward-rectifying K channels in GH_3/B_6 cells and rat pituitary. *J Neuroendocrinol* **12**, 263–272.

Zhang YM, Hartzell C, Narlow M & Dudley SC (2002). Stem cell-derived cardiomyocytes demonstrate arrhythmic potential. *Circulation* **106**, 1294–1299.

Zhao LR, Duan WM, Reyes M, Keene CD, Verfaillie CM & Low WC (2002). Human bone marrow stem cells exhibit neural phenotypes and ameliorate neurological deficits after grafting into the ischemic brain of rats. *Exp Neurol* **174**, 11–20.

Acknowledgements

The excellent technical assistance of Romy Kempe and Silvia Feldmann is gratefully acknowledged. This work was supported by an InnoRegio BioMeT-grant of the Bundesministerium für Bildung und Forschung to B.B., by a grant of the Deutsche Gesellschaft für Kardiologie-Herz-und Kreislaufforschung to I.Z., by a MeDDrive-grant of the Medizinische Fakultät Carl Gustav Carus, Dresden University of Technology, to J.F.H and by a grant of the Sächsische Ministerium für Wissenschaft und Kunst to J.F.H and U.R.